5-1-2016

Statistical Behavior of Distributed Microgrids with Cascading Model Predictive Control

Yasser Yasaei

Yasser Yasaei

Candidate

School of Engineering - Dept. of Electrical and Computer Engineering

Department

This dissertation is approved, and it is acceptable in quality and form for publication:

Approved by the Dissertation Committee:

Prof. Andrea A. Mammoli , Chairperson

Prof. Majeed M. Hayat

Prof. Meeko K. Oishi

Prof. Manel Martinez-Ramon

Statistical Behavior of Distributed Microgrids with Cascading Model Predictive Control

by

Yasser Yasaei

B.Sc., Sharif University of Technology
M.Sc., Sharif University of Technology

DISSERTATION

Submitted in Partial Fulfillment of the
Requirements for the Degree of

Doctor of Philosophy
Engineering

The University of New Mexico

Albuquerque, New Mexico

May, 2016

Dedication

To my parents, Sedigheh and Hooshang, for their support, encouragement and love.

To my beloved sister, Salva, for her kindness and love.

"You don't write because you want to say something; you write because you've got something to say"

– Scott Fitzgerald

Acknowledgments

I would like to thank my advisor, Prof. Andrea Mammoli for his support and encouragement as well as his outstanding knowledge. He helped me understand what an engineering problem is. I would also like to thank Prof. Majeed Hayat for providing the opportunity of working on an important problem for me and our group, along with his constructive comments during this project.

I also want to express my great acknowledgements for Prof. Meeko Oishi for teaching me hybrid-systems theory as well as supporting me on one of the most important contributions of this manuscript. Also thank you to Prof. Manel Martinez-Ramon for his time and accepting to be on the board.

And finally, I like to thank Defense Threat Reduction Agency (DTRA) for their support during these years. The present study was conducted under grant number HDTRA1-13-1-0020.

Statistical Behavior of Distributed Microgrids with Cascading Model Predictive Control

by

Yasser Yasaei

B.Sc., Sharif University of Technology
M.Sc., Sharif University of Technology

PhD, Engineering, University of New Mexico, 2016

Abstract

The problem of integration of distributed energy resources into the grid is addressed in this study. The main objective is to deploy such resources as an alternative for conventional resources in a power system, and to increase renewable resources share in the generation-mix. Distributed energy resources in general come with small capacities, and may have an intermittent nature. The former characteristic limits their impact on large scale grid applications, while the latter characteristic can induce serious stability problems in the system. As the first step, an appropriate model is developed to mathematically describe the behavior of such resources and to facilitate developing applications that address performance and control issues of a power system. Also, design of an appropriate mechanism that can facilitate participation of distributed resources is presented in this manuscript. Specifically, optimal participation for distributed resources, while maintaining the stability of the system at different levels is of interest. Model predictive control provides a framework to address both optimal performance and stability concerns. The ability of the proposed platform to be a part of operating reserve capacity in a power system is addressed in a deterministic sense for standalone case, and in a statistical sense for system-wide implementation.

Contents

List of Figures

List of Tables

Glossary

BESS	Battery Energy Storage System
CAISO	California Independent System Operator
PCC	Point of Common Coupling
DER	Distributed Energy Resource
DoD	Department of Defense
DoE	Department of Energy
DR	Demand Response
DSO	Distribution System Operator
ES	Energy Storage
EWH	Electric Water Heater
GE	Gas Engine
HVAC	Heating, Ventilation and Air Conditioning
ISO	Independent System Operator
MGCC	Microgrid Central Controller

MIP	Mixed-Integer Problem
MPC	Model Predictive Control
NERC	North American Electric Reliability Corporation
PEV	Plug-in Electric Vehicle
PFC	Primary Frequency Control
PG&E	Pacific Gas and Electric
PV	Photovoltaic
QoS	Quality of Service
RTP	Real-Time Pricing
SFC	Secondary Frequency Control
SoS	System of Systems
T&D	Transmission and Distribution
TCL	Thermostatically Controlled Load
TFC	Tertiary Frequency Control
TSO	Transmission System Operator
TW&AA	Tactical Warning and Attack Assessment
UPS	Uninterruptible Power Supply
VPP	Virtual Power Plant
WMD	Weapon Mass Destruction

Chapter 1

Introduction

The electricity grid in the United States served 4113 billion Kilowatt hours energy in 2013 for more than 300 million people. In this period, 127.89 million residential, 17.78 million commercial and 740+ thousand industrial customers had, respectively, 33.91%, 32.68% and 23.79% contribution to the total energy consumption [4] as shown in Fig. 1.1. The power network, as a man-made complex system, has evolved during 100+ years to provide an extremely reliable service to end-users. However, the last decade was marked by numerous large blackouts that raised questions about the resiliency of the system against severe disturbances. In addition to the observed fragility, there has been a growing trend recently to deploy renewable resources for providing electric energy and replacing polluting fossil-fuel-based generation internationally. This trend comes with its associated challenges due to the intermittent nature of renewable resources. Specifically, renewable resources are non-dispatchable in their basic implementation, which places a barrier to their deployment as power resource in a highly reliable electric power system. These two issues as well as the perspective of a liberalized (or at least less regulated) energy market are among main drivers for modernizing the power system infrastructure.

The electricity demand in the current grid is primarily met by the power that is generated at

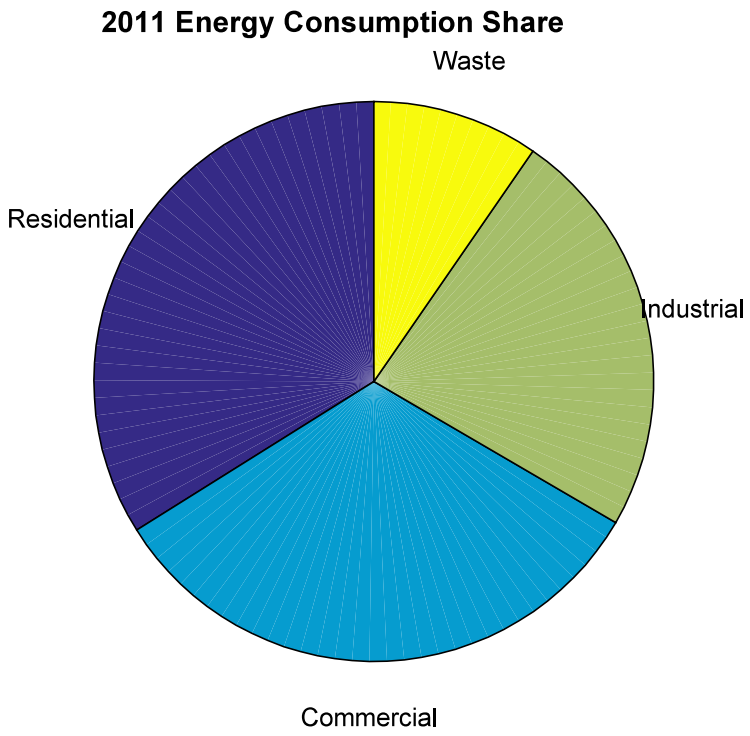

Figure 1.1: Energy consumption share of each sector in the U.S. power system, 2011.

large centralized sites, including but not limited to fossil-fuel-based generation, nuclear and hydro power plants as well as transmission-level scale wind farms. This system has recently shown increasing frequent and non-negligible signs of fragility [5, 6, 7, 8]. According to the President's Council of Economic Advisers, the U.S. Department of Energy (DoE)'s Office of Electricity Delivery and Energy Reliability, and the White House's Office of Science and Technology, severe weather conditions were the main cause of more than 679 widespread power outages in the United States between 2003 and 2012 [9]. In addition to severe weather conditions, there are also concerns about the resiliency of the system against possible malicious attacks.

The inflation-adjusted average annual net cost of weather-related power outages has been approximated as between US$18 to US$33 billion, meaning around $100 per capita. In the case of the power outage caused by super-storm Sandy [10, 11] in 2012, the associated cost was approximated as between US$27 to US$52 billion. The variation in the values is due to the methods and considered assumptions for cost evaluation.

In June 2011, President Obama's office released "*A Policy Framework for the 21st Century Grid: Enabling Our Secure Energy Future*" for modernizing the electric grid [12]. The initiative was addressing grid technologies for decreasing vulnerability of the power system against weather-related outages as well as the restoration time with focus on increasing the grid efficiency, reliability as well as resilience.

Furthermore, there has been a growing interest in the community for using renewable power generation in recent years due to environmental concerns as well as financial incentives [13], that has affected the energy network to replace more fossil-fuel generation with renewable resources. The scale of renewable resources ranges from roof-top solar photovoltaic (PV) panels to large wind farms at the transmission-level scale. The "*duck curve*", which is shown in Fig. 1.2, is a well-known graphic that illustrates the predicted share of solar PV power in the generation-mix of California Independent System Operator (CAISO) for the horizon up to the year 2020 [1]. In this plot, the actual net loads for 2012 and 2013 (when the study was conducted) as well as the predicted values until the year 2020 are shown. The net load is derived from subtraction of the actual (predicted) renewable generation production from the actual (predicted) demand. The objective of the plot is to demonstrate likely evolution of the power system as the share of renewable resources, mainly from PV, in providing energy increases. It also illustrates that integration of PV power into the grid comes with challenges, including the high ramp of the net load at the end of the day, when PV panels no longer generate power at the same time that loads increase due to people returning home from work. This ramp should be covered by conventional resources in the grid, which at best, are available for a high price.

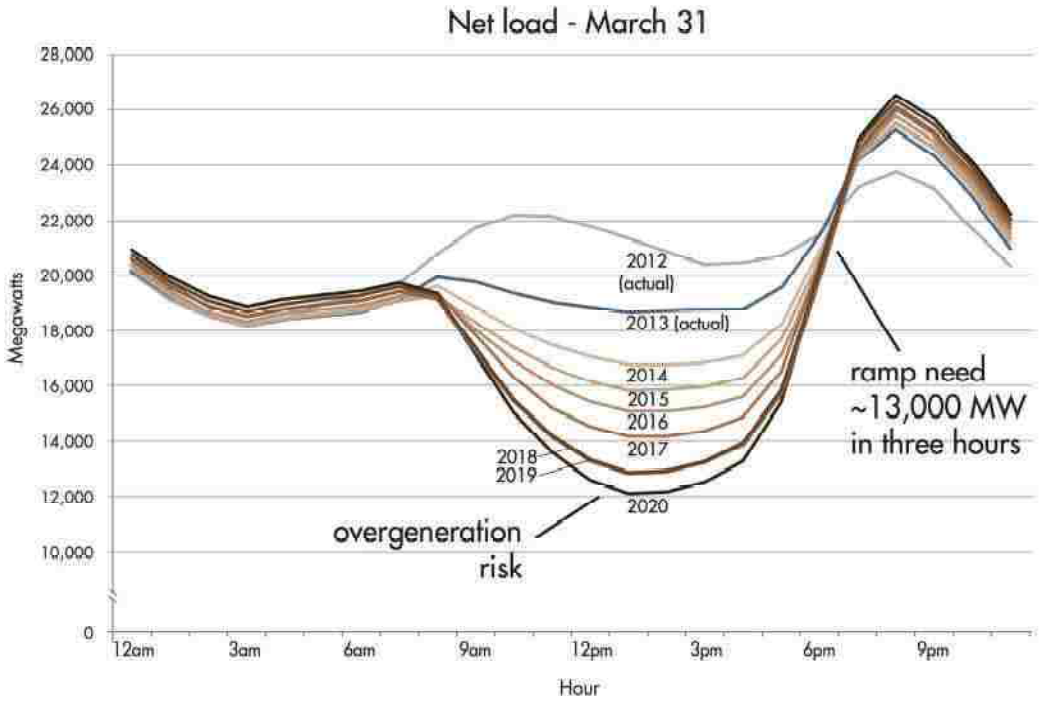

Figure 1.2: Actual (predicted) net load in CAISO for a fixed date from 2012 to 2020. As the share of renewable resources in the generation-mix increases, some issues including high ramping at the end of the day may emerge. Source: CAISO [1].

Finally, the current operation of the power system is based on a vertical integration of utilities that run as regulated monopolies. An important issue in a power system is providing the flexibility needed for maintaining perfect balance between demand and generation in real-time. Except basic prevalent time-of-use rates that has a limited effect on the demand profile, there has not been a mechanism that could significantly adjust the load, to make it contribute to the needed flexibility for the supply-demand balance. Due to the lack of sufficient financial incentives in the current paradigm, an inelastic consumer behavior has emerged in the electricity market, forcing the supply-side to provide almost all the

required elasticity in the system. Oldwurtel *et al.* in [14] have discussed the effect of utilizing distributed energy resources (DERs) on the demand-side in increasing the elasticity of the load. The demand-side participation facilitated, consequently, could open gates to a liberalized (or at lease less regulated) market.

The need for enhancing the system resiliency in addition to the necessity for less polluting power generation within a liberalized market together have directed significant research efforts to the subject of modernizing the power network. The structure of a modern power system, with a significant share of renewable resources in its generation-mix, and the control mechanism that maintains system reliability/stability are the major concerns of this study.

1.1 Background and Challenges

The challenges that the current electricity grid is facing are at different scales. For example, stability issues associated with integration of renewable resources such as solar PV are typically at lower levels of the power system structure than that of the issues regarding nation-wide large blackouts which in general are at the transmission-level. In the present study, a platform that can act as an interface between different levels of the control architecture is studied. The platform of interest consists of a distribution feeder microgrid structure equipped with an appropriate control framework that addresses performance objectives and stability requirements. It is expected that system-wide implementation of this platform throughout the grid could facilitate execution of applications that assist control solutions at higher levels by leveraging resources at lower levels of the power system. This inter-layer interaction, however, should not violate system reliability at any of the targeted layers.

1.1.1 Microgrids and Mitigating Stress On the Grid

It was just a few minutes after 4 PM EDT on August 14th, 2003 that sections of the Midwest and Northeast United States as well as Ontario, Canada lost their electric power in one of the largest blackouts experienced ever. Fifty million people with more than 60 GW of average daily electric load were affected for four to seven days. Large blackouts such as this reveal vulnerabilities of the system, unfortunately at significant costs. The estimated cost of this single 2003 large blackout was approximated as between US$ 4 billion and US$10 billion on just the U.S. part [15]. The cost of this single blackout was equivalent to 0.05% of the net GDP of 2003.

Researchers have conducted several studies on the reasons and underlying dynamics of such outages, trying to develop models that describe what happens in large blackouts. Baldick *et al.* [16] have provided an initial review on the essential concepts, methods and tools needed for analyzing what happens in large outages. Also, Hines *et al.* [8] have studied large blackouts in North America from a statistical point of view; the occurrence frequency of large blackouts conveys information that can be used for planning purposes in the power system. In the case of 2003 large blackout, for example, it was shown that the outage was the result of cascading component failures in the system [15]. In a cascading failures event, a disruptive factor imposes stress on the grid, and causes initial component failures. These failures, consequently, impose further stress on the grid, and a chain of outages happen in the system, resulting in a large blackout; It is thought that a load reduction of less than 1% could have averted the 2003 blackout [15].

In a cascading failures event, the amount of load on the system is an important factor in the progress of component outages [17, 18, 19, 20]. The standard practice in dealing with such a phenomenon is to curtail load. On the other hand, there is reluctance in system operation to cut the service as it reduces the quality of service (QoS) for the end-users, and the load is likely removed from the system when the time for corrective actions has passed.

Furthermore, studies have addressed the importance of a new architecture for the power system that facilitates better handling of disruptive stresses. Among the proposed solutions, the concepts of microgrid and virtual power plant (VPP) have gained considerable interest recently [21, 22]. These architectures usually offer improved system resiliency as well as opportunities for extending resource heterogeneity in the generation-mix. In the present study, the concept of the distribution feeder microgrid structure is used.

According to the DoE, a microgrid is a group of interconnected loads and distributed energy resources with clearly defined electrical boundaries that acts as a single controllable entity with respect to the grid [and can] connect and disconnect from the grid to enable it to operate in both grid connected or island mode [23].

As Asmus stated in [21], "perhaps the most compelling feature of a microgid is the ability to separate and isolate itself from the utility's distribution system during brownouts or blackouts". This feature, when considering the cascading component failures phenomenon, is promising for mitigating stress on the system as it is possible to completely disconnect an entity and its associated load from the grid in the worst case scenario in a grid-stress situation. However, a microgrid can offer more by providing a controllable entity as discussed later in this manuscript.

A load reduction scheme facilitated by a microgrid, however, is different from a regular load curtailment scheme in the sense that the microgird is still able to serve its critical loads in island mode autonomously, utilizing its local available resources. The microgrid central controller (MGCC) maintains the internal stability of such a structure. More precisely, the microgrid framework provides a controllable entity for the system in contrast to the current non-dispatchable scheme of load in the network. The controllability feature of such a structure, provides an opportunity to shape the associated load, and not limiting the control actions to a simple switching fashion.

1.1.2 Integration of Fluctuating Renewable Resources into the Grid

There are also challenges in the power system at smaller scales, down to the distribution-level. As an example, integration of the power generated from roof-top solar PV panels can be categorized in this level, which can trigger problems including voltage stability and protection issues. In general, adoption of renewable resources in the power network is limited by their intermittent nature.

The fluctuations associated with renewable resources can cause gaps between generated power and demand. At small scales, large rotating mass of synchronous generators absorb the associated intermittencies in the grid. At large scales of renewable power penetration, however, gaps can influences the system frequency stability by affecting the supply-demand balancing requirement [24]. Such a problem can take place either in normal operating conditions or when the system is at risk, weakening the ability of the system to withstand sudden disturbances [25]. There are also voltage and reverse load flow issues associated with intermittent renewable resources [26, 27] at distribution level scale.

So far, penetration of the electricity generated by renewable resources has been managed by different methods at larger scales, including deployment of reserve generation and large rotating mass of synchronous machines. Reserve generation can be used to compensate low frequency variations, while large rotating mass of synchronous generators behaves as a low-pass filter in the system. This feature eliminates the effect of rapid fluctuations at limited scales [28].

Another approach for eliminating fast fluctuations at smaller scales is to use battery energy storage system (BESS). A storage device, in general, acts as a buffer for the intermittencies associated with the power that comes from a renewable resource. When an intermittent resource is combined with a storage device, it becomes a partially dispatchable resource. Although using a battery seems promising on the surface, the storage capacity of the battery

is limited by economic factors. As the size of the storage device gets larger, the financial justification of the method shrinks, until it reaches a point where using battery would not be financially attractive.

Thus, penetration of renewable resources into the network in the current operation paradigm is limited by the capacity of the grid to absorb the associated fluctuations provided by the system inertia, reserve generation and conventional storage devices. However, there are methods that can boost system capacity for absorbing intermittencies. These methods, which are implemented through power system services, in general utilize the capacity of DERs in services that maintain the stability of the system. It is worth mentioning that a system service, in general, is an external influence on the behavior of a part of the grid in favor of a reliability requirement or efficiency improvement.

The DERs of interest include, but are not limited to, local fossil-fuel-generation, storage technologies as well as dispatchable loads. The term dispatchable load refers to a load the power consumption profile of which can be changed by an external control action.

Deployment of DERs for intermittency absorption applications, and in general other system applications, is limited by their small capacities. For example, storage devices and dispatchable loads have limited power capacity, while local fossil-fuel-based generation typically comes with low ramping capacity. Despite typical low capacities of distributed resources, a control mechanism that can facilitate a coordination among several small distributed resources, while maintaining stability requirements, is able to provide a higher aggregated capacity. Such a collective capacity, then, can be used, for example, in boosting the power system to tolerate higher levels of renewable resource power penetration.

Although the potential of an aggregation scheme implemented over distributed resources is widely accepted, its implementation structure is not fully yet determined. There is a hypothesis that fast control actions should be highly local and decentralized while slow control actions are more suitable to be centralized [29]. Due to the presence of rapid variations in

the power generated by renewable resources, the corresponding control mechanism that uses distributed resources to absorb fluctuations should be highly decentralized. A microgrid offers an architecture, in which the essential control mechanism for integration of renewable resources can be practically implemented via the associated microgrid central controller (MGCC).

1.2 Solution, Objectives, Tools and Performance

In the present study, the concept of a microgrid structure is used to address several problems at both the transmission and distribution levels. At the distribution level, applications can be developed in this architecture to optimally integrate renewable resources. The highly decentralized structure of a microgrid provides the opportunity to implement fast control actions in response to high frequency fluctuations of renewable resources in a local scale, and consequently to boost a power system capacity for increasing renewable generation share in the generation-mix by absorbing destabilizing associated intermittencies [30].

As an example for the applications in higher levels of the power system, moreover, coordination between controllable loads, local generation and storage devices, once implemented in this platform, can provide a controllable entity with a large capacity for a utility company. This capacity could be used in system reliability services such as load reduction applications when the grid is under stress.

Microgrids in this study participate in the utility scale applications via demand response (DR) schemes. Demand response, as defined by Albadi, *et al.* are "all intentional modifications to consumption patterns of electricity of end-use customers that are intended to alter the timing, level of instantaneous demand, or the total electricity consumption" [31].

Demand response schemes utilize the dispatchable capacity of a microgrid and can alter the microgrid's load profile at various time scales in favor of the grid performance and stability.

Microgrids usually have fast response time and high ramping capacity, while their power and energy capacities are limited as compared to conventional large generators. Similar to the internal coordination scheme of DERs in a microgrid platform, a utility company can orchestrate an aggregation mechanism over the controllable capacity of a considerable number of microgrids to obtain a significant collective capacity that can replace conventional resources.

In the long run and concerning the market of the power system, a microgrid-based architecture for the grid increases the demand elasticity. This elasticity, consequently, can provide an opportunity to facilitate shifting the current regulated energy market towards a liberalized/competitive one. This economical improvement, however, does not come with compromising costumer quality of service (QoS).

1.2.1 Research Objectives

The concept of a recently developed type of microgrids, namely the distribution feeder microgrid is developed in this work specifically. According to Asmus [32], in the most common configuration of a microgrid, a group of DERs are tied together on their own feeder, which is then linked to the larger utility grid at a single point of common coupling (PCC). In this architecture, distribution feeders already existing on the distribution network adopt the structure of a microgrid and provide a level of controllability that could be used for load management purposes at the system scale. This wide scale adoption of microgrid platform is what is referred to in this manuscript as microgrid-based structure hereafter.

Distribution feeder microgrids are also assumed to have high levels of power penetration from renewable resources, including solar PV. The ability of such a structure to integrate renewable resources and the capacity that a microgrid-based architecture for the power system may have in reducing the level of stress on the grid is evaluated in the present research. The main objective of this project is specifically to study the essential control requirements for

converting feeders into microgrids.

In Fig. 1.3, an example of the microgrid type of interest is shown. In this figure the physical boundary of the Studio-14 feeder, serving Mesa del Sol community located in south of Albuquerque, New Mexico, as well as the already connected facilities and the foreseen ones are depicted. The PV panels installed in the Prosperity site provide 500 KW solar PV power capacity to the feeder. This set of panels is an example of the general highly intermittent renewable resources that distribution feeder microgrids are expected to encompass.

Figure 1.3: An example of a distribution feeder microgid. The location is south of Albuquerque, New Mexico, and the feeder serves Mesa del Sol community. The installed and foreseen facilities are shown with their associated capacities.

In the present study, design of a control mechanism that addresses stability requirements as well as an optimal performance is addressed. Specifically, the performance of the system is formulated in terms of realistic costs. The advantage of this approach is that it better reflects the financial justification of implementing distribution feeder microgrids in the power network.

1.2.2 Tools

The control mechanism of interest is in charge of fulfilling performance requirements and maintaining the internal stability of the structure by utilizing available distributed resources to the extent possible. The focus of this study is on local fossil-fuel-based power generation, distribution-level controllable loads, energy storage (ES) devices and renewable power resources available on a feeder.

Although based on converting the stored energy of fossil fuels into electricity, local fossil-fuel-based generation (e.g. a gas engine (GE)) has the advantage of lower carbon footprint and high efficiency as compared to, for example, a coal plant. When integrated in a combined heat and power design, the resulted by-product heat from the local power generation can be used for thermal energy needs in residential/commercial buildings such as producing hot or chilled water, which consequently increases the efficiency of the system.

Loads that offer some levels of controllability can also be used for the objectives of this study as they provide a dispatchable resource once enabled by a proper control scheme [33]. Loads that have a hysteresis property are candidates for becoming controllable. The hysteresis property is illustrated in Fig. 1.4. A hysteresis-driven load is associated with a thermal mass. An example of a hysteresis-driven controllable load is heating, ventilation and air-conditioning (HVAC) system of a building. Based on the thermal mass of a building, it is possible to, e.g., postpone its power demand in a load management application without compromising end-users' comfort. The controllability property results in part from technological

progress in the communication and sensing technologies.

Dispatchable loads are not limited to the loads that have hysteresis property. For example, there have been efforts to develop applications for turning computing servers into dispatchable loads [34]. In such an application, the performance of the resource, and consequently its power consumption, is reduced in favor of a higher priority requirement in the power system.

1.2.3 Research Questions

Coordination among distributed resources can provide a higher aggregated capacity that can be used for fulfilling a control mechanism objectives. The problems that should be addressed for designing such a coordination mechanism are as follows:

a. To develop a unified consistent model that captures the major features of distributed resources in a simple yet accurate fashion to be used in the control framework. Such a model should capture main attributes and the physical properties of the system elements as well as practical constraints, including power, energy and ramping capacities. The elements of interest include controllable loads, energy storage devices and local fossil-fuel-based generators.

b. To choose an appropriate control framework that can address performance and stability objectives, using the developed model in the first step. It is also essential to formulate the performance and stability requirements in a way that can be fed into the applied control framework.

The control framework of interest in the present study is the model predictive control (MPC), that suits the objectives of the research. Broadly speaking, the MPC framework uses the current state of the system in a feedback mechanism as well as prediction of the external factors, solves an optimization problem and provides a set of control actions for a finite horizon at each time step.

While model development and control problem formulation are two aspects of this study, the computational cost of the solution should also be tackled. Specifically, the MPC framework is a real-time optimization process. Thus, the time that it takes to calculate control actions for the optimization part does matter.

The platform studied in this research is also supposed to enhance the power system resiliency against disturbances at the transmission level. The enhancement could be achieved if a system-wide adoption of distribution feeder microgrids takes place over the network.

An important factor in grid-stress situation is the amount of load on the grid. Especially, higher levels of load on the system play a significant role in propagation of component outages in a cascading failures event. As mentioned earlier in this chapter, the common approach in a power system operation is to curtail substation loads. Also, load is generally inelastic in the system emerged through years of the network evolution and due to the lack of financial incentives. This phenomenon translates into the fact that all the necessary flexibility for meeting the variations in the demand should be provided by the generation side. In a modern power system, the essential flexibility should be transferred partially to the demand-side. A microgrid-based structure provides an opportunity for such a transfer. The improvement that a microgrid-based architecture could provide is from two aspects; time and energy.

A microgrid-based structure as being interactively connected to the utility central controller has a short response time for grid requests. Also, it provides an opportunity to utilize distributed energy resources in an implementable way. Specifically, there are communication and computational barriers in direct integration of distributed resources into the grid. A microgrid-based structure facilitates a hierarchical control platform in which the problems associated with direct integration of distributed resources are bypassed. Thus, the flexibility that is provided by the studied structure enhances the resiliency of the system against disturbances through increasing controllability level over the system. Thus, system operators may be able to use the provided flexibility on the demand side for reducing the stress without

needing to compromise users' QoS as in a regular load shedding scheme.

The improvement in the resiliency of the system should be characterized in a measurable way. The scenarios that result in stress on the grid are heterogeneous and include a wide range of possibilities from severe weather conditions to malicious attacks including Weapons of Mass Destruction (WMD)-induced ones in the extreme case. The direction of a related and recent study, where a probabilistic model for cascading failures event has been developed [35], is followed here for assessing resiliency enhancement offered by the proposed platform. Some meaningful metrics are derived in this research that can be coupled into the probabilistic model of cascading failures, and how a distribution feeder microgid-based architecture for the power system can likely mitigate vulnerabilities against severe disturbances is shown.

The developed metrics address two important factors: response time and capacity. Time plays a significant role in taking remedy actions for reducing stress on the grid during a cascading failure event. Reactions take time in the current centralized structure, and slow responses come with a significant price. It will be shown that the proposed architecture has the advantage of fast reaction in the case of a severe crisis, and consequently can enhance system resiliency.

Another important factor when facing a large disturbance in the grid is the capacity of the system to endure against the disruption. This capacity can be defined in terms of the energy that a microgrid structure can survive with in an island mode, while maintaining the service for its own critical loads. In the grid connected mode, this capacity determines the amount of imported energy from the grid that a microgrid can reduce to help a power system in a grid-stress situation. The endurance capacity of the proposed structure is assessed by introducing a suitable metric later in this manuscript.

1.3 Significance of the Project

The platform of interest in this research is well suited to address the needs of suburban communities, where more than 50% of the U.S population live [36], with high levels of renewable power generation. Working at the scale of distribution feeders also makes it possible to attain finer control over the available resources. Also, it is possible to add some levels of controllability to small loads and turn them into distributed dispatchable resources. The connected nature of future devices through ever-developing communication infrastructure also in part enables this leveraging mechanism.

Based on the scale of the distribution feeder microgrid, the cooperation between dispatchable loads, generation and storage devices makes it possible to minimize the size of needed conventional resources, and hence the associated cost of implementing a service, e.g. for stability requirements. The advantage of the proposed system is based on its capability to control and deploy a wide-range of resources either in the form of generation or storage device ranging from those with small power/energy capacity to large ones, relying mostly on the available infrastructure.

Finally, the proposed framework will enable utility companies to go beyond the current limits associated with deploying renewable resources. At the system scale, it also increases the level of control over the grid that will increase the resiliency of the system against large disturbances.

1.4 Structure of the Dissertation

The remainder of this manuscript is structured as follows. In chapter 2, a brief review on studies related to the concerns of the present research is provided. In chapter 3, a novel framework for characterizing the time-scale of services that DERs can participate in is introduced. For this characterization, a specific control mechanism is designed and

implemented to act as the essential aggregation mechanism over small capacity distributed resources. In chapter 4, the control mechanism that addresses performance and stability requirements of a distribution feeder microgrid is discussed from a frequency stability point of view. The control mechanism of interest is a price-driven scheme that captures realistic costs associated with implementation of each of the utilized technologies. Also, a recursive feasibility condition is determined which is neglected in many studies conducted so far. In chapter 5, a cascading mechanism is introduced as an extension to the primary results to optimize the computational costs associated with using the control mechanism introduced in chapter 4. Finally, the effect of reconfiguring the current power system control paradigm based on the proposed platform in the current study is assessed from a probabilistic point of view in chapter 6. Chapter 7 concludes the manuscript.

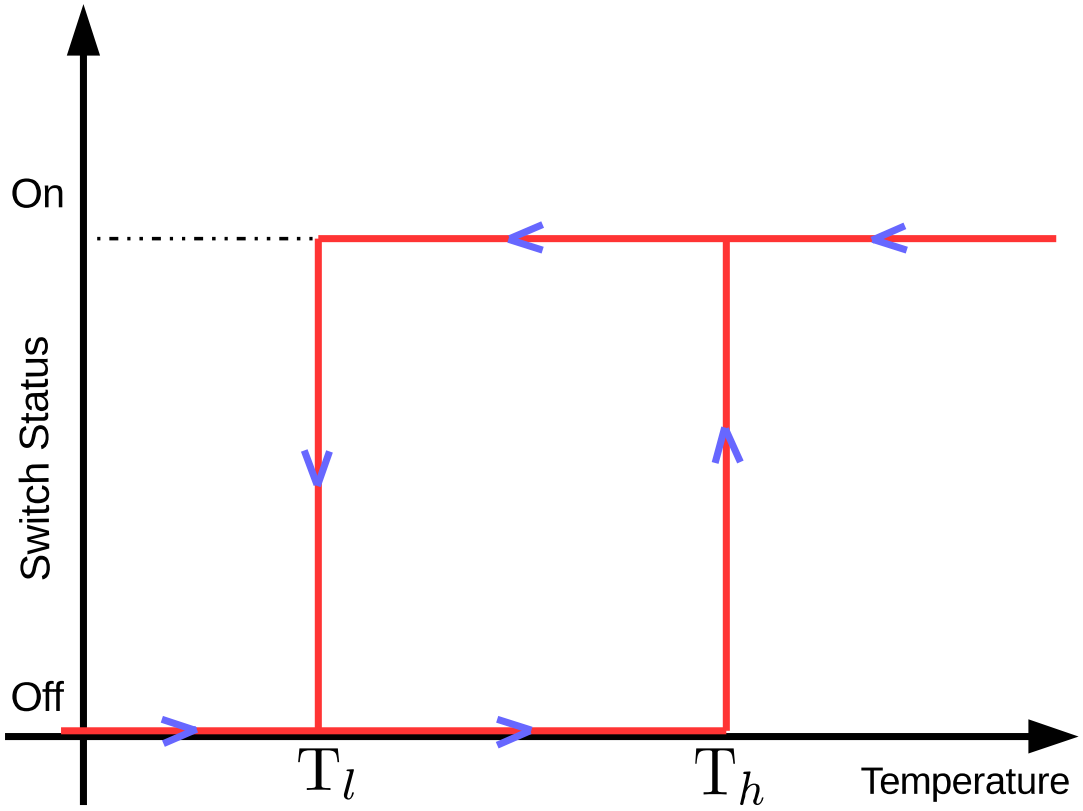

Figure 1.4: Graphical explanation of the hysteresis property. A thermostatic device remains off until its temperature reaches the upper bound of the dead-band T_h. Then the device switches on and start using power to reduce its internal temperature until it reaches the lower dead-band T_l, where it switches off again. This cycle repeats depending on the environmental conditions.

Chapter 2

Literature Review

Although originally introduced in the 1950's, the concept of *System of Systems* (SoS) received attention in engineering societies in the 1990's [37]. According to the Department of Defense (DoD), "A system of systems brings together a set of systems for a task that none of the systems can accomplish on its own. Each constituent system keeps its own management, goals, and resources while coordinating within the SoS and adapting to meet SoS goals" [38]. In this architecture, generally, services are delivered by independent preexisting subsystems that collectively fulfill a requirement.

The SoS structure can be considered as the child of technological progress in communication and computing fields, making individual systems *smarter*. Despite the lack of common understanding on the features of such a structure, according to Maier [39] SoS has five main characteristics as follows:

- Operational independence: in the sense that subsystems are able to operate individually even if the SoS is disassembled.

- Managerial independence: in the sense that self-governing operation is not only a can, but a should.

- Geographic distribution: in the sense that subsystems exchange information and not a considerable amount of mass or energy. However, this term has ambiguity in its definition.

- Evolutionary development: in the sense that subsystems can constantly adapt new functionalities, objectives and structure.

- Emergent behavior: in a synergistic sense, meaning that an SoS performs a task as an emergent behavior of individual subsystems performance.

The SoS architecture has become an interesting topic in engineering fields to address resiliency issues, which are difficult to resolve by simple systems methods. In such cases, the scale of the system becomes so large that the simple systems paradigm does not have sufficient tools to deal with the problems. For example, *tactical warning and attack assessment* (TW&AA) system of the U.S. DoD is composed of large evolving independent subsystems that collectively fulfill a certain objective [40]. The Internet is another well-known example of an SoS structure. The question, here, is whether a power system can adopt such an architecture to address its increasing challenges. The proposed configuration of the power system in this study, at least to some extent, has some of the features of an SoS structure. Whether the proposed platform perfectly fits an SoS structure, however, is discussed later in this chapter after introducing the control mechanism of interest.

As mentioned in the chapter 1, the U.S. power system is facing challenges at different scales. These challenges put the stable operation of the grid at risk. Thus, to have an understanding of the power system operation under normal and grid-stress conditions seems essential before developing any control mechanism. In the first section, a brief review on the current power system structure and operation is presented. This section is followed by a brief introduction to the concept of *smart grids*. Grid operators in a power system use different services to deal with destabilizing situations. A brief introduction on different power system services is presented as well. These services currently utilize conventional resources in a power system to

meet their objectives. In a modern power system, however, the resource set that services use can be extended by including small scale, yet aggregated, distributed resources. A review on various DERs, and in specific the ones of interest in the present study is provided afterwards.

Also, the concept of a microgrid is used to define the structure in which such utilization can be implemented. Specifically, a distribution feeder microgrid as a special type of this structure is considered, and a brief discussion on the microgrid concept is provided. Also, an appropriate control mechanism that addresses performance and internal stability requirements of a microgrid is introduced and reviewed at the end.

2.1 Current Power System - Configuration, Operation and Complications

The U.S. power system is a complex interconnected network of generation sites, transmission facilities and distribution systems. In this network, electric energy is mainly provided by bulk generation at centralized plants. Transmission and distribution (T&D) networks provide the infrastructure for delivering the generated power to the end-users. The end-users mainly include residential and commercial customers as well as industries. In Fig.2.1, a schematic topology of the current power system is shown.

2.1.1 Power System Operation

In the current paradigm, large generation sites collectively provide the main portion of the needed power for the consumers. The contribution of each site to the demand is determined by transmission system operators (TSOs) through running optimal dispatch routines according to various factors from load forecasts to weather conditions. The dispatching process takes place at various time scales depending on the transmission system size and physical

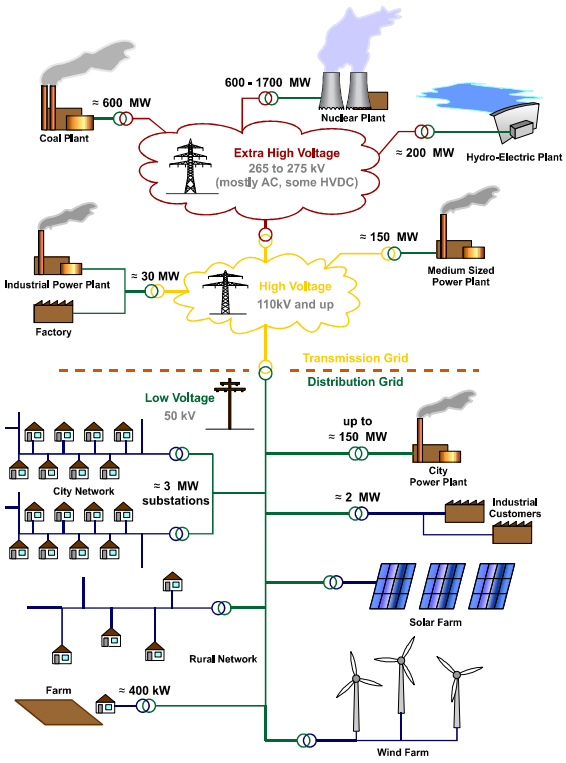

Figure 2.1: Current power system topology. The power system is a complex interconnected network of generation sites, transmission facilities and distribution systems. Source:wikipedia.org [2]

constraints of devices [41]. It should be noted that the dispatch mechanism also considers a safety margin to address robustness of the system due to unforeseen events, following the North American Electric Reliability Corporation (NERC) standards [42].

While bulk power generation sites provide the main portion of electrical energy needs, peaking energy generation at a lower level of the grid structure provides an additional capacity during peak hours. These smaller scale facilities maintain reliability of the power system. In addition to peaking energy generation, ancillary services are also in charge of maintaining the reliability of the system. These services include, but are not limited to, operating reserves, voltage regulation, load following and contingency reserves [43].

2.1.2 Power System Control Paradigm and Challenges

The U.S. power system has shown numerous non-negligible signs of fragility during the past decade, causing concerns about its resilience in more severe conditions such as WMD-attacks as an extreme case. The traditional approach to address power system reliability, so far, has been based on a hierarchical control architecture defined by time-scale separation.

One of the most important issues in a power system is the demand-supply balancing issue which affects the system frequency stability. In the current paradigm, and based on the NERC standards, bulk power generation along with smaller scale resources are in charge of meeting the demand in a highly reliable fashion. They also should compensate possible variations, e.g. demand changes during a day. Depending on the time-scale of the variations, there are methods to compensate the gap between scheduled supply and demand. For lower frequencies, conventionally, system operators redispatche generation resources by ramping them up or down to match the demand and the supply. For higher frequency variations, governors, which are the frequency-sensing devices installed on conventional generation resources, automatically adjust electric power output.

Moreover, there has been a growing trend in the power system community during recent years to increase the share of renewable resources in the generation-mix [44]. The scale of these resources varies from roof-top solar PV panels, typically 1-10 KW, to large transmission-level wind farms at the scale of hundreds of megawatts. This trend is the result of various factors, including decreasing cost of associated technologies [45], efficiency incentives and renewable portfolio standards [46].

Renewable resources are highly intermittent and in general non-dispatchable. They seldom come with frequency reserve capabilities as in the conventional generation facilities. Thus, increasing the share of renewable resources in the generation-mix, especially by replacing conventional generation, decreases the inertia of the system. This inertia reduction weakens the capability of the system to deal with high fluctuations. Based on their highly dynamic

nature and lack of on-site dispatching technologies, renewable resource-derived power penetration is limited due to the capacity of control mechanisms for compensating high frequency fluctuations [47]. Thus, higher levels of penetration requires more flexibility in the system to maintain demand-supply balancing requirement. A sample of the power generated in the Prosperity site, located in south Albuquerque, NM is shown in Fig.2.2. The site is connected to the Studio14 feeder, serving the Mesa del Sol community. The power spectral density of the signal shows the distribution of the power over a frequency spectrum.

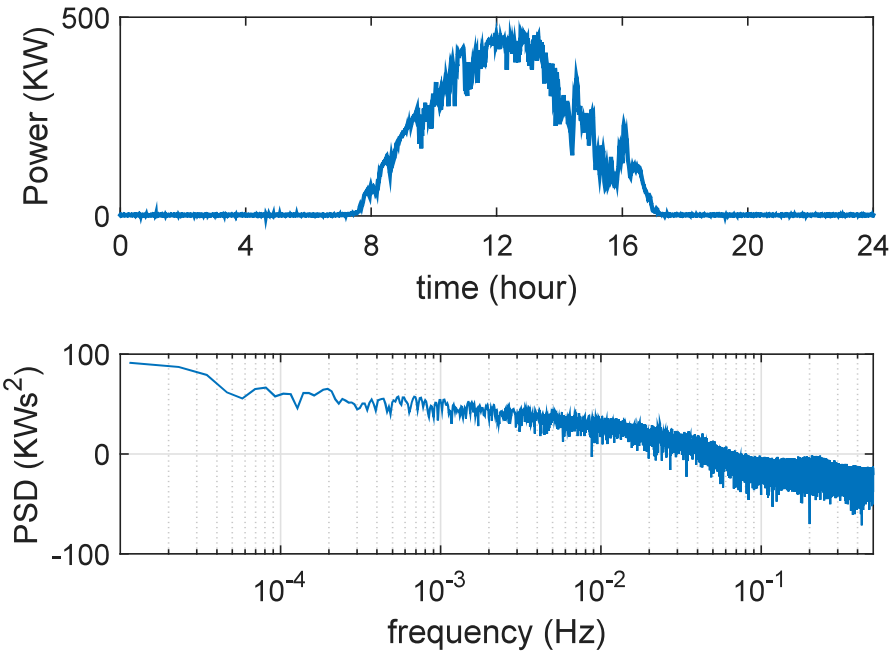

Figure 2.2: A sample output of the Prosperity site, located in south of Albuquerque, NM. The upper plot shows the actual output of the site, and the bottom plot is the associated power spectral density (PSD) of the same signal.

In the current paradigm, moreover, demand-supply balancing applications rely only on the elasticity of the supply-side and not the demand-side. In other words, loads in this framework are considered non-dispatchaple and they do not contribute to the balancing issue. From a reliability perspective, on the other hand, a flexibility that comes from the demand-side is

equally valuable to what comes from the supply-side, provided that demand-side flexibility can provide the needed level of accuracy and reliability. One major concern in the power engineering society nowadays is to enable/increase levels of controllability of the loads at different system and time scales. This increased level of flexibility makes these loads assets for power system management.

In contrast to the current top-down management scheme in the power system, alternative control approaches have been explored, mainly in decentralized fashion. The objective of such efforts has been to facilitate integration of distributed resources into the grid, while addressing the reliability issues. They are based on the potential of DERs and load to be used as complementary resources for affordable and reliable power delivery. Integration of DERs can provide higher efficiency in the power system, along with a lower carbon footprint. However, the system architecture that facilitates this integration and the corresponding building blocks for such an architecture are not yet fully determined.

2.2 Smart Grids

Aligned with the major concerns regarding the power system architecture and operation paradigm, the concept of *smart grid* has gained attention in recent years. According to Manz *et al.* [48], concerns regarding the structure and functionalities a power system include management of distributed solar power, wind power, energy storage for short-term frequency regulation, demand management, distributed generation and maintaining grid resiliency via microgrids. "The *smart grid* is the application of technologies to all aspects of the energy transmission and delivery system that provide better monitoring, control and efficient use of the system" [49]. The independent system operator (ISO)'s goal is to enable and integrate all applicable smart technologies while operating the grid reliably, securely and efficiently. Functionalities associated with a smart grid are expected to enable diverse generation including utility-scale renewable resources, demand response, storage and smaller-scale

solar PV technologies to fully participate in the wholesale market as well as to increase grid efficiency and reliability, while providing enhanced physical and cyber-security.

There are several technologies in the smart grid road-map that a modern power system is expected to feature, including a reliable communication infrastructure [50, 51] as well as an enhanced demand response capability. Demand response by definition [31], are "all intentional modifications to consumption patterns of electricity of end-use customers that are intended to alter the timing, level of instantaneous demand, or the total electricity consumption". A demand response program is targeted to use demand-side resources to support supply-demand balance equation. Demand response technology is expected to be implemented via market policies including incentives and penalties [52]. Also, physical constraints of devices according to their corresponding characteristics should be well-maintained in any realistic implementation. It seems essential that a data acquisition program be a part of the technology to exchange necessary information including devices' state [1].

2.3 Power System Services - Performance and Reliability

The objective of services in a power system in general is to address reliability issues or system efficiency. Services that may be considered by operators in a power system differ from one system to another. In a two-part survey, Rebours *et al.* provided a comprehensive reference on various power system services in different regions from two perspectives: ancillary services and market services [53, 54]. The former is mainly addressing reliability issues in a power system, while the latter are used for improving the efficiency of the system. The focus of the present study is the ancillary services.

Ancillary services are characterized by their corresponding time resolution and zero-mean period. The time resolution represents the time interval between successive actions of a

particular service. Moreover, services are usually designed to account for deviations of a quantity from a nominal/scheduled operating point. Thus, it is easy to understand that control signals may have a zero-mean characteristics over an expected period of time. In other words, while a service adjusts a quantity in a specific direction, it is expected that the same service performs the adjustment in the opposite direction at some other time. By zero-mean period, the period of time over which the signal is expected to have a zero integral is determined.

Ancillary services in a power system are a set of heterogeneous applications, each of which addresses a reliability issue in a power system. These services include a wide range of applications from operating reserves, voltage regulation and load following to contingency reserves. An important category of ancillary services is the operating reserves category which is closely related to the frequency stability of the system, and is also the main concern in the present study.

Operating reserves are the real power capabilities in a power system by which a grid operator maintain the balance between load and generation [55]. Although these services are implemented for different time scales and different purposes, they together keep the system frequency stable.

2.3.1 Grid Operating Reserves

The balance between power generation and consumption is a key factor in frequency control in a power system. If the generated power exceeds the demand, positive frequency deviation happens in the system, i.e. the frequency goes up. Similarly, negative frequency deviation happens when the generation is less than the demand [56]. Thus, several techniques in different time scales have been developed to maintain the power system frequency. The underlying feature of all these methods is to change supply and/or demand in a way that the balance is maintained.

The alteration of frequency deviations is traditionally implemented in three different time-scales [57]. Primary frequency control (PFC), is designed to respond to a frequency deviation in the fastest mode. This decentralized control mechanism is implemented through governors in the system. For this purpose, speed of the synchronous generator is used as the measure to detect frequency deviation and compensate the deviation locally in a feedback mechanism. Primary frequency control is not able to completely compensate a frequency deviation by itself. Secondary frequency control (SFC) mechanism, after the PFC, is in charge of what is so-called as steady state error. This mechanism is a centralized control scheme that is exerted into the system within minutes of a contingency. The tertiary frequency control (TFC) mechanism is mainly implemented in the system for optimal dispatch of generators, based on economical factors.

In a future power system, it is expected that the heterogeneity of resources for frequency control purposes will increase, especially by demand-side participation. For example, Mercier *et al.* reported a study on using energy storage systems for frequency control purposes in [58]. In addition to the conventional storage devices such as batteries, loads are also favorable for frequency control purposes. The magnitude of this participation ranges from residential buildings [59] to industrial loads [60].

There are five types of operational reserves: 1) frequency response reserves, 2) regulating reserves, 3) ramping reserves, 4) load following reserves, and 5) supplemental reserves. Time-scale characteristics of these resources are shown in Table 2.1. Note that spinning reserves must be synchronized to the system while non-spinning reserves are not necessarily synchronized.

In normal operating conditions, regulating and load following reserves are used for, respectively, random and non-random variations in the power flow. Load following reserves have a slower time scales as compared to regulating reserves. Frequency response reserves, a.k.a governor response, provide initial frequency response during a contingency, while supplemental reserves are used to replace faster responding reserves in longer contingencies. For the in

	Frequency Response Reserve	Regulating Reserve	Ramping Reserve	Load Following Reserve	Supplemental Reserve
Response Timescale	sec	sec	min-hrs	min	min-hrs
Spinning Reserve	Yes	Yes	Yes	Yes	Yes
Non-Spinning Reserve	No	No	Yes	Yes	Yes

Table 2.1: Operating Reserves Taxonomy

between, e.g. wind forecast error, ramping reserves are used.

2.3.2 Ancillary Services Taxonomy

In general ancillary services can be categorized according to the system level at which they are implemented; transmission-level or distribution-level [14]. At the transmission-level, ancillary services can be categorized based on their time-scale characteristic as follows:

- Very fast services: primary frequency control belongs to this category. The period over which the signals are expected to be zero-mean is about 5 minutes.
- Fast services: this time scale addresses the secondary frequency control (a.k.a. load frequency control). The period over which the signals are expected to be zero-mean is also 5 minutes with the time resolution of 1-10 seconds.
- Medium-speed services: a wide range of services can be categorized in this time-scale. Load following reserve is an example of the services that are categorized in this time-scale. Moreover, the time resolution of the signals are assumed to be in the order of minutes. It is observed that the signals are not zero-mean in practice.

At the distribution-level, two main time-scale characteristic are the fast and slow time scales. The former is mainly associated with voltage support, while the latter is more appropriate for peak shaving purposes.

2.4 Distributed Resources - Revealing a Hidden Potential

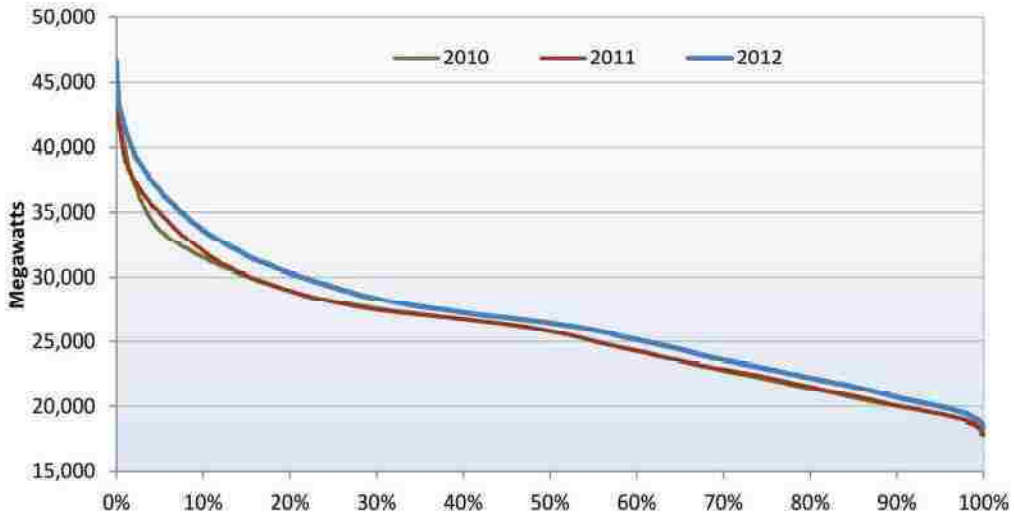

Figure 2.3: Load-duration curve of CAISO for 2010-2012. Soure:CAISO [3]

A major problem in a power system takes place during the peak. The capacity that is needed for peak-demand in a power system contributes to 10%-20% of the overall cost for just 100 hours during a year [55]. This is the direct result of demand-side inelastic behavior

in the system. In Fig.2.3 the load-duration curve of CAISO for the years 2010,2011 and 2012 is shown. A load duration curve illustrates the relation between generation capacity requirements and capacity utilization. The plot shows that a significant capacity is needed for just a small duration in a year.

Technological progress in the communication infrastructure as well as sensing technologies have provided an opportunity for developing new solutions in the power system operation and control paradigm, using distributed resources instead of conventional ones. Specifically, to replace capital-intensive reserve capacity with modern resources with less cost is of interest. In a modern paradigm, the essential flexibility for maintaining power system resiliency is partially transferred from the current fully supply-side contribution to the demand-side, decreasing the need for reserve generation as well as transmission capacity [61].

Demand-side resources are in general small in capacity. Thus, demand-side participation should happen through a coordination mechanism by which a collective capacity becomes available in an aggregated form. This collective capacity provides additional resources to be used in system services. It is also expected that this asset can contribute to increasing the share of renewable resources in the generation-mix. However, new coordination mechanisms may require a new system structure. This participation brings up several challenges including developing a coherent mechanism that can capture heterogeneous DERs small capacities with different characteristics.

In the previous section, various ancillary services were introduced. These services currently use conventional resources to fulfill a specific objective, such as maintaining system frequency stability. In a modern power system, on the other hand, these services could be implemented by utilizing not only the conventional resources, but also available DERs. Whether a distributed resource is appropriate for a special service or not depends on its characteristics. According to Oldewurtel *et al.* [14], these characteristics determine:

- the level of the service: whether a distributed resource can participate in a transmission-

level or a distribution-level service.

- the time-scale of the application: that can be characterized by the duration over which the control signal is expected to be zero-mean. If a distributed resource has the energy capacity is the major factor.

- accuracy level: in general this should be higher for ancillary services than that of market services. The level of accuracy that a distributed resource can provide differs. For example, the flexibility of a switching device in a standalone application is limited to two levels in its output power.

Several load types have the capacity to contribute to system services. The level of granularity of this control ranges from discontinuous switching to finer-grained control, such as set points on thermostatic devices for the former and dimmable lighting levels for the latter [62]. Plug-in electric vehicles (PEVs) are also among the resources envisioned to be used in future power systems [63, 64].

The focus of the present study is on dispatchable loads, storage devices and local fossil-fuel-based generation. A brief review of such dispatchable loads and electrical energy storage devices is brought in this section. Local fossil-fuel-based generation, such as a gas engine (GE) or a fuel cell, is considered as a scaled down version of large plants. Moreover, the focus is on using distributed resources in operating reserves rather than market services, as they address the stability of the system. Market services that enhance the efficiency of the system are beyond the scope of this study.

2.4.1 Battery Energy Storage Systems

Depending on its characteristics, a battery energy storage system (BESS) could have a wide range of applications in a power system from peak shaving to frequency control. In demand-supply balancing mechanism, a system operator may need to use reserve generation to fill

the gap between the load and scheduled generation during a day. The needed resources come with significant costs as compared to the bulk generation resources. The faster the compensation needs to be, a higher cost it comes with. This is mainly because that faster resources are more expensive than slower ones. For example in a peak shaving application, a system operator uses a storage capacity to defer a load in the system for a period of time, and thus to provide a window for necessary corrective actions.

Load deferral is in general an application in slow or medium speed category. Some types of BESSs are able to respond so quickly that they can be used for frequency control in the system. There is no doubt that this type of batteries is more expensive than the ones used for slower applications [65]. Application of BESSs are not limited to peak shaving and frequency control. Also, frequency control mechanism only becomes essential during a limited time in a year. Because batteries age even without being in use, there are methods that suggest using BESSs for multiple applications, and not to confine them to some specific services [66, 67]. A prioritizing mechanism that can manage utilizing BESSs, without compromising their primary tasks is of interest. These extensions to BESS tasks contribute to reducing the associated cost. Divya *et al.* in [68] and Hall *et al.* in [69] have independently provided a comprehensive review on the BESS applications.

The main difference between a battery as a storage device and a dispatchable load in ancillary services applications is that a dispatchable load typically has other primary task(s) to fulfill, and provides services as a complementary objective, while the main responsibility of a storage device is to store and deliver energy as directly needed in services. Also, in contrast to a dispatchable load, it is assumed that the reliability does not change with the level of aggregation in an BESS. An example of using battery in system level services, which requires an aggregated capacity of BESSs, is presented in [70] where the storage devices are in charge of mitigating fluctuations of wind farm output power fluctuations.

Characteristics of BESS

Despite their different technologies [71, 72], batteries come with relatively high implementation cost that limits their usage in power system services. A comprehensive review of various energy storage devices was provided by Beaudin *et al.* and Ibrahim *et al.* in [72] and [73], respectively. In both of these important research studies, a wide range of different storage technologies was discussed, including pumped hydro storage, compressed air energy storage, batteries, superconducting magnetic energy storage, hydrogen storage, flywheels, capacitors and super-capacitors. Batteries themselves include lead-acid batteries, nickel-cadmium batteries, sodium-sulfur batteries, lithium-ion batteries, zinc-bromine batteries and vanadium redox batteries.

Characteristics of storage devices determine whether a specific technology is appropriate to be used in a certain application. For example, in a peak-shaving application the energy capacity of the technology is the most important criterion, while in a power quality application, the ramping capacity is the most important player. Different technologies are associated with different characteristics, including implementation costs. Beaudin *et al.* in [72] have addressed this implementation cost. While acknowledging that the storage devices are expensive, they recognized the necessity for improving system's capacity to integrate power from renewable generation. Ibrahim *et al.* in [73] emphasized the importance of an optimization mechanism in order to incorporate different aspects of a storage system to derive implementable and cost benefit plans.

The main costs associated with batteries are the operating costs including the degradation cost. The term degradation refers to several phenomena that happen in a battery which results in a finite lifetime. In fact, degradation causes the internal resistance of a battery to increase and reduces its capacity. Regardless of the direction, the lifetime of a battery decreases as the power flows. It is hard to calculate the degradation cost as it is a nonlinear function of a set of variables including temperature, state-of-charge and charging/discharging

rate [74, 75].

Despite the recent technological progress in manufacturing lower-cost BESSs, the predicted cost per installed kWh is estimated to be around $335 [76] for the horizon of the year 2020 (based on the exchange rate of Euro and U.S. Dollar in the year 2016).

BESS and Power System Services

Due to their high implementation cost, BESSs are more appropriate for vary fast and fast ancillary services rather than medium-speed services. Consequently, they are inappropriate for market services which are in slower time-scales as compared to ancillary services. Based on their fast reaction time and high ramping capacity, BESSs are possible candidates for ancillary services, although they come with high implementation cost.

A technical challenge in utilizing BESS for current frequency control mechanisms is that it is not guaranteed that the signals to be zero-mean within a short time-frame, meaning that in the cases with small energy/power ratio, it is essential to develop methods that can compensate this problem [77, 78, 79]. The common practice in facing this issue is to only control the zero-mean portion of the deviations by the BESS, while the remainder of the signals are taken care of by other methods.

An example of utilizing BESSs is in mitigation of fluctuations associated with the power from low-voltage PV panels is reported by Demirok *et al.* in [80]. Due to high implementation cost of BESS technologies, an optimization procedure seems essential when using them in various services to make sure that operational cost of the system does not exceed benefits from better utilization of grid tariff structure. In addition to the single costumer level, there are applications for BESS at the distribution level [81, 82]. Battery energy storage systems are also able to provide system level services through an aggregation mechanism. This is mainly because of the scalability of this technology.

2.4.2 Dispatchable Loads - Thermal Mass and Hysteresis

Although the potential of demand-side participation in improving system reliability and performance is well recognized, only simple DR schemes so far have been used in this regard. In a simple DR program, loads are curtailed in favor of power system reliability, compromising end-users' quality of service (QoS) [47]. In current DR schemes, customers at different consumption scales are subject to the control actions exerted from a utility company or a third party acting on its behalf. As a result of such a program, a portion of the overall load of the costumer (non-critical) load is curtailed during a period of time. Demand response is a limited way for utilities to reduce the need for peak capacity investments by shedding some non-critical loads at peak times, and thus to keep rates lower.

In contrast to a simple DR program, there are dispatchable loads that can provide an opportunity to implement more flexible services. Dispatchable loads usually have a hysteresis property that can store energy. This stored energy can be used in a dispatching application. An example of such a load is heating, ventilation and air-conditioning (HVAC) system of a building. In the present study, the focus on two types of dispatchable loads with hysteresis property: thermal load of a building, and thermostatically controlled loads.

Thermal Load of Buildings

The thermal mass associated with the thermal load of a building acts as an energy storage device. This feature is because of the presence of the hysteresis property in this system. The stored energy in the thermal system of a building can then be used in power system services under the same principles as in the BESSs. However, it should be noted that the primary objective of the this type of resource, which is maintaining a healthy air condition in the building for residents, should not be compromised.

As an example, the thermal energy stored in a commercial building can be used in a power deferral application, or in general to shape the demand by shifting the load in time. This

shaping, however, can be performed without compromising residents' comfort. The buildings of interest range from campuses to warehouses. The size of these buildings play an important role as their energy consumption is multiple times more than a residential building. Moreover, larger-size buildings are usually equipped with a kind of automation system that controls the energy consumption of the building. Such an automation system facilitates implementing the control actions.

Characteristics of Thermal Load of Buildings:

The percentage that a thermal load contributes to the total load of a building depends on various factors including the type of the building, the occupancy and the geographical situation. Also, the share of this load that can be used in power system services depends on the defined comfort zone in each building. Thus, the power and energy capacities associated with the dispatchable thermal load of a building varies from one to another [83].

With respect to the ramping capacity, the design of the automated system in charge of the thermal load of a building plays a significant role in this characteristic. Also, the communication structure of the system has an important role in the ramping capacity of the buildings [84]. In general, the load shedding processes take from 1.5 to 30 minutes [85]. The same time window applies for a pre-cooling process.

Thermal Load of Buildings and Ancillary Services:

In this study, the focus is on the operating reserve applications, and not the market services. Regarding fast services at the system level, there are contradictory studies assessing if these devices are capable of participating in such services. Hao *et al.* showed a successful case in this regard [86], while Kiliccote *et al.* [87] showed the deficiency of thermal loads to be used in fast demand response schemes. For medium speed services, there are several studies addressing some pilot projects to integrate thermal load of buildings in non-spinning reserve services using open automated demand response communication protocol (openADR [88]) and via a price-driven mechanism [89].

For the distribution level, and in [90], the effectiveness of DR programs in peak shaving using commercial-size buildings has been assessed as a distribution grid support. In customer support services, commercial-size buildings can be used in two different ways: for peak reduction [91] and for load shifting [92, 93].

Thermostatically Controlled Loads

Example of thermostatically controlled loads (TCLs) include electric water heaters (EWHs), heat pumps, and refrigerators. Thermostatically controlled loads, similar to a building envelope, have thermal inertia that can be used in various services. Small temperature deviation does not affect user's comfort [94]. This potential can be released by adding a level of controllability to the device. The application can be implemented by changing the set point [95] or using the on/off switching mechanism [96]. The latter can provide the opportunity for non-disruptive control [97, 98] by limiting the modifications to the hysteresis dead-band.

Characteristics:

Thermostatically controlled loads have primary tasks that they should fulfill. Due to the small capacity of TCLs, an aggregation mechanism should provide a meaningful capacity for power system services [99]. Thus, the characteristics of this type of resource is based on the aggregation mechanism itself. Based on the control signal that acts on the devices and the decision making mechanism, there are different approaches for using TCLs.

Aligned with the framework of this research there are two types of implementation mechanisms. One is based on control signal, and the other one is based on a pricing signal. In the former framework, a control signal is sent to each individual device from an aggregator, which toggles the switch and not the set point. Depending on the decision making mechanism, there are two separate subsets in this framework; centralized decision making and decentralized decision making. In the centralized one, the signal that is provided by the aggregator is able to override the local switching pattern. In this mechanism, a feedback

control is needed to support the decisions at the aggregator level. Due to some problems in acquiring the state of the devices individually [100], state estimation mechanisms are used for this purpose [101]. In the decentralized decision making approach, utility or the third party in charge is not able to override local decisions. In other words, the utility tries to induce the consumers to take some actions in favor of the system reliability, for example via changing the tariffs [102].

There are also some methods that use pricing mechanism to implement control actions. In this method, however, the decisions are made just by local mechanisms and not centralized ones. This mechanism needs lower communication infrastructure, while lacking the feedback mechanism loop in a typical control signal approach [94, 103].

The power capacity of the aggregated devices depends on the power capacity of individual devices participating in a service. Several factors influence the energy capacity including the consumption pattern, bandwidth of each of the devices as well as the size of the appliance in which TCLs are installed. Methieu *et al.* in [104] have provided a good reference for the characteristics of different TCLs in a state-wise assessment in California. It should be noted that TCLs come with small capacities. However, it is possible to derive a significant controllable entity from such devices through an aggregation mechanism.

The other characteristic of this resource is the dead-time effect of some TCL devices. For example, in the case of a refrigerator, a compressor is not able to undergo two successive switchings unless it passes a certain amount of time, say 5 minutes for example. This feature, puts a limit on controllability of such resources.

TCLs and ancillary services:

The primary step in using TCLs is to develop a model to represent aggregated behavior of these resources [95, 105, 106, 107, 108]. The state estimation presented in [109, 108], moreover, reduces the size of the infrastructure needed for this purpose. Such a model then can be used in different control frameworks.

At the distribution level, remote control of air conditioners by the utilities in a switching mechanism is now implemented in California by Pacific Gas and Electric (PG&E) company [110]. This program provides a direct control opportunity for PG&E over cooling loads of buildings. As an incentive, PG&E compensates the clients that participate in this program. This participation occurs through control devices that are installed in AC units [110]. There are also some applications for distributed TCLs, for example to support PV in small scales in a load-shift application [111].

2.5 Microgrids - Building Blocks of A Modern Power System

In the future, distribution systems are likely to play two major roles; delivering power to or among customers and aggregating DERs. The importance of the interconnection between DERs to be utilized in power system reliability services has been addressed in numerous studies [112]. However, the architecture of such an integration is not fully determined yet. Such an architecture should incorporate both DERs and intermittent renewable resources.

Due to the intermittent nature of renewable resources, it is hard to directly integrate these resources into the grid. In general, there are two approaches for such an integration: centralized [113] versus decentralized [114]. The centralized architecture has the advantage of highly reliable implementation as it is directly connected to a specific control center. The disadvantage of this approach, however, is that the communication infrastructure needed for this purpose is cost intensive. Also, there is a potential fragility with a centralized structure as it is highly dependent on the communication infrastructure. Once the communication system fails, the system loses its control over resources.

Regardless of the implementation fashion, the fundamental requirement for an integration architecture is that distributed resources operate in parallel with the utility at all times and

supply sensitive loads [115].

One of the proposed architectures is VPP [116] which was developed to enhance control over household appliances for the system operators. Another architecture in this direction is microgrid. A microgrid is a cluster of interconnected distributed generators, loads, and intermediate storage units that cooperate with each other to be collectively treated by the utility grid as a controllable load or generator [117].

The integration at the distribution level and in the form of a microgrid would have advantages at both the transmission level and the distribution level [118]. Microgrids provide the opportunity to indirectly integrate renewable resources into the grid through a combination of facilities like storage devices [119] as well as supervisory control and dispatchable loads [120]. Also, a microgrid maintains its internal stability by implementing control actions exerted by the associated MGCC [121, 122, 123].

The control hierarchy associated with a microgrid that is connected to a power system is in charge of several tasks including participating in energy markets, provision of ancillary services and load sharing among DERs. This hierarchical structure has several layers as stated by Katiraei *et al.* in [124]:

- Grid level: where coordination of several microgrids at the distribution level is happening. A Microgrid central controller (MGCC) provides the interface for the interactions between a microgrid and a distribution system operator (DSO) or possibly among microgrids. The MGCC is in charge of the microgrid's internal performance and reliability issues.

- MGCC: is in charge of reliability of the microgrid, including restoration control as well as load management and production management.

- Field level: At this level, internal controllers of the facilities are implemented. For example, internal controllers for building heating and cooling system.

Via this architecture, it is possible to implement several applications for the benefit of both the power system and end-use stakeholders [125]. From the consumers point of view, energy security is provided, and from the utility company point of view, a microgrid-based structure promises to relieve existing power system from current levels of stress [126]. For example, MGCC can communicate with the loads and directs them to isolate from the grid in real time to reduce overall demand load on the system in peak-load hours [127]. At a higher level, long-term sustainability and reduced green house gas emissions are among the contributions of a modern power system to the society's concerns.

As well as the architecture and engineering perspective, the mechanism by which this implementation can be implemented is a concern. Flexibility, though often hard to define, is an important characteristic that needs incentives to become active when needed. According to Chassin *et al.* [128], real-time pricing (RTP) technologies will be a central component in a future so-called "smart grid". In this approach, the reliability of the system and the design of the market are closely tied. System operators, planners, and reliability regulators cannot make changes to its mechanisms to meet reliability without some recognition of how the electricity market is designed. Likewise, market designers cannot create new or modified designs without recognizing the reliability needs of the system [129].

There are four levels in control strategies that may exist in a smart grid [128].

- Passive: This level of control is the implemented strategy of the current power system control paradigm.
- Active: In this level, there are two factors that determine consumers' behavior. A real-time price signal that is sent from the utility (or an aggregator) to the end-user and the set-point of a device that is determined by the consumer. In this approach, a passive controller receives a price signal and provides this information to the end-user to adjust the behavior, e.g. by changing the set-point.
- Interactive: This method is similar to the *active* method, except that there is a feedback

mechanism that provides information to the utility company (or aggregator) so that it can adjust the pricing signal for deriving its desired behavior from the consumers.

- Transactive: This method is the highest level of control in this taxonomy, in which the passive controllers in the *active* and *interactive* methods are replaced by interactive controllers. These interactive controllers that act as agents on behalf of the consumers, then, exchange information with the utility company (or aggregator) automatically to alter the behavior and price and settle in a stable condition.

2.6 Model Predictive Control - Optimal Actions in Uncertainty

Due to the physical constraints of DERs, it seems inevitable to use optimization techniques to leverage them for various services applications [130, 131]. Among optimization frameworks, model predictive control has gained interest in dealing with the problem based on the variations associated with the players. For example Su *et al.* in [132] used the MPC framework because of the uncertainty parameters associated with plug-in electric vehicles (PEVs) including charging time and initial battery state-of-charge to minimize the operational cost. In the case of using PEVs, Zhang *et al.* [133] have reported another study with an MPC application to provide a power buffer.

In DERs integration applications discussed earlier in this chapter, and regardless of the architecture and the scale of the problem, some form of energy storage devices play an important role to justify the MPC framework. For example, Ma *et al.* in [92], used MPC as the optimization framework to control the operation of building cooling system equipped with a cold water tank. Using forecasts on building load and weather conditions, then, an MPC was in charge of optimal thermal energy storage in the tank by taking a hybrid dynamical model approach. The objective function to be minimized in the study was the

electricity bill.

Model predictive control has also applications in grid operations. In [134], a case study of a demand response scheme was presented. In that case, the objective was to minimize the cost associated with using an electric space heating in the presence of partial thermal storage in a linear programming application. The proposed control is optimized according to dynamic prices, shifting the power demand from peak price periods to the cheapest hours.

An important application of MPC in DERs integration schemes is in the frequency control problem. Galus *et al.* used MPC approach for a set of CHPs, PEVs and thermal load of buildings gathered in a cluster (without well defined boundaries like a microgrid) to support frequency control in the grid [135]. In another study on the frequency control Vrettos *et al.* [136], assessed a novel hierarchical control algorithm to enable simultaneous participation of aggregations of TCLs in power system frequency control. The study was based on active distribution network management in order to increase the integration of intermittent renewable resources. The studied platform was based on a two-way communication infrastructure and was consisting of two phases: day-ahead scheduling and real-time operation. The main objective of the study was to maximize share of renewable resources in the system. The study was closely related to another study in the same group for the case of operation of a building [137].

Model predictive control provides a unique opportunity to address several issues within a single framework. These issues include optimal operation of various devices as well as stability requirements. In addition, with improved load and generation forecasting, and the introduction of local control and coordination algorithms, DERs could easily provide timely services to the grid and could be integrated into the current power grid. At the same time, these technologies will facilitate the long-term transformation to a future grid that leverages all assets, regardless of their placement at the distribution or transmission level.

2.7 Microgrids and System of Systems Structure

A microgrid based structure for a power system has some characteristics in common with an SoS architecture. First of all, as a microgrid is able to work independently from the grid, the operational independence is served. However, this independence comes with scarification of the full service. To some extent, the marginal independence is also maintained in a microgrid structure. As microgrids are distributed over the power network, the geographic distribution is served. Although microgrids can exchange information, they can also exchange energy among themselves in the future. Also, microgrids are able to adopt new functionalities, objectives and configuration.

The only feature that distinguishes a microgrid-based structure form an SoS structure is the emergent behavior of subsystems. Specifically, microgrids are implemented in a hierarchical fashion. Thus, their collective behavior is controlled and not emergent from their independent operation.

Chapter 3

Characterizing Aggregated Response of TCLs at the Distribution Level

The shift from the current inelastic load condition to a partially elastic one requires augmenting loads with an appropriate control mechanism. Once augmented with a control mechanism, a load could turn into a dispatchable asset that can be deployed in power system services that maintain the reliability of the system. Specifically, dispatchable loads can reduce the need for conventional storage devices. For thermostatically controlled loads (TCLs), there are two main control platforms that have received interest to make such resources controllable: 1) real-time pricing and 2) direct control.

In a real-time pricing scheme, a central controller sends a price signal to each individual device, based on which a decision is made at the device level and the behavior of a TCL is altered. In the direct control scheme, a control signal is sent from a central controller to the device. The decision in this case is made at the central controller level, and is implemented via a communication infrastructure. The communication channel typically is bidirectional to provide devices' state information for the central controller[1]. The costs associated with

[1]Mathieu *et al.* have studied state estimation techniques to reduce the dependency on the communication infrastructure [109].

this approach includes the device cost, implementation cost as well as the costs associated with the communication infrastructure.

For the situations that these two platforms are not implementable, for example due to regulatory rules or the cost of communication infrastructure, a platform is proposed by which TCLs can become partially controllable. However, the main contribution of this chapter is where a novel framework is provided to determine the time-scale of the applications that TCLs can be used in. As a special case, the proposed platform is examined. The framework, however, is not confined to the proposed platform, and can be used for other control schemes such as price-based mechanisms as well.

3.1 Problem Definition

Among all possible types of load, TCLs have received significant attention for use in demand-side participation programs based on their thermal inertia and power capacity.

The hysteresis property of thermostatic devices provides an opportunity to store energy within a physical boundary. For example, a refrigerator keeps the temperature of its internal space within the specified dead-band for a while after being disconnected from the electricity resource. During this time, the internal temperature of the appliance increases, that can be translated into a depletion mechanism for a storage device. The stored energy in TCLs, similar to any storage device, has a potential to participate in power system services [104]. However, the platform that releases such a potential may be different from a conventional storage device.

In addition to the hysteresis-driven energy capacity, TCLs are typically associated with considerable power capacity. Cooling loads, for example, contribute 13% of the average load of a commercial-size building in the U.S. [138], and can even reach 40% on a hot summer day [139]. Two plots in Fig. 3.1 correspond respectively to the cooling load of a single residential

building and the aggregated cooling load of 1000 similar scale buildings. As shown, a single TCL has a step-wise load pattern due to its switching nature. The aggregation of such loads, on the other hand, shows a continuous load profile from a distant as long as their are working independent from each other. The aggregated load shows a significant and, to some extent, a continuous behavior that potentially can be used in replacing conventional resources.

A control platform is aimed to make a coordination among a big number of TCLs in order to provide a useful capacity as a reserve. Regardless of the type of platform, it is implemented at two levels; at the central coordinator level and at the device level. The central coordinator uses either a real-time pricing mechanism to make the coordination happen [94] or a direct control approach [109]. In the former approach, the central mechanism is combined with local/decentralized decision making at the device level, while in the latter the decisions are made at the central controller level that it enforces devices to undergo a control action [109]. No matter if made locally or at a higher level, decisions at the device level are applied through either 1) adjusting the set point of a TCL or 2) a simple on/off switching mechanism.

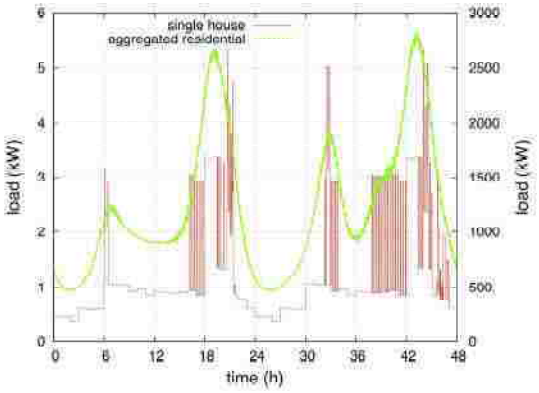

Figure 3.1: Simulated cooling loads of residential buildings in two forms: single vs. aggregated for a 48 hours period

However, it is possible that the two mentioned platforms would not be implementable; local regulatory may prohibit a real-time pricing mechanism or the communication infrastructure for implementing a direct control would not be available[2]. For such cases a platform is proposed that does not come with the implementation problems associated with the current standard approaches. The proposed platform in this chapter has constituents at both the

[2]It should be noted that there are also fully distributed control mechanisms that are beyond the scope of this research.

central coordinator and device levels, similar to common studied platforms so far. At the central controller level, a gain-scheduling approach is used to design a control signal. At the device level, the platform is based on using a ramp rate control mechanism combined with the inherent switching of a TCL. The control signal sent from the central coordinator in collaboration with the local ramp rate decision making mechanism causes the overall system to modify its collective behavior.

Moreover, one of the key features that many of the studies have not (At least directly) addressed so far is the switching dead-time of thermostatic loads. Dead-time in a thermostatic device refers to the period of time that a TCL (such as a refrigerator or a building cooling system) takes before undergoing the next switching action due to its mechanical constraints. This feature places a barrier to implementation of a desired behavior from the system, as TCL does not respond to any control action before passing the dead-time.

Dead-time issue as well as implementation barriers associated with the current control mechanisms are addressed in this chapter by a new proposed platform. However, the main contribution lies where a novel framework is suggested to determine the time-scale of the services that such a platform can be used in. This framework is not limited to the proposed platform and can be used for other schemes as well, including the real-time pricing and direct control mechanisms.

For the mentioned purposes, it is first necessary to model the system of TCLs in a simple yet accurate way that can be used for control objectives. There are also several studies that have addressed technical benefits of treating distributed TCLs located in residential buildings, e.g. at the scale of a distribution feeder, in an aggregated form rather than individually [105, 140, 141]. The study conducted in this chapter is aligned with such an aggregation approach.

At the final step after modeling the aggregated system and designing a control platform, the time-scale of the power system services that TCLs under the introduced platform can

participate in is derived in this chapter through a novel framework. The aggregated behavior of devices is modeled as a large BESS. Also, a metric is introduced to determine how fast these devices can act and how much power they can contribute to various services.

3.2 Modeling - Single TCL as the Building Block

A well-known dynamical model for describing behavior of a single TCL in discrete-time domain is described by eq. 3.1. This simple model is accurate enough, yet comes with smaller computational costs in comparison with continuous-time models [142]:

$$T(t+1) = aT(t) + (1-a)(T_a(t) - T_g m(t)), \tag{3.1}$$

where $a = 1 - \frac{1}{\tau}$. The parameter τ is the time constant of the system in which the thermostatic device is placed. In this model, $T(t)$ and $T_a(t)$ are the device and the ambient temperatures, respectively, while T_g represents the thermostat gain. Thermostat gain corresponds to power consumption when the device is *on*. Finally, $m(t)$ is the state of the thermostat. Here, $m(t) = 0$ when the device is *off*, and $m(t) = 1$ otherwise. In this study, the ambient temperature is assumed constant, i.e. $T_a(t) = T_a$ as its rate of change is negligible in comparison with the time-scale of control actions and the dynamics of the device.

The case study, here, is at a distribution feeder scale, meaning that the central controller is placed at the point of common coupling (PCC) of a feeder to the transmission network. An aggregation of 1000 residential-size building HVAC units, as the most significant TCL-type single contributor to the residential power demand is considered. Their set points are uniformly distributed over $[22.5,\ 23.5]^{\circ}$C with a 3°C dead-band. Switching dead-times are equally 5 minutes. Finally, the parameter τ is uniformly distributed over $[1000, 1400]$ seconds, meaning that it takes around 14 minutes on average for the thermostatic devices to get to their lower temperature bands from the corresponding upper ones in a condition that the ambient temperature is 36°C.

3.3 Control Platform

Real-time control actions by pricing mechanisms are prevented by local regulations in many situations. Instead, a possible agreement between the utility company and the end-users is assumed here for implementing a probabilistic control mechanism. This scheme is an indirect control approach. At the controller level, the utility (or a third party) sends a signal which represents the desired collective behavior of the aggregation of TCLs from the central controller view. This signal is received by smart control units installed at the device level. In the absence of dead-time constraint, each smart control unit generates a random number from a uniform distribution function. If the generated number is less than the one reflected in the received reference signal, the device will switch its operating status from on to off or vice versa [143, 108]. For example, if the referred value by the control signal is 0.2, then it is expected that 20% of the overall addressed devices, on average, switch their operating state by the end of the time step.

At the device level a ramp rate control approach is combined with the switching mechanism of the device for executing control actions. Ramp rate, by definition, is the time derivative of power. In this platform, the end-users are responsible to react to the reflected *changes* in the reference signal. In other words, the unit continues its normal operation until it captures a change in the received signal. In Fig. 3.2 a general schematic version of the control policy that turns a portion of the devices on is shown. In this figure, the reference signal $u(t)$ represents the normalized desired behavior that the central controller expect to see from the aggregated loads. Thus, $1-u(t)$ is the portion of the devices that is expected to be off. The resultant gain g_{on} then is:

$$g_{\text{on}} = \frac{u_2 - u_1}{1 - u_1} \tag{3.2}$$

In a similar way it can be shown that the following equation holds for switching a portion

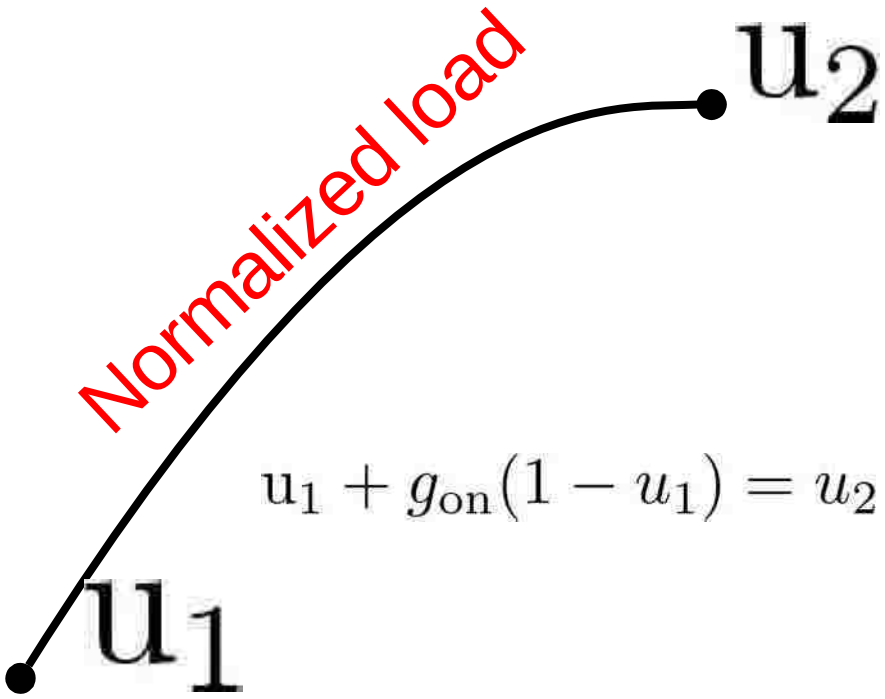

Figure 3.2: Switching on mechanism for the platform of interest. The gain scheduling mechanism is derived from the shown equation based on the received signal $u(t)$.

of the devices off:

$$g_{\text{off}} = -\frac{u_2 - u_1}{u_1}. \tag{3.3}$$

Now that the central controller is assumed to send a continuous signal $u(t)$ to devices, and based on a fine enough 1 second time resolution assumed for signal updates, the following approximations for g_{on} and g_{off} can be made as follows:

$$g_{\text{on}}(t) = \frac{u(t) - u(t-1)}{1 - u(t-1)}, \tag{3.4}$$

$$g_{\text{off}}(t) = -\frac{u(t) - u(t-1)}{u(t-1)}, \tag{3.5}$$

at discretized time step t. Note that the gain scheduling policies g_{on} and g_{off} are derived by neglecting the dead-time effect. Although an open-loop control is considered here, moreover, there is always a room for designing a closed-loop control system.

3.4 Dead-Time Effect and Availability of TCLs For Exerting Control Actions

One of the main physical limitations of TCLs to participate in a load management program is the switching dead-time of thermostatic devices. Because of this physical constraint, it is not possible to drive a fast desired behavior from TCLs either in single or aggregated modes with the associated full capacity. Here, this parameter is assumed to be 5 minutes equally for all TCLs. In Fig. 3.3 the time distribution of the state of 1000 TCLs at an arbitrary time instant is shown, depicting the introduced dead-time as well. In this plot, each bin represents 10 seconds time interval and the number of devices in each time interval is also shown, categorized by the state if on or off. Based on this plot, a considerable portion of thermostatic devices cannot undergo any switching action because of the dead-time constraint.

The temperature distribution of the unperturbed system in shown in Fig. 3.4 for two scenarios. The first plot shows the state of the devices that are already *off*, and if ready to turn *on*. The available devices for switching are those that have been in their current state longer than the dead-time, depicted by red-ish colors. Those that are shown with the blue-ish colors are the devices that have not passed their dead-time yet. As expected, the lower half is more populated with the devices that have lower temperatures, while the upper half is more populated with those that are close to their upper temperature band. The second plot in the same figure shows the availability of devices for switching *off* according to their temperature and last switching. Colors can be interpreted in the same way as in the first

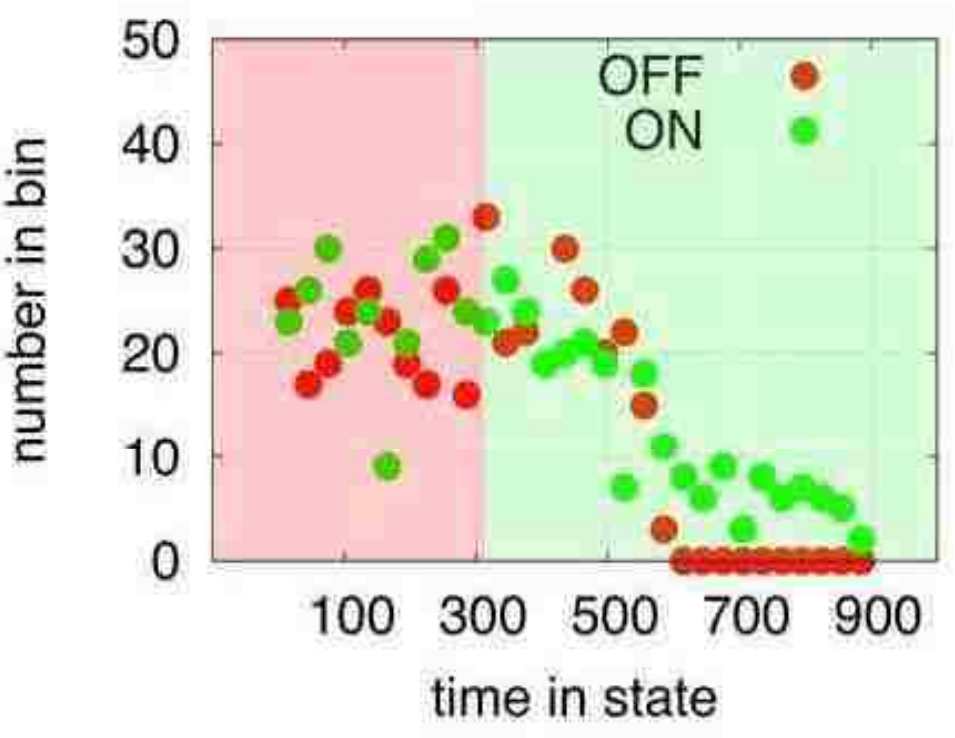

Figure 3.3: Distribution of 1000 TCLs state in time. Each bin represents 10 seconds and the number of devices in each bin is shown on the y-axis.

plot.

The discussed dead-time effect in this section puts a barrier to simply derive a desired behavior from the population of TCLs by the eqs. 3.4 and 3.5.

3.5 Characteristics of A Population of TCLs

As mentioned in section 3.1, hysteresis-driven loads can be considered as storage devices, once become controllable. As compared to a BESS, a TCL is in its charging cycle when it is *on* and is reducing its surrounding space temperature. Upon reaching the lower temperature

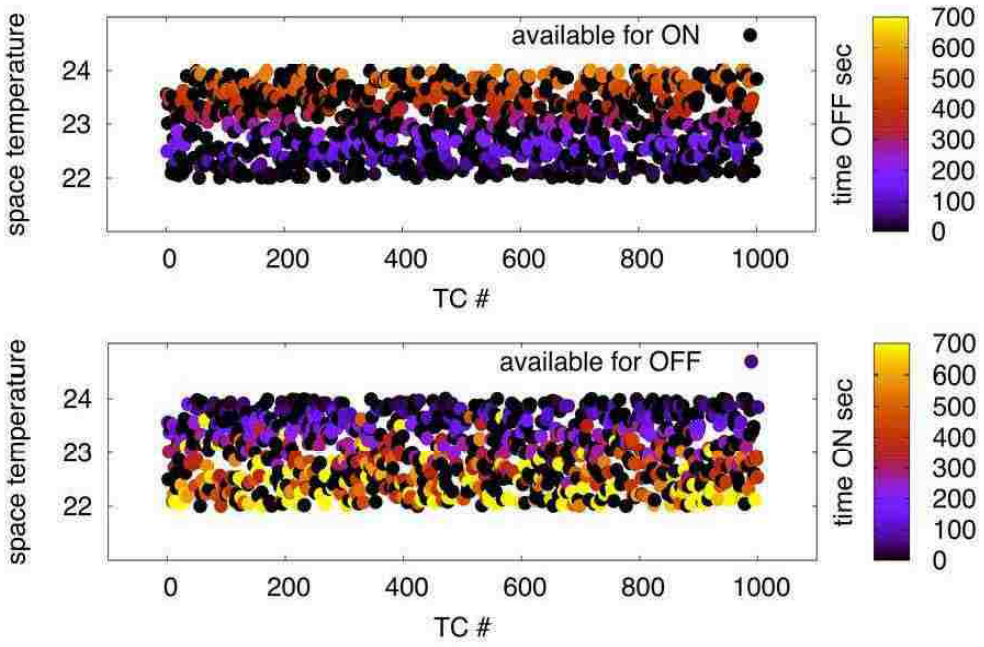

Figure 3.4: The distribution of temperatures of the unperturbed system according to availability for switching 1) ON (upper plot) and 2) OFF (bottom plot)

band, the cooling cycle stops and the temperature starts increasing again. This new cycle can be interpreted as a discharging cycle as it is depleting the stored energy. By this approach, it is possible to model a population of aggregated TCLs as a single BESS. A comparison with a conventional BESS is made here to characterize such a storage capacity. Specifically, the objective is to determine the time-scale of the power system services that the platform introduced in section 3.3 can contribute to. For this purpose, the aggregated behavior of a population of TCLs is investigated and compared to a BESS. The comparison is made in the frequency-domain.

3.5.1 Characteristics of a BESS

Regardless of the power capacity which is normalized in this study, two important characteristics of a BESS are: 1) maximum ramp rate and 2) energy capacity. These two characteristics are illustrated in Fig. 3.5 for a typical lead-acid battery. In the shown plots, the upper halves of the sinusoidal signals show the charging cycles, while the lower halves are associated with the discharging cycles. The energy capacity, thus, is proportional to the area under the charging cycle. Three scenarios for charging/discharging are examined by sinusoidal signals that are respectively 1) too fast, 2) well-matched and 3) too slow for the battery to follow. In the first and last scenarios, the battery is not able to exactly track the input signal based on its maximum ramp rate and energy capacity respectively, while in the second scenario the BESS is able to perfectly follow the sinusoidal command signal.

To characterize the behavior of an ideal storage device a tracking ratio is introduced. This ratio is derived from dividing the area under the absolute value of the output signal by the one corresponding to the input command signal. Then, this ratio is calculated at various frequencies as shown in Fig. 3.6 for the case of a lead-acid battery. Followed by the plots of Fig. 3.5, it is expected that the BESS follows a sinusoidal command signal perfectly in a middle frequency range. The boundary of the frequency band of interest is determined by the associated energy capacity and the ramping capacity. The former characteristic determines the lower bound of the frequency band, while the latter one specifies the upper counterpart.

In the case of TCLs, the introduced characteristics are affected by the switching dead-time feature. These characteristics are, then, compared with the one associated with a battery as follows:

Energy capacity: In Fig. 3.7, a snapshot of temperature distribution of an affected population of TCLs by a low frequency sinusoidal command signal in the middle of a charging cycle is shown. As the period of the command signal is long, a considerable portion of devices

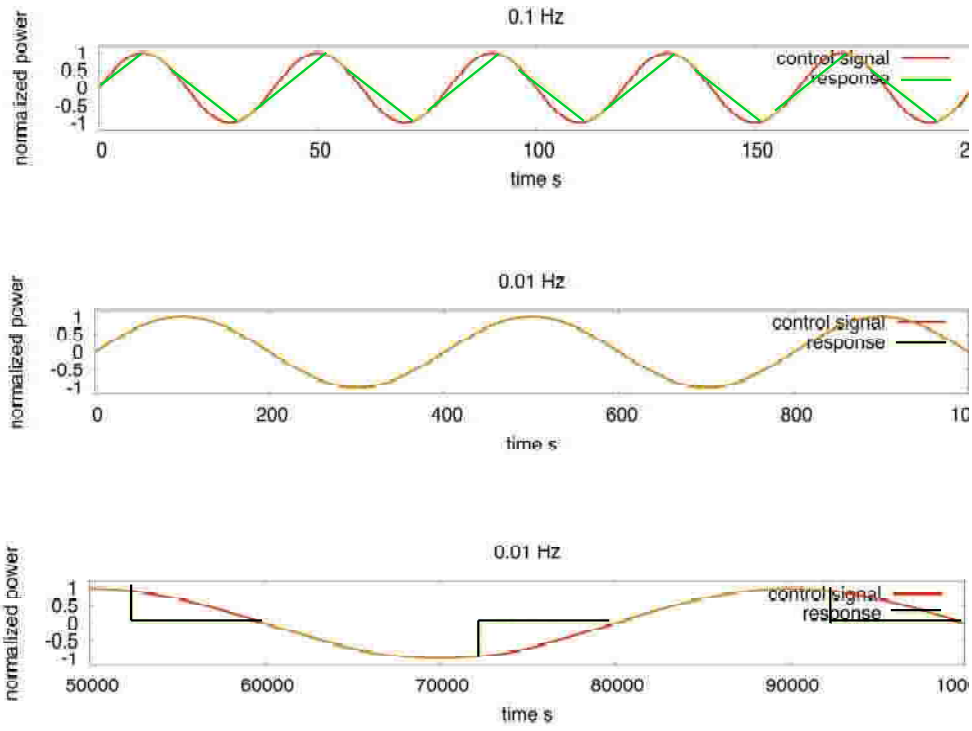

Figure 3.5: Maximum ramp rate and energy capacity of a battery. The upper figure illustrates the ramp rate limit of a battery as it cannot track a high frequency signal. The bottom figure shows energy storage capacity of the device as it stops charging in the middle of the cycle. The one in the middle corresponds to the case where the sinusoidal signal does not violate the ramp rate capacity, nor the energy capacity.

have become *on* and are ready to turn off. Vice versa, those that are off are pretty much young and are not available for exerting control actions on them. The collective behavior is showing the energy capacity associated with the population of TCLs in an aggregated way.

Maximum ramp rate: Ramp rate capacity of a storage device reflects the fact that changes do not happen immediately. A snapshot of the temperature distribution of affected TCLs is shown in Fig. (3.8) at the end of a fast charging cycle. As illustrated, there is a considerable number of devices that are ready to switch but have not been used. Also, a considerable

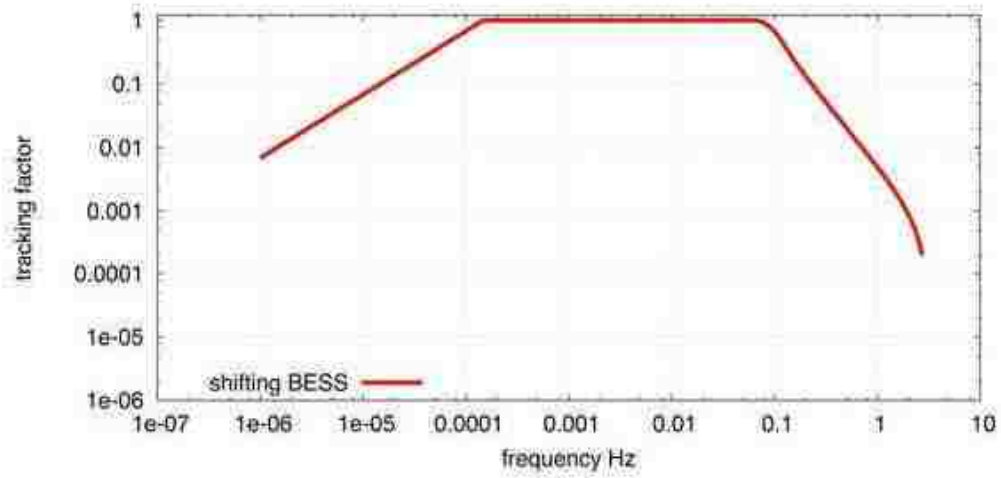

Figure 3.6: The frequency response of a lead-acid battery against sinusoidal input signals with various frequencies.

portion of the devices are not able to undergo a control action as they have not passed their dead-time from their previous switching; this figure addresses the effect of dead-time on the maximum ramp rate of the aggregated devices as well.

3.5.2 Reference Signal and Error Definition

In the previous subsection, it was described how (normalized) sinusoidal reference signals with different frequencies can reveal two important characteristics of a storage device. The same methodology can be applied in the case of TCLs; the aggregated behavior of TCLs against a single frequency sinusoidal signal should be investigated. As introduced in the pro-

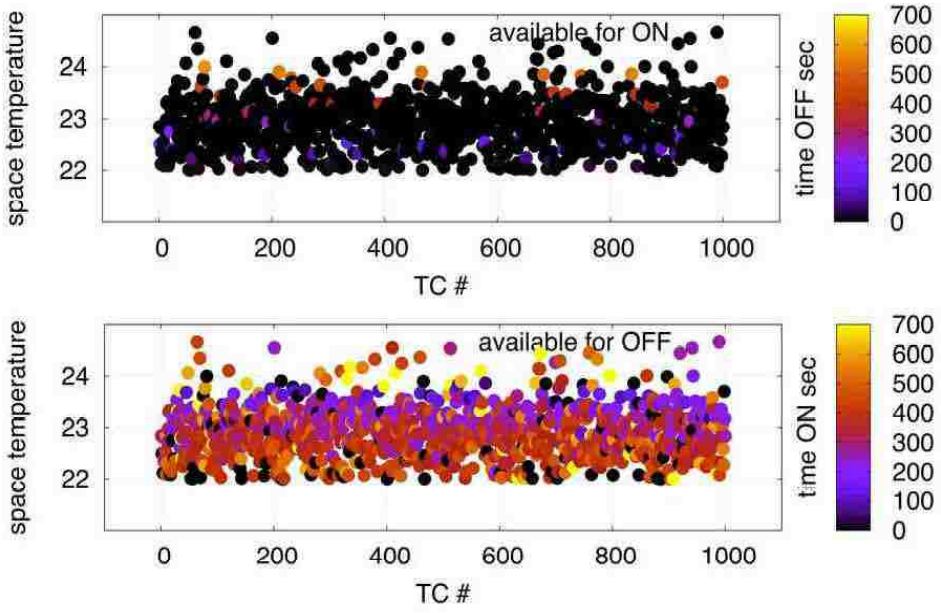

Figure 3.7: A snapshot of the temperature distribution in the middle of the charging cycle. The target devices have almost reached their energy capacity in the middle of the charging cycle.

posed platform, this signal is sent from the central controller and represents the normalized desired collective behavior of the system. Each individual device captures the changes in this reference signal and respond based on the discussed probabilistic mechanism, governed by eqs. 3.4 and 3.5. Consider a single frequency sinusoidal signal

$$p(t) = \frac{1}{2} + \frac{1}{2}\sin(\omega t), \tag{3.6}$$

that changes between 0 and 1 as a normalized behavior with the frequency $f = \frac{\omega}{2\pi}$. Based on the discussed physical constraints, there will be a mismatch between the input and the (normalized) collective response of the system. The output of the system for the case of $f = \frac{1}{500}$Hz signal is shown in Fig. 3.9.

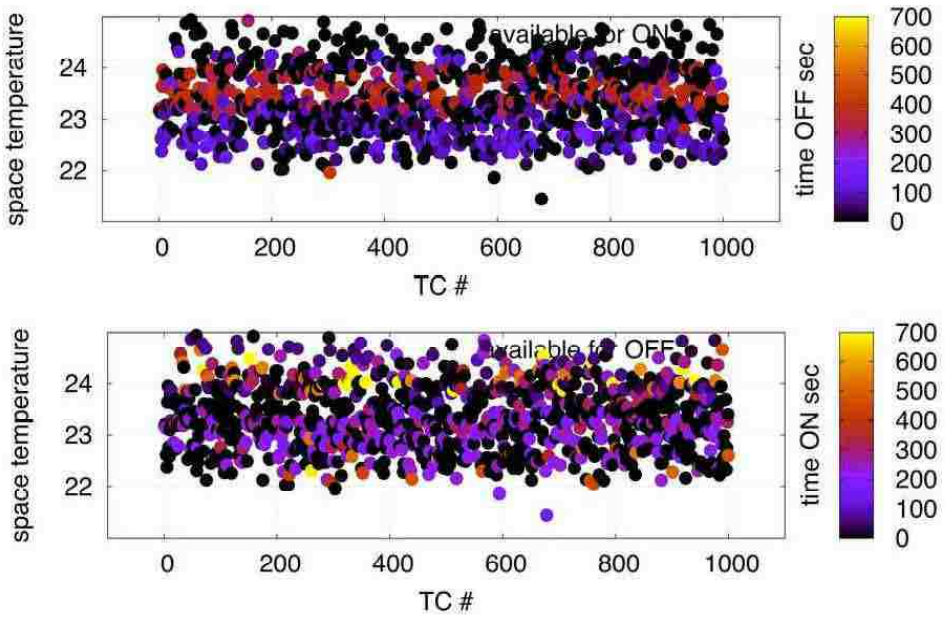

Figure 3.8: A snapshot of the temperature distribution at the end of a fast charging cycle. A considerable portion of the devices are not used, while another large portion have not passed their dead-time from their previous switching. The dead-time effect thus, limits the maximum ramp rate of the collective capacity.

The error term is also illustrated in this figure. The shaded area represents the error of the tracking for one cycle. This error is normalized by the total area under one cycle of the absolute input signal when the mean-value is removed. This division generates a normalized error corresponding to a specific frequency. As shown in Fig. 3.10, in the absence of switching dead-time, the system can better track the command signal, meaning that the tracking ratio is highly affected by the switching dead-time feature of TCLs.

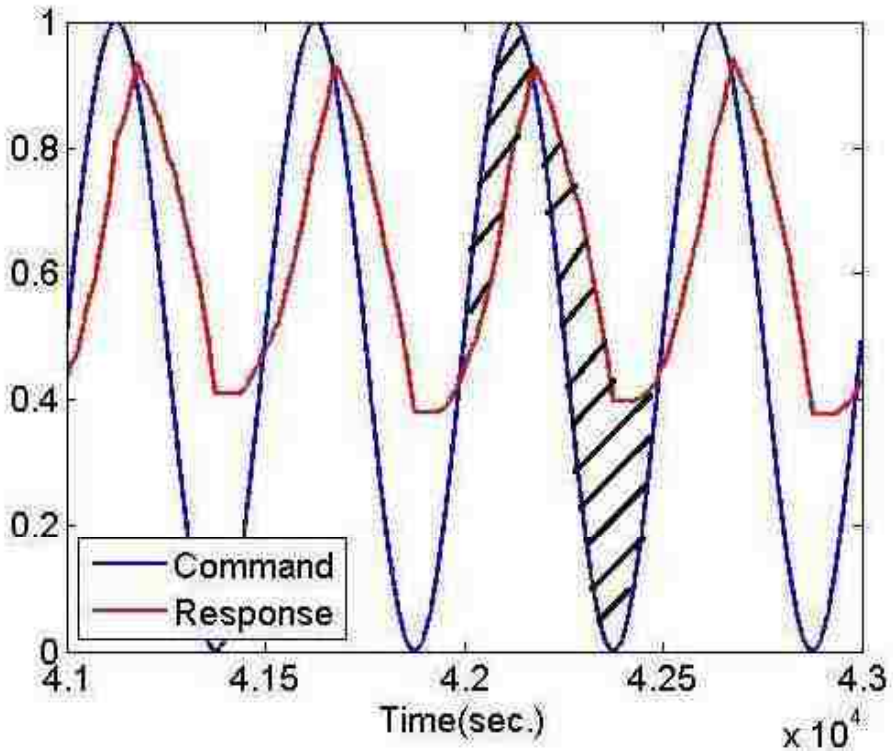

Figure 3.9: The ability of a population of TCLs to collectively track a sinusoidal reference signal is affected by the dead-time feature of such devices. The command signal in this case is too fast for the system to track. The shaded area depicts the error.

3.6 Frequency Response and Time-Scale Characterization of Power System Services

The collective behavior of a population of TCLs for a range of different frequencies is evaluated, akin to what was seen in the case of a BESS; for each case the tracking ratio is calculated and the results are plotted against corresponding frequencies. Three plots are shown in Fig. 3.11. The blue plot depicts the behavior of the system against various frequencies characterized by the tracking ratio which is derived by subtraction of the defined error metric from 1.

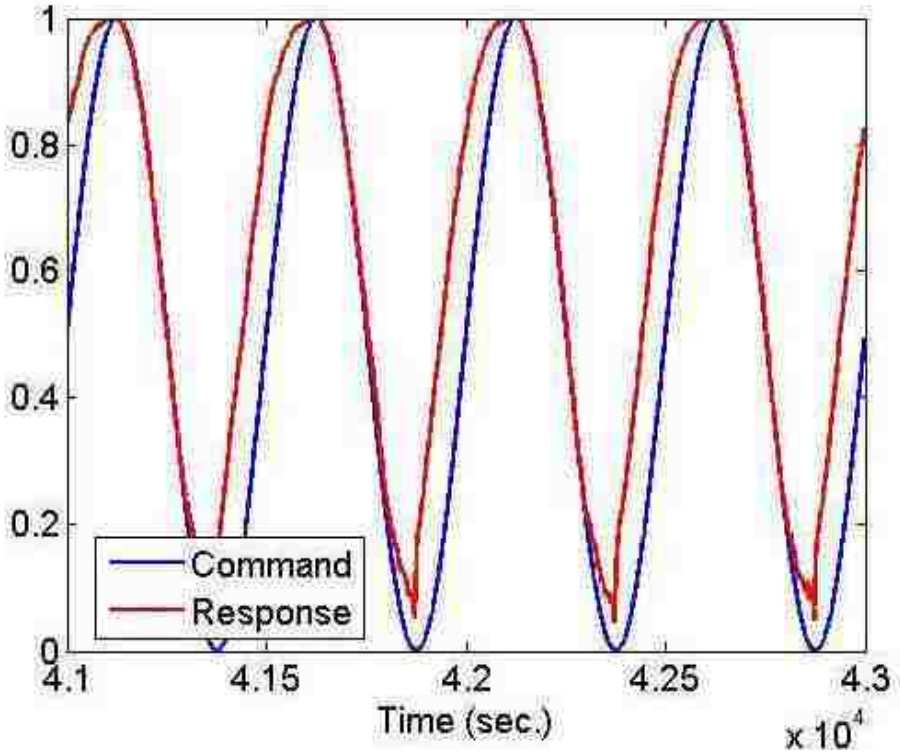

Figure 3.10: In the absence of switching dead-time, the system tracks the command signal better as compared to the presence of such a feature.

The other two curves shown in green and red depict the reliable areas for load shaping purposes. It was shown in Fig. 3.9 that a population of TCLs has a limited capacity to follow a sinusoidal command signal. Specially, the amplitude of the collective response is less than that of the input command signal. Thus, the aggregated system can better follow a limited input signal which translated into a fraction of the net power capacity. In other words, the depicted two curves by red and green represent equivalent capacity associated with TCLs in the form of an ideal battery. With the green plot scenario, a load management system can use roughly 1/3 of the total power capacity of existing loads, while in the scenario of the red curve, 1/2 of the total power capacity can be taken into account. If assumed that each single load is associated with 300 Watts power consumption, the green scenario represents a

battery with 100 KW power capacity, while the red one represents 150 KW power capacity. This increase comes with the cost of a smaller frequency band.

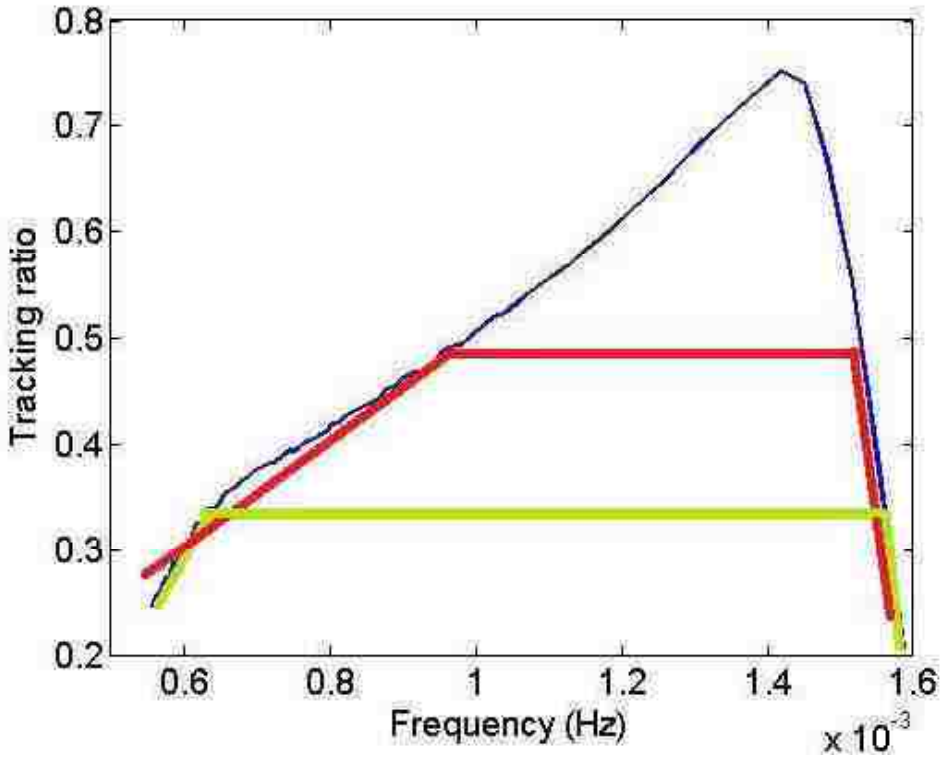

Figure 3.11: The frequency response of the system of aggregated TCLs versus sinusoidal input signals with various frequencies.

The specified frequency bands in each case determines the time-scale of the power system services in which the proposed platform can participate. For example in the situation that is shown by the red curve, the energy management system can rely on the collective capacity of TCLs for services in the time-scale from 11 to 20 minutes. In the green curve scenario, the associated time-scale is from 10 to 30 minutes. This time-scale is mainly resulted from the dead-time property of TCLs. It should be noted that this level of reliability is not just addressing a power curtailment application (which typically comes with a rebound after

removing the control signal), but also any plausible load shaping that can be translated into charging and discharging cycles with appropriate frequencies.

3.7 Discussion and Conclusions

In this chapter, a platform was proposed for enhancing controllability of TCLs in an aggregated form in the cases that not a direct control nor a pricing mechanism were viable. The platform essentially was consisted of a control signal sent from a utility company (or a third party on behalf) combined with a local decision making mechanism. This enhanced level of controllability would play an important role in system services of emerging power networks.

The implementation cost of such a platform would not be high in the sense that the communication infrastructure is almost available everywhere, besides that the control signals only need a unidirectional channel. Also it was considered that the state of the devices are not available, which circumvents probable costs and complications associated with using such an information. Although, there would be a room to implement a feedback mechanism to enhance the system performance.

Finally, a novel framework was proposed for evaluating the power network in which such a participation can take place. This framework, however, is not confined to the proposed platform and can be applied to other platforms such as direct control and price-driven applications as well.

The results also showed that the switching dead-time affects both the time-scale of the power network in which TCLs (in an aggregated form) can be used for system services as well as their power capacity for load shaping purposes in the proposed platform.

Chapter 4

Stable Integration of DERs In A Distribution Feeder Microgird

The ability of distribution feeder microgrids to operate as a controllable entity from a utility point of view is assessed in this chapter. The concept of distribution feeder microgrid is introduced, and a control mechanism that fits such a structure is proposed. The control mechanism fulfills optimal performance requirements, while maintaining the internal stability of the microgrid of interest. When equipped with the proposed control mechanism, distribution feeder microgrid is shown to have the potential for increasing the heterogeneity of resources in the generation-mix and releasing the capacity of under-utilized distributed energy resources. Participation of DERs in power system services can reduce the dependency on capital-intensive conventional resources.

4.1 Introduction

On August 14^{th} 2003 before evening, people in sections of Midwest and Northeast United States as well as Ontario, Canada found themselves in the middle of one of the largest

blackouts in the power system history. Fifty million individuals with more than 60 GW of average daily electric load were affected for four to seven days. The estimated cost of this single blackout was approximated as between US$ 4 billion and US$10 billion on just the U.S. part. Analyses and investigations showed that the blackout started with a limited scale failure caused by a disturbance in the system, but the resultant mismatch between generation and demand increased the size of the blackout by a chain of device outages in a domino-effect-like event [15].

Although the August 2003 blackout was one of the largest outages in the U.S. power system's history, it was only one among many since the beginning of this century [8]. More than 670 large outages in the U.S. power system between 2003 and 2011 [9], solely induced by severe weather conditions, have increasingly raised questions about the resiliency of the power system against large disturbances. In addition to weather-induced disruptions, there can be other sources of perturbations that can threaten system performance and reliability, e.g. malicious attacks.

In the early 2000's, the resiliency of the power network was investigated in numerous research studies by analyzing large blackouts, for example by Dobson *et al.* in [18] and [17]. Investigations had shown that cascading component failures was the phenomenon that had caused many large blackouts [15]. An important factor in progress of outages in a cascading failures event is the load on the grid.

4.1.1 Power System Configuration and Control Paradigm

The current power system configuration is based on vertical integration of utilities that serve electric power to consumers via a complex architecture. This architecture is composed of large centralized power plants, nation-wide high-voltage transmission system as well as lower-voltage distribution systems working under a top-down centralized control scheme.

Moreover, the frequency stability of the power system is highly related to the balance between

generated power and load. Once generated power exceeds demand, a positive deviation in the system frequency happens. Similarly, a negative deviation takes place in the system frequency if demand exceeds power supplied [56].

In the current control paradigm of the power system, large generation sites including hydro, nuclear and fossil-fuel plants as well as transmission-level scale wind farms collectively provide the main portion of the needed power in the grid. This translates into the fact that the balance between load and generation is mainly handled by bulk power generators. The share of load supported by each site is determined by system operators through running optimal dispatch routines subject to various constraints from load forecasts to weather conditions in different time-scales [41].

While bulk power generators provide the main portion of electrical energy needs, peaking energy generation and operating reserve resources at lower levels and shorter time-scales provide additional capacities for deviations during a day. In this approach, the balancing issue is extremely, if not totally, dependent on the flexibility of the generation side. In other words, the demand side has an inelastic presence in the current power system control paradigm, contributing almost nothing at the grid scale to the supply-demand balancing requirement. The current control system architecture has posed extra costs by pushing the flexibility to the generation side along with showing significant signs of vulnerability. About 100 hours worth of annual operation of the peaking capacity costs 10%-20% of the overall grid design investment [55].

Furthermore, a mismatch between load and demand causes deviation in the system frequency. Once the deviation becomes excessive, protection relays trip generation sources. Failure of supply facilities, moreover, intensifies stress on remaining sources, which consequently increases power flow on the corresponding transmission lines to meet the unchanged demand. Lines also fail once the power flow passing through them exceeds their capacity. This failure propagation mechanism was among main causes of the August 2003 large blackout [15].

A possible approach to maintain the balance between generation and demand, when there is not enough supply source available, would be load curtailment. However, there is a reluctance to shed load because of the drastic reduction in service, not to mention the cost of a compensation that a utility company should pay in return. Also, loads are likely removed from the system when the window of opportunity for corrective action may have passed.

4.1.2 Characteristics of A Modern Control Paradigm

A new power system control paradigm seems inevitable in light of the vulnerabilities observed in the past decade as well as the operational costs to maintain the reliability of the system. In a new control paradigm, the essential flexibility in the system is partially transferred to the demand side to the extent possible. Such a paradigm is also likely to call for a new architecture for the control system.

Several architectures, coming with their own control paradigms, have been proposed to deal with system fragilities since early 2000's when the necessity for modernizing the power system was widely accepted in power engineering society. The solutions mainly involved with relying on the potential of distributed energy resources (DERs) and availability of renewable power generation within an appropriate structure, e.g. a virtual power plant (VPP) architecture as discussed by Pudjianto *et al.* in [116].

Distributed resources that could be utilized in modern power systems include but are not limited to dispatchable loads [102], battery energy storage systems (BESSs) [68, 69], plug-in electric vehicles (PEVs) [63, 64] and local fossil-fuel generation. Among dispatchable loads, there are thermal loads with hysteresis property resulted from their associated switching control mechanism [144], dimmable lights and even computing servers [34].

A dispatchable load demand profile, in general, can be altered based on power system requirements in a demand-side participation program. The hysteresis property of switching thermal loads is illustrated in Fig.4.1. A hysteresis-driven load is associated with a thermal

mass. An example of such a load is heating, ventilation and air-conditioning (HVAC) system of a building. Based on the associated thermal mass with an HVAC, it is possible to, e.g., postpone its power demand in a load management application without compromising end-users' comfort. The controllability property results in part from technological progress in the communication and sensing technologies. As another example, it is possible to reduce the performance of a computing server for a short period of time to decrease the associated power consumption with the load, and consequently, stress on the grid in favor of the system resiliency.

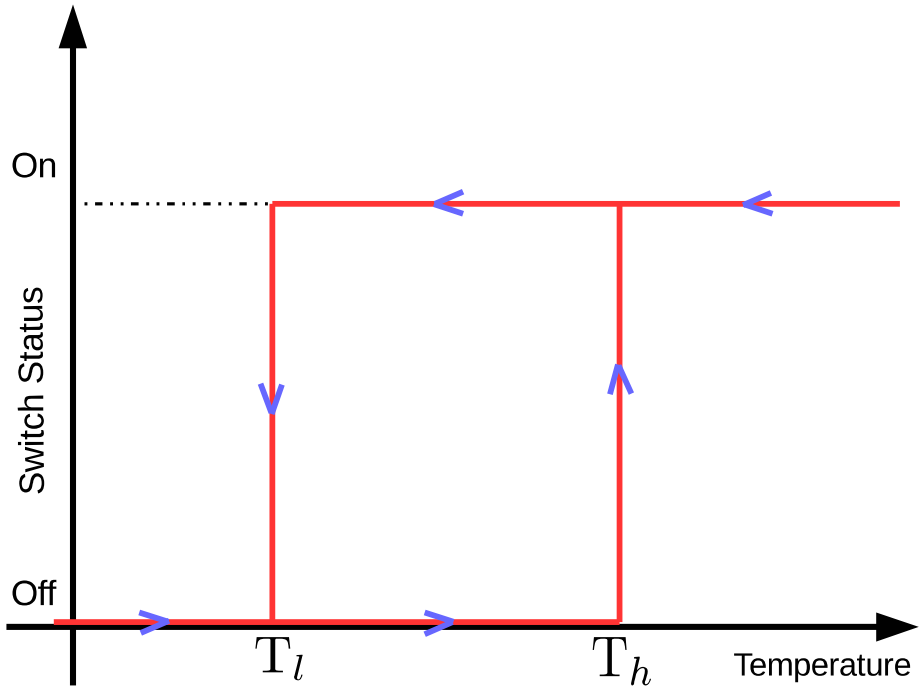

Figure 4.1: Graphical explanation of the hysteresis property. The device remains off until its temperature reaches the upper bound of the dead-band T_h. Then the device switches on and start using power to reduce its internal temperature until it reaches the lower dead-band T_l, where it switches off again. This cycle repeats depending on the environmental conditions.

In general, DERs come with small capacities as compared to conventional resources. Thus,

a proper control mechanism is needed to integrate a set of small distributed resources to provide a meaningful collective capacity that can be used as a resource in the system.

Although the potential of an aggregation mechanism over DERs for being used in power system services (via demand-side participation programs) is widely approved in the power engineering society, the architecture in which the integration of DERs should take place is still under investigation. Typically, there are two approaches for such an integration: centralized [113] versus decentralized [114]. A centralized control mechanism has the advantage of highly reliable implementation as resources are directly connected to a specific control center. The disadvantage of this approach, however, is that the essential communication infrastructure is capital-intensive. Hypothetically, a direct control over distributed resources by a utility company comes with a significant communication infrastructure cost, not to mention the computational cost associated with handling a large number of devices in a centralized fashion.

Moreover, it is hard to directly integrate renewable resources such as solar photovoltaic (PV) power into the grid due to their highly intermittent nature. Renewable resources are in general non-dispatchable, and do not come with frequency reserve technologies found in conventional generation facilities. Based on their highly dynamic nature and lack of on-site dispatching technologies, increasing the share of renewable resources in the generation-mix is limited because of the small capacity of control mechanisms to compensate high frequency fluctuations [47].

To be implementable, a new architecture should provide a viable scale for the integration of DERs as well as the essential control mechanism that can facilitate using DERs and renewable resources such as solar PV power, while maintaining reliability requirements.

4.1.3 Microgrid

A microgrid can provide an architecture in which several issues associated with integration of distributed and renewable resources can be addressed simultaneously. According to the Department of Energy (DoE), a "microgrid is a group of interconnected loads and distributed energy resources with clearly defined electrical boundaries that acts as a single controllable entity with respect to the grid and can connect and disconnect from the grid to enable it to operate in both grid connected or island mode" [23, 123]. Within a microgrid structure, distributed and renewable resources interconnect and cooperate with each other to collectively meet performance and stability objectives.

The integration of DERs at the distribution level and in the form of a microgrid have advantages at different levels in a power system [118]. Microgrids provide the opportunity to indirectly integrate renewable resources into the grid through a combination of facilities such as storage devices [119] and dispatchable loads [120] enabled by an IT-rich control paradigm. Also, the local interconnection scheme reduces the cost of communication infrastructure as distributed resources are only connected to a local control center at a limited scale.

From a utility company point of view, a microgrid presents itself to the outside world as a controllable entity [117]. The microgrid central controller (MGCC) in this architecture is in charge of the microgrid internal operation and stability. Thus, the controlled loads embodied within the microgrid structure collectively provide an elastic resource that can be used in power system management. Such a demand-side contribution to the essential flexibility in the power system, consequently, will decrease the necessity for new generation and transmission capacity [61], provided that a sufficient number of such structures are available at the distribution level. Specifically, power system operators can deploy demand-side resources in power system services to maintain reliability of the system. For example, the needed capacity for the frequency stability of the system during peak can be addressed by utilizing distributed resources such as local generation and battery energy storage systems

rather than conventional resources. A microgrid architecture seems aligned with a modern power system control paradigm in which the essential flexibility for maintaining power system resiliency is partially transferred from the supply-side to the demand-side, causing the latter to have an elastic participation in the power system.

In summary, a microgrid offers an appropriate architecture for implementing a new robust power system control paradigm. Specifically, a microgrid-based evolution of the power system can enhance the scalability of the network to finer levels, promising higher scales of system resiliency [22].

In this study, control requirements for implementing a microgid from the power system frequency stability point of view is investigated. Specifically, a special type of microgrid, namely distribution feeder microgird is of interest. In this type of microgrid, a distribution feeder adopts the microgird architecture and the utility company can treat a feeder as a controllable entity at the point of common coupling (PCC). Working at the scale of distribution feeders also makes it possible to attain finer control over the available resources. Resources in this structure are not limited to conventional ones. modern resources such as hysteresis-driven loads also can be utilized in this scale, reducing the need for capital-intensive conventional resources. An example of such resources are TCLs, integration of which was addressed in chapter 3. The appropriateness of architecture of a distribution feeder microgrid for the purpose of integration of DERs and renewable resources into the grid is examined as well.

4.2 Problem Definition

As a remote area in the middle of the California desert connected to the grid with a lengthy transmission line, Borrego Springs is a well-known example of a community that is supported by a distribution feeder microgrid structure [145]. This community obtains the majority of its electrical energy needs from small scale distributed resources, mainly scattered roof-top solar PV panels. While relying on local resources, the lengthy transmission connection of

this microgrid to the distribution system supports the community in the cases that local resources are not sufficient, available or may be financially justifiable to meet 600+ residential, commercial and industrial costumers' needs. The associated MGCC orchestrates an optimal combination process for the power imported from the main grid and the local generation to meet local demand [146].

The Borrego Springs microgrid demonstration project had targeted several objectives from reducing peak load on the feeder to implementing an information-rich control platform. The demonstration was among pioneer efforts in the U.S. aligned with the trend of modernizing the current system by turning a distribution feeder into a controllable entity, opening the gates towards a self-healing infrastructure [147].

The key technologies used in this microgrid include fossil-fuel (diesel) generators, energy storage systems, solar PV panels and an MGCC that makes the essential coordination among resources happen. The coordination is implemented based on a price-driven demand response (DR). Demand response by definition [31], are "all intentional modifications to consumption patterns of electricity of end-use customers that are intended to alter the timing, level of instantaneous demand, or the total electricity consumption". A DR program is aimed to use demand-side resources to support supply-demand balance requirement.

The objective of the present research is to address some control requirements associated with implementation of a distribution feeder microgrid by designing an appropriate control mechanism. Large scale adoption of feeder microgrids which relies heavily on renewable resources requires increased level of distributed control, and would shift the current centralized generation paradigm to a more decentralized one [29]. Consequently, the control infrastructure and mechanisms should also be changed to suit this paradigm shift. The microgrid studied is based on the current and future facilities installed on the Studio-14 feeder located in south of Albuquerque, New Mexico, serving Mesa del Sol suburban community. The microgrid also embodies a distribution-level solar PV site, namely the Prosperity site [82] that partially fulfills consumers' needs during the day.

Similar to the Borrego Springs microgrid, a price-driven DR scheme is supposed to alter the microgrid power import from the grid, while the MGCC is in charge of performance and stability requirements. Such a scheme is supposed to use BESS, hysteresis-based dispatchable loads of residential and commercial buildings as well as local fossil-fuel generators. A price-based control paradigm is also aligned with the shift from the current market to a less regulated one by taking into account the financial justification of introducing non-conventional resources in the system as compared to conventional resources. This aspect is not widely discussed in the current literature.

To design the control mechanism, a coherent mathematical model for the system and its components should be developed. Such a model can be used later to address performance and stability criteria. These criteria that form the control requirements in the problem should be formulated according to the developed model. Finally, a consistent framework should incorporate the developed model and the control requirements in a unified way to facilitate the microgrid management automation.

The first step is to model individual components of the system. The *Power node* model is an attempt in this regard that models both intermittent renewable resources and storage devices in a unified way to be used in a frequency stability problem [148]. This model captures energy and power attributes in a device. Although mentioned as a possibility, the ramping capacity of a device, which is the time derivative of the power, is not clearly specified in this model. Consequently, the study resulted in a first-order dynamical model for each device. The *Energy hub* model presented by Arnold *et al.* in [149] takes a similar approach for modeling local fossil-fuel generators as well as energy storage devices by a first-order dynamical model. Again, the main attributes of the model are power and energy. In both of the mentioned models, power signal acts as the control input to the system, while the energy specifies the state of the device/component. In the present study, a second-order dynamical model is introduced that captures energy, power and ramping capacities associated with each device. The model studied here is an extended version of the *energy hub* model, while capturing the

ramping constraint. In contrast to the *energy hub* model, the ramp rate associated with the device, which is the time derivative of the power signal, acts as the control input. The state of the device, instead, is represented by both the stored energy and the instantaneous power.

The second step is to formulate the performance and the stability requirements in the system based on the developed model. The performance concern in the system is mainly the optimal dispatch of available resources, while meeting demand perfectly. The reliability of the system is limited to the frequency stability. Formulation of performance criteria, moreover, should reflect the associated realistic costs with utilizing each technology in the framework. Traditionally, researchers use quadratic cost functions in their optimization problems. The main rationale behind using quadratic costs is mainly the resultant well-behaved convex problem along with the extensive availability of quadratic solvers. However, realistic costs are better realistically modeled by linear and in some cases by absolute value functions. For example, fuel costs are better approximated by the former, while the degradation cost is suited to be formulated into the latter form. Another significant cost in some devices is the maintenance cost, e.g. in a gas engine (GE), which generally is neglected. In the present study, all these costs are investigated with a more realistic formulation.

Frequency stability, conventionally, is addressed in three different time-scales [57]. Primary frequency control (PFC), is designed to respond to a frequency deviation in the fastest mode. This decentralized control mechanism is implemented through governors in the system. Primary frequency control only compensates the high frequency fluctuations. Secondary frequency control (SFC) and tertiary frequency control (TFC) in a power system, on the other hand, are in charge of lower bandwidths of fluctuations. In this chapter, the control automation implemented on the microgrid is in charge of maintaining the low frequency stability of the system. In Fig.4.2, a schematic version of associated bands with different categories of frequency control is depicted.

At the final step, control requirements which consist of both the performance and stability requirements of the system should be addressed within a unified framework simultaneously.

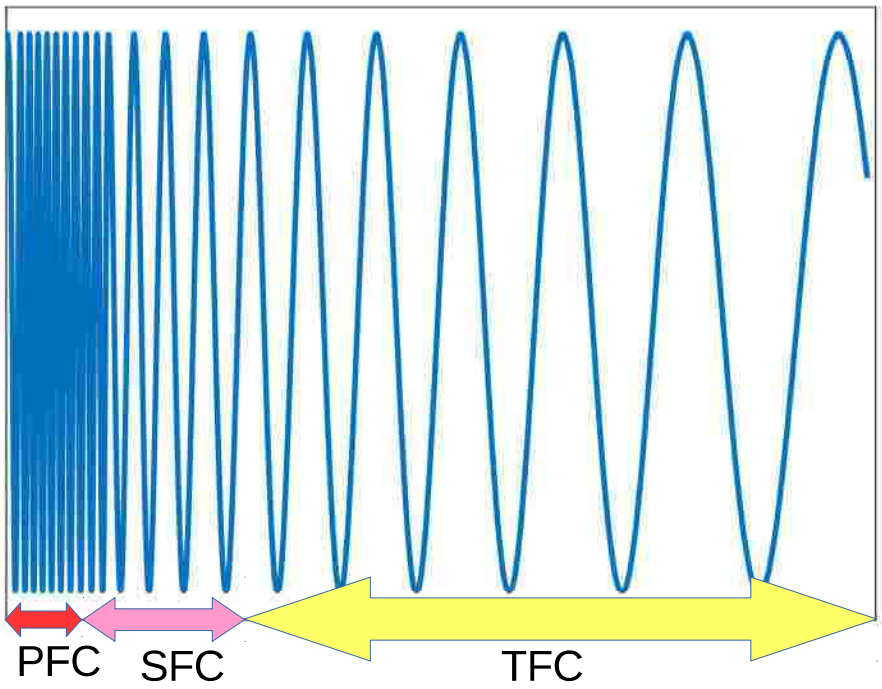

Figure 4.2: A scheme of associated frequency bands with the primary, secondary and tertiary frequency control.

Performance concerns in this study address the costs of using a resource as well as possible deviations from pre-determined operating settings. Stability issues are mainly the balance between load and generation, as well as avoiding exhaustion of storage devices. An optimal control framework seems appropriate to address the performance and stability concerns of this study. A widely used optimal control framework is the model predictive control (MPC). The MPC framework provides an opportunity to deal with several objectives at the same time. Motivations to apply this method include the necessity to work with uncertainty in the system and presence of a storage device in the system.

A strong feature of MPC is its capability in dealing with uncertainties and changes in the system in an online fashion. For example in [132], uncertainty parameters associated with PEV including charging time and initial battery state-of-charge were the rationale behind

using MPC for minimizing the associated operational cost.

Another key motivation in the literature to use MPC framework has been the presence of some form of energy storage. An optimal deployment of the energy capacity in a storage device necessitates using such a framework. For example, Ma *et al.* in [92] used MPC as the optimization framework to control the operation of building cooling system equipped with a cold water tank.

Model predictive control also has applications in grid operations. As discussed by Ali *et al.* in [134], MPC was used in a case study of a demand response scheme for grid operation purposes. In that case, the objective was to minimize the cost associated with using an electric space heating in the presence of thermal storage by a linear programming application. The proposed control was in charge of an optimized dispatch according to dynamic prices, which shifts the power demand from peak hours to the periods with less expensive tariffs.

An important application of MPC is in the frequency control problem when utilizing DERs in the system. In this study also MPC constitutes the main part of the chosen automation framework technology. Specifically, a similar framework as what Vrettos *et al.* used [136, 137] is deployed here. In this framework, a hierarchical control algorithm is used for active distribution network management in order to leverage distributed resources in a modern system architecture. The platform studied consists of two phases: day-ahead scheduling and real-time optimal dispatch performed by the MPC.

When working with distributed resources, it is essential to consider that such resources come with small capacities in contrary to conventional resources. This limited capacity may cause the recursive problem to become infeasible. For example, the optimization procedure may exhaust a resource in favor of reducing operational costs. Another important contribution is this study is addressing the essential recursive feasibility condition in the MPC problem. A mathematical tool based on optimal control theory is provided to guarantee the recursive feasibility criterion.

4.3 Modeling Framework

The prototype utility-feeder microgrid considered here has an architecture with high PV penetration in either centralized (utility-owned) or distributed (customer-owned) forms, supported by battery energy storage systems, dipatchable loads and a gas engine as a local fossil fuel generation. These resources have a potential for demand-side participation in load management problem in near future. In Fig.4.3, a simple scheme for a distribution feeder microgrid based on the current and future configuration of Studio-14 feeder, introduced in the previous section, is shown.

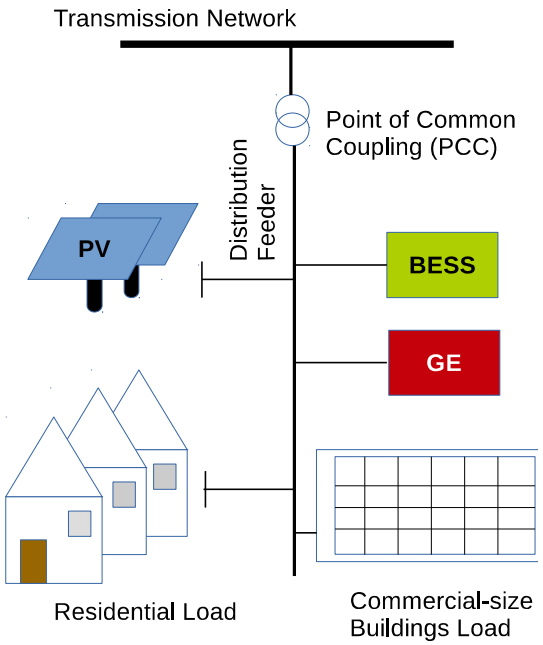

Figure 4.3: Example of a distribution feeder microgrid, encompassing renewable resources (PV), storage devices (BESS), local fossil-fuel-based generators (GE) as well as residential and commercial loads.

In the present study, the generated solar PV power from all different resources are aggregated

as a single renewable resource power. It is assumed that within the structure of the microgrid, intermittent renewable resources are directly connected to the system, providing a non-dipatchable resource. From the MGCC point of view, the power fed by the PV panels act as a negative load in the feeder structure.

Moreover, a large BESS is considered as the energy storage device of interest. Dispatchable loads with hysteresis property can be modeled as a BESS with corresponding characteristics. Thus, they can be dealt in the similar way in the problem. For the objectives of the present chapter, a BESS suffices. To use more BESSs in the system, it is just needed to scale up the problem in the same fashion.

To allow for the heterogeneity of distributed energy resources that will form the future "smart grid" infrastructure, a unified model that captures the essential features of various dispatchable resources despite their different nature is used[1]. These features are energy and power capacities as well as maximum ramp rate. In this framework, the ramp-rate signal which is the time-derivative of the device output power acts as the control signal, adjusting the state of any individual dispatchable resource.

The state of each device at time step k is described by a 2×1 vector $x_k = (E_k, P_k)^T$, where E_k is the stored energy at the time step k, and P_k shows the instantaneous power. Negative values of P_k show that the storage device is receiving energy in a charging cycle.

As devices are controlled by a ramp-rate input signal, each storage device has a second-order dynamical model as follows:

$$\begin{pmatrix} E_{k+1} \\ P_{k+1} \end{pmatrix} = \begin{pmatrix} 1 & -t_s \\ 0 & 1 \end{pmatrix} \begin{pmatrix} E_k \\ P_k \end{pmatrix} + \begin{pmatrix} -t_s^2/2 \\ t_s \end{pmatrix} u_k, \tag{4.1}$$

where t_s is the sampling time, and u_k is the associated ramp-rate at time step k. Also, constraints apply to each of the described variables. Storage devices have limited capacity

[1]A dispatchable resource is any type of resource in the system that can be controlled by an input signal. It includes BESS, dispatchable loads, local fossil fuel generation as well as the main grid.

to store energy. The power input or output capacity of a DER as well as its ramp rate are also constrained by physical limitations:

$$\begin{aligned} 0 &\leq E_k \leq E_{\max}, \\ P_{\min} &\leq P_k \leq P_{\max}, \\ u_{\min} &\leq u_k \leq u_{\max}. \end{aligned} \tag{4.2}$$

This modeling approach offers to model every local dispatchable resource as an energy storage device with its associated finite capacities, while the grid can be modeled in the same way, but with infinite capacities.

Expressing the above difference equation in the general form of $\boldsymbol{x}_{i,k+1} = A_i \boldsymbol{x}_{i,k} + B_i \boldsymbol{u}_{i,k}$ and forming the corresponding matrices A_i and B_i, the aggregated dynamics $\underline{\boldsymbol{x}}_{k+1} = A\underline{\boldsymbol{x}}_k + B\underline{\boldsymbol{u}}_k$ is described by:

$$\begin{aligned} A &= \begin{pmatrix} A_1 & \mathbf{0} & \dots & \mathbf{0} \\ \mathbf{0} & A_2 & \dots & \mathbf{0} \\ \vdots & \vdots & \ddots & \vdots \\ \mathbf{0} & \mathbf{0} & \dots & A_m \end{pmatrix}, \\ B &= \begin{pmatrix} B_1 & \mathbf{0} & \dots & \mathbf{0} \\ \mathbf{0} & B_2 & \dots & \mathbf{0} \\ \vdots & \vdots & \ddots & \vdots \\ \mathbf{0} & \mathbf{0} & \dots & B_m \end{pmatrix}, \end{aligned} \tag{4.3}$$

where $\underline{\boldsymbol{x}}_k$ is the aggregated state, and $\underline{\boldsymbol{u}}_k$ is the control input at the time step k. The state vector $\underline{\boldsymbol{x}}_k$ is the $2m \times 1$ column-vector of aggregated state vectors $\boldsymbol{x}_{i,k}$: $i = 1, \dots, m$ associated with each of the m available resources as $\underline{\boldsymbol{x}}_k = (\boldsymbol{x}_{1,k}^T \dots \boldsymbol{x}_{m,k}^T)^T$. In the same fashion, the $m \times 1$ control input $\underline{\boldsymbol{u}}_k$ is composed of the single control input of each of the devices as $\underline{\boldsymbol{u}}_k = (\boldsymbol{u}_{1,k} \dots \boldsymbol{u}_{m,k})^T$. Moreover, the signals $\boldsymbol{x}_{\text{sch},i}$ and $\boldsymbol{u}_{\text{sch},i}$ are the corresponding scheduled values. This aggregated dynamical model will be deployed in optimization procedures later in this study.

4.4 Day-ahead Scheduling

A two-level optimization approach is proposed in this study: a day-ahead scheduling combined with an MPC framework. The former level is a single shot optimization that takes place every 24 hours, while the latter level is a dynamic programming problem that balances supply and demand in real-time. In this section, the day-ahead scheduling process is considered, and the real-time adjustment procedure is discussed in the next section.

The price-based mechanism implemented in the current control paradigm of the power system is based on time-of-use rates. In the current scheme, importing power form the grid is more expensive at early evening than early morning. This approach induces consumers to import less power from the grid during the peak, and consequently reducing the stress on the network. On the other hand, this mechanism provides room for purchasing power from the grid and use it later if a storage technology is present and financially justifiable, provided that legally permitted. A well-defined day-ahead scheduling optimization can be used to assess this possibility.

In a microgrid system, the variable price of the electricity provided by the grid as well as forecasts of load and model of DERs can be fed into an optimization problem to derive the set points of various devices on the microgrid. The objective of such an optimization is to minimize the cost of meeting predicted demand during a day. Broadly speaking, the day-ahead scheduling optimization will charge storage devices when the cost of purchasing power from the grid is low (e.g. after midnight), using the stored energy when the cost is high (likely late afternoon and early evening).

A simple configuration for the microgrid is investigated in this study. As mentioned in the previous section, the studied microgrid embodies an aggregated solar PV resource, which is the collective form of small scale roof-top solar panels and/or as many centralized sites as installed on the microgrid structure. Also, the structure of interest comes with a large energy storage system. Based on the model introduced for system elements and from the

optimization point of view, it does not matter if the storage is a conventional battery or a non-conventional resource such as a hysteresis-driven dispatchable load. Without loss of generality, a BESS is considered here. Other type of storage devices can be fed into the problem with their corresponding characteristics. Also, a gas engine is placed in the system structure that provides power by converting chemical energy into electrical energy when financially justifiable.

The costs associated with each resource should be appropriately formulated to be used in the optimization problem. The price of the power imported from the grid is specified by the time-of-use rates from the utility company. Solar PV panels are non-dispatchable resources, the cost of which does not affect the optimization problem. Indeed, the optimization process is just in charge of optimal performance of dispatchable resources. The price associated with other resources should be formulated according to the introduced mathematical model. The optimization problem of interest for the day-ahead scheduling part can be formulated as:

$$J = \sum_{k=0}^{N-1} J_k, \tag{4.4}$$

assuming N equal time intervals for the dispatch routine. In this equation, J_k is the overall cost associated with using all the available resources at time step k.

4.4.1 Costs Associated With A Gas Engine

Regarding the gas engine, the two most important costs are the fuel cost and the maintenance cost. The fuel cost is the cost of gas burned to produce electricity. The maintenance cost, on the other hand, is a fixed rate for deploying a gas engine to produce electricity. This fixed rate should be added to the fuel cost as long as the gas engine is in use, no matter how much power it produces. The maintenance cost can be approximated by the total scheduled maintenance cost for a gas engine divided by its lifetime.

The fuel cost for a gas engine at each step can be determined with the equation

$$\begin{aligned} J_{\mathrm{GE,f},k} &= q_{\mathrm{GE,f},k}(E_{\mathrm{GE},k} - E_{\mathrm{GE},k+1}) \\ &= q_{\mathrm{GE,f},k}(t_s P_{\mathrm{GE},k} + \tfrac{t_s^2}{2} u_{\mathrm{GE},k}), \end{aligned} \tag{4.5}$$

according to the model introduced in eq. 4.1. In this equation, $J_{\mathrm{GE,e},k}$ represents the cost associated with the energy conversion from the time step k to $k+1$ in a gas engine, and $q_{\mathrm{GE,e},k}$ is the price for conversion of a unit energy into electricity expressed in ¢/KWh.

The maintenance cost at each time step can be expressed as:

$$J_{\mathrm{GE,m},k} = I_k q_{\mathrm{GE,m}}, \tag{4.6}$$

where $q_{\mathrm{GE,m}}$ is the maintenance cost per unit of time expressed in ¢/h, and I_k indicates whether the GE is *on* ($I_k = 1$) or *off* ($I_k = 0$).

4.4.2 Cost Associated with BESS

The main costs associated with batteries are the operating costs including the degradation cost. The term degradation refers to several phenomena that happen in a battery which reduce its ability to store energy. In fact, degradation causes the internal resistance of a battery to increase and shrinks its capacity. Regardless of the direction, the lifetime of a battery decreases as power flows through it. It is hard to calculate the degradation cost as it is a nonlinear function of a set of variables including temperature, state-of-charge and charging/discharging rate [74, 75]. In this study, a simplifying assumption is made and the degradation cost is approximated by the average implementation cost over the total expected energy transformation during the lifetime of the battery. The equation below describes the degradation cost as a function of the state of battery.

$$\frac{d}{dt} J_{\mathrm{BESS}} = q_{\mathrm{BESS}} \left| \frac{d}{dt} E_{\mathrm{BESS}} \right|, \tag{4.7}$$

where q_{BESS} is the approximated degradation cost per unit energy. Thus, between the time steps k and $k+1$, the degradation cost can be calculated by

$$\begin{aligned} J_{\text{BESS},k} &= \int_{t_k}^{t_{k+1}} q_{\text{BESS}} |\tfrac{d}{dt} E_{\text{BESS}}(t)| dt \\ &= \int_{t_k}^{t_{k+1}} q_{\text{BESS}} |p_{\text{BESS}}(t)| dt. \end{aligned} \tag{4.8}$$

As the total cost function is the summation over all J_k, the presence of an integration over a norm-1 function will be problematic, when working with a solver. Thus, an approximation is made here to translate the problem into an interpretable one for available solvers. For the approximation, the time duration between t_k and t_{k+1} is divided into M equally spaced time intervals $\Delta t = (t_{k+1} - t_k)/M$. Then, the cost function $J_{\text{BESS},k}$ at each time step k is approximated as

$$J_{\text{BESS},k} \approx \sum_{i=0}^{M-1} \frac{|p(t_k + i\Delta t)| + |p(t_k + (i+1)\Delta t|}{2} \Delta t, \tag{4.9}$$

using a trapezoidal integration approach. In this equation, $p(t)$ is the short form for $p_{\text{BESS}}(t)$.

4.4.3 Day-Ahead Optimization

Now that the associated costs with each technology is determined, the overall cost at each step is then given by:

$$\begin{aligned} J_k &= J_{\text{GE,f},k} + J_{\text{GE,m},k} + \\ &\quad J_{\text{BESS},k} + \\ &\quad J_{\text{grid},k}, \end{aligned} \tag{4.10}$$

where $J_{\text{grid},k}$ corresponds to the cost associated with importing power from the grid, and is similarly calculated as $J_{\text{GE,f},k}$.

The step cost function J_k, now, should be fed in the day-ahead scheduling problem. Regardless of the maintenance cost, the objective function of interest is a summation of different

linear and absolute value of linear costs. The constraints also are linear. Thus, the optimization problem is a disciplined convex programming problem [150], a special type of convex problems.

However, the step cost $J_{\text{BESS},k}$ cannot be dealt easily by available solvers as it includes an indicator function. Presence of an indicator function turns the problem into a mixed integer problem (MIP). To deal with the MIP problem developed, the *Branch and Bound* (B&B) method is used in this study, which is described in detail as follows. Specifically, the developed problem is a mixed boolean convex problem, and the B&B method should be combined with a convex solver to derive optimized results.

Branch and Bound Algorithm

Branch and bound algorithms are non-heuristic methods that may find applications in non-convex problems [151]. In the most general form, they provide a provable bound on the optimal value of interest. The computational effort grows exponentially in the worst case scenario with the size of the problem, which put B&B-based solutions generally in slow applications in an optimization tool set.

The type of B&B problems studied here is the mixed boolean convex problem, applicable to combinatorial problems. A simple statement of the algorithm is as follows.

Consider the following optimization (minimization) problem as a function of variables x and z:

$$\begin{aligned} \text{minimize} \quad & f_0(x,z) \\ \text{subject to} \quad & f_i(x,z) \leq 0 \quad i = 1,\ldots,m \\ & z_j \in \{0,1\} \quad j = 1,\ldots,n, \end{aligned} \tag{4.11}$$

where the $f_i; i = 0,\ldots,m$ are convex functions of the optimization variables x and z. The search space contains 2^n convex optimization problems. Although the branch and bound

algorithm cannot guarantee a better performance than the exhaustive search method, it is often the case that this method converges to the global solution considerably faster [151].

The algorithm at the first step applies a convex relaxation to the original problem and converts it to:

$$\begin{aligned} \text{minimize} \quad & f_0(x,z) \\ \text{subject to} \quad & f_i(x,z) \leq 0 \quad i=1,\ldots,m \\ & 0 \leq z_j \leq 1 \quad j=1,\ldots,n, \end{aligned} \tag{4.12}$$

making the variables z_j continuous in the interval $[0,1]$ rather than boolean. This relaxation also allows using widely available convex solvers for the relaxed problem. It can be easily concluded that the optimal value derived from the recent problem is a lower bound for the optimal value of the original problem as it is a relaxed version of the original problem.

The branching step occurs next. One of the indexes $j=1,\ldots,n$ is picked. Assume that this index is denoted by k and two subproblems are generated as follows. The first subproblem is

$$\begin{aligned} \text{minimize} \quad & f_0(x,z) \\ \text{subject to} \quad & f_i(x,z) \leq 0 \quad i=1,\ldots,m \\ & 0 \leq z_j \leq 1 \quad j=1,\ldots,n, \\ & z_k = 0, \end{aligned} \tag{4.13}$$

while the second subproblem is

$$\begin{aligned} \text{minimize} \quad & f_0(x,z) \\ \text{subject to} \quad & f_i(x,z) \leq 0 \quad i=1,\ldots,m \\ & 0 \leq z_j \leq 1 \quad j=1,\ldots,n, \\ & z_k = 1. \end{aligned} \tag{4.14}$$

It can be easily seen that each of the new-born subproblems are also convex, the optimal solution of which gives a lower bound on the optimal value of the original problem. Another

conclusion is also that the optimal solution of each of the subproblems will not be less than that of their parent problem.

The branching process grows a tree by adding leaves to a tree structure from developing subproblems as shown in Fig. 4.4. The next step after solving each of the subproblems is to choose the next parent problem among the most recent child subproblems. In this study, the one with the lower optimal value is chosen, and the branching process continues on this leaf (node) in the same way as performed on its own parent leaf.

This branching process continues until all the boolean variables are fixed. Once the process reaches to final leaves that have all their z_j variables fixed, the optimal values derived are the actual optimal value associated with each of the most recent subproblems. Specifically, the derived values are not only a lower bound for each of corresponding subproblem, but also the exact optimal value associated with each of them. The leaf with the smallest value is a candidate for the optimal value of the original problem.

The next step is the *pruning* process. Once a candidate for the optimal value is derived, it can be easily concluded that all the previous leaves with lower bound not less than the candidate optimal value will not generate a better candidate if the branching process continues on them. Thus, they can be removed from the tree.

The branching process will then be continued on the remaining leaves until the best candidate is derived. Such a best derived value is the actual optimal value of the original problem. In Fig. 4.4, an illustration of the process is provided.

Simulation Results

As an example, a variable price for the power imported from the grid implemented through time-of-use rates is considered here, as shown in Fig. 4.5. In this example, the price is high early evening and low after midnight. The BESS degradation cost is assumed to be 0.0625 ¢/KWH. Regarding the gas engine, the associated fuel cost is assumed to be 1 ¢/KWH and

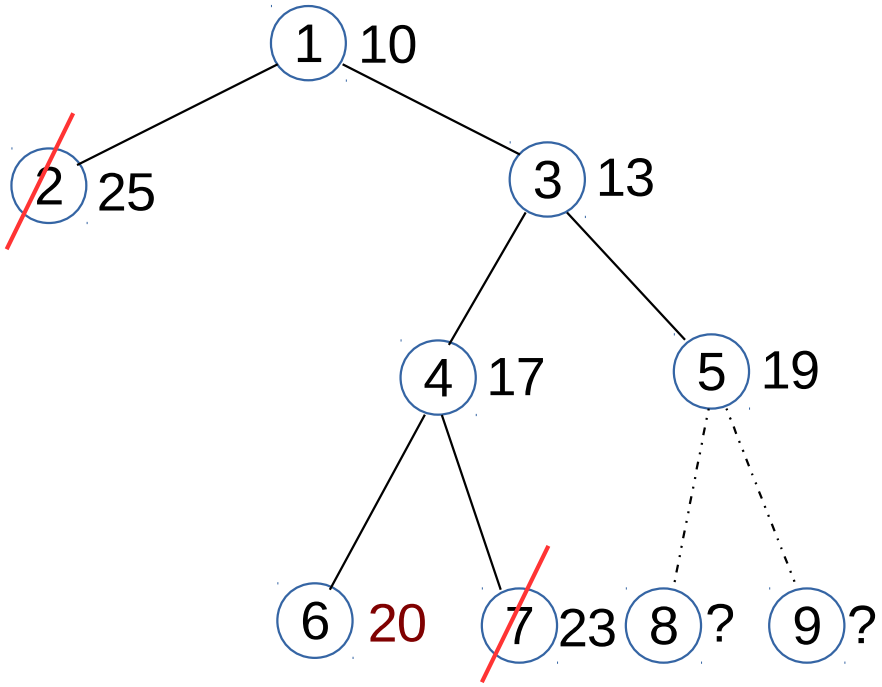

Figure 4.4: Branch and bound algorithm developed for a mixed boolean convex problem with three boolean variables. The relaxation procedure happens as ordered by the number shown within the circles. Values depicted right next to each of the nodes are the associated optimal values. These values are lower bounds for the actual optimal value of the original problem. After deriving an optimal candidate on node #6, the pruning procedure removes all nodes with associated lower bounds not less than that of the derived candidate.

the maintenance cost is 15 $/Hour.

For the scheduling purposes, an average net load profile is considered. This profile is derived from the historical data for the time period of one month. The net load is the difference between the averaged actual load and the averaged generated PV power during the period considered. As discussed in the previous section, solar PV power is treated as negative load in this study. The average net load profile studied is shown in Fig. 4.6.

This averaged net load should be met by available resources (here a BESS, a GE and the grid) in an optimal fashion with respect to the associated costs mentioned above. The

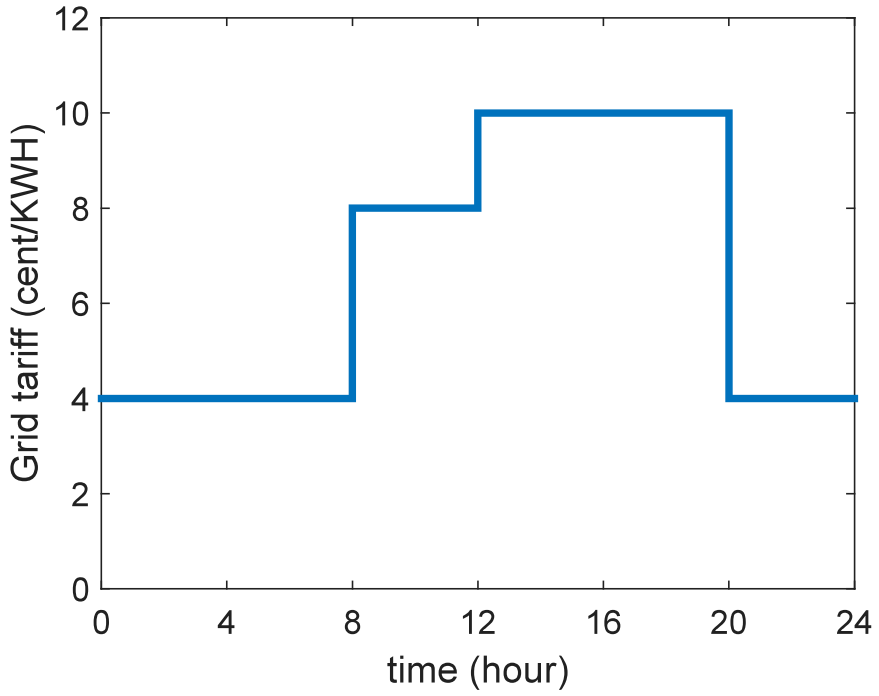

Figure 4.5: An example of varying price throughout a day used for the day-ahead scheduling. In this example, the price is high early evening and low after midnight.

characteristics of the studied resources are presented in Table 4.1.

Table 4.1: Resource Characteristics for the Day-ahead Scheduling Problem

Resource	Power capacity	Energy capacity	Ramp rate
Gas Engine	[0,350] KW	Unlimited	0.56 %/sec
Energy Battery	[-250,250] KW	500 KWH	1.67 %/sec

Also, the balancing requirement is a constraint on the optimization problem of interest. This translates into the following equality constraint for the optimization problem as:

$$\underbrace{(0\ 1\ \ldots\ 0\ 1)}_{2m\times 1} \cdot \boldsymbol{x}_k = P_{\text{ref},k}, \tag{4.15}$$

where $P_{\text{ref},k}$ is the reference power demand at time step k, and m is the number of resources

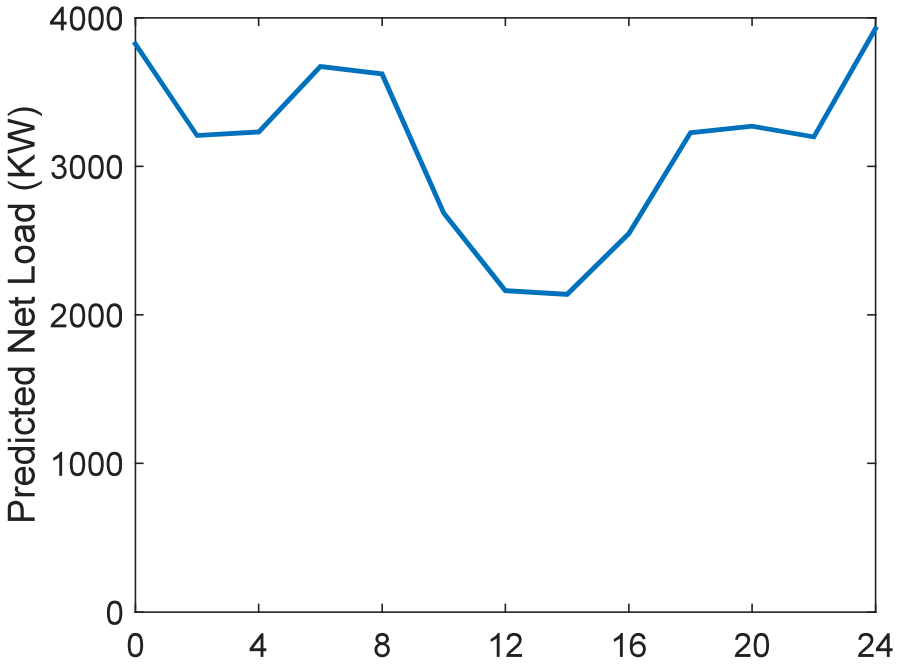

Figure 4.6: Average net load used in the day-ahead scheduling problem. This curve is derived from historical data of demand and PV generation for the course of a month. The steepness in the middle of the day results from penetration of solar PV power into the system.

available. In summary the optimization problem has the following general form as:

$$
\begin{aligned}
\underset{\underline{\boldsymbol{u}}_0,\cdots,\underline{\boldsymbol{u}}_{N-1}}{\text{minimize}} \quad & J(\underline{\boldsymbol{x}}_0, \underline{\boldsymbol{u}}_0, \ldots, \underline{\boldsymbol{u}}_{N-1}) = \sum_{k=0}^{N-1} J_k(\underline{\boldsymbol{x}}_k, \underline{\boldsymbol{u}}_k) \\
\text{subject to} \quad & \underline{\boldsymbol{x}}_{k+1} = A\underline{\boldsymbol{x}}_k + B\underline{\boldsymbol{u}}_k \qquad\qquad k = 0, 1, \ldots, N-1 \\
& \underline{\boldsymbol{x}}_{\min} \leq \underline{\boldsymbol{x}}_k \leq \underline{\boldsymbol{x}}_{\max} \\
& \underline{\boldsymbol{u}}_{\min} \leq \underline{\boldsymbol{u}}_k \leq \underline{\boldsymbol{u}}_{\max} \\
& \underbrace{(0\ 1\ \ldots\ 0\ 1)}_{2m\times 1} \cdot \underline{\boldsymbol{x}}_k = P_{\text{ref},k}.
\end{aligned}
\tag{4.16}
$$

The optimization problem, then, is fed into the B&B algorithm to obtain an optimal sched-

ule for available resources. As mentioned in the general description of the branch and bound algorithm, each step is associated with fixing a subset of boolean variables to some fixed values. The fixation of parameters adds another set of constraints to the optimization problem. In the case study here, boolean variables are the indicator functions that determine weather the GE is on or off. If the gas engine is off during the time step k to $k+1$, translated into $I_k = 0$, the following set of constraints is added to the optimization problem:

$$\begin{aligned} (0,1).x_{\mathrm{GE},k} &= 0, \\ u_{\mathrm{GE},k} &= 0, \end{aligned} \tag{4.17}$$

where $x_{\mathrm{GE},k}$ is the state of the GE at time step k, and $u_{\mathrm{GE},k}$ is the associated ramp rate of the device which acts as the control input. The first equation is equivalent to say that $P_{\mathrm{GE},k} = 0$.

In Fig. 4.7, the result of such an optimization based on the information provided is depicted for the course of a day. As one can expect, the BESS is charged after midnight and depleted in the early evening when the price is high. Also, due to the presence of maintenance cost, it is reasonable that a GE should either work on full capacity or it should be turned off.

Generally, branch and bound method and its variants provide a suboptimal solution within a guaranteed bound around the actual optimal value. Once the algorithm reaches a guaranteed boundary, it stops further search. However, the method used here, which is a mixed boolean convex programming problem as a special variant of branch and bound method, provides an exact optimal solution by continuing the search completely to the end which has the advantage over suboptimal solutions. Although a variant of branch and bound methods is used here, there are other methods that could be used instead, such as tabu search [152, 153].

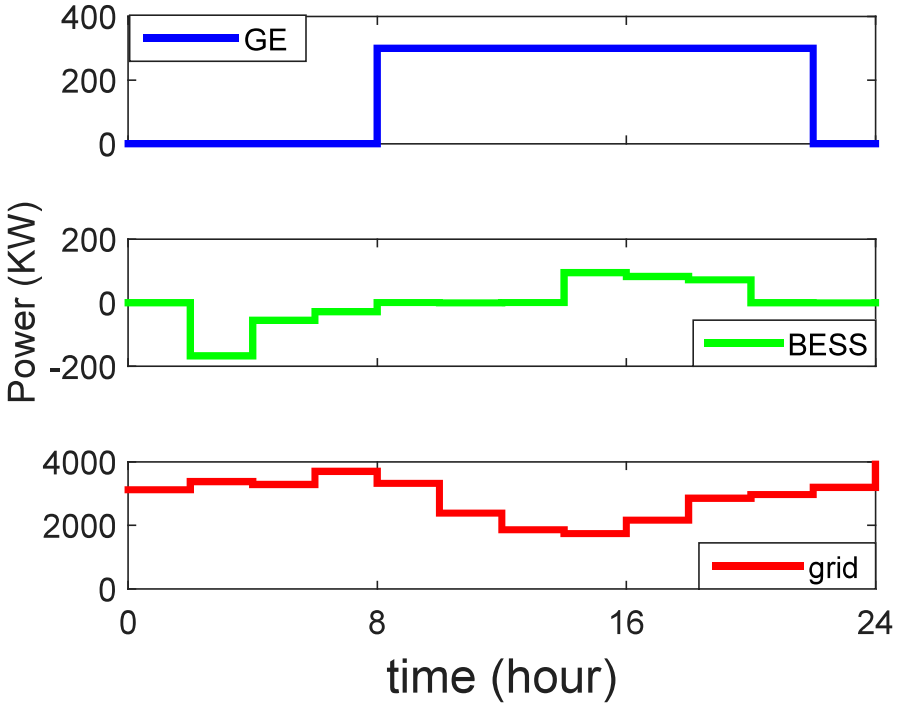

Figure 4.7: Scheduled values derived from the day-ahead optimization. The most top plot is associated with the GE. The one in the middle is the scheduled profile of the BESS. The lowest one corresponds to the grid.

4.5 Online Control Mechanism

Based on the fact that no forecast is perfectly accurate, an online dispatch mechanism should adjust the output of the resources in a way that the cost of deviations from the scheduled values is minimized. The cost of deviation should again account for battery degradation, fuel costs, and so on. A model predictive control with a proper cost function is a well-known approach for the purpose of real-time cost minimization [154], [149].

The MPC is a real-time optimization technique that takes future predictions of the system state for a finite horizon into account and determines a set of control actions which minimizes a cost function. In this control technique, an optimization problem is solved at each time

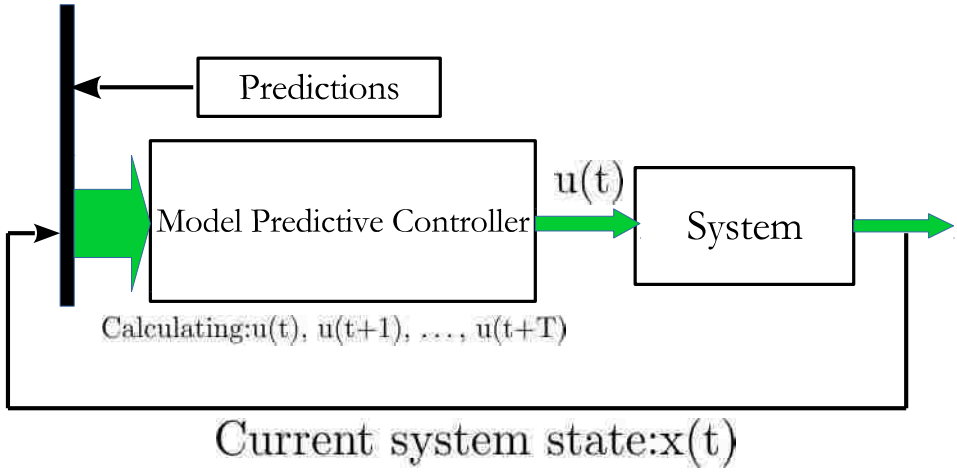

Figure 4.8: Diagram of an MPC framework for the finite horizon T. At each time step, the MPC framework is updated with the current state of the system as well as prediction of quantities of interest for the finite horizon T. The first calculated input $u(t)$ is then applied to the system.

step to specify a set of control actions for the finite horizon over which the prediction is performed. The first calculated control action, then, is applied to the system. The same process takes place at each successive time step taking into account the updated estimates of future quantities of concern. The control policy is a feedback system as it uses the the current system state at each time step. In Fig. 4.8, a schematic version of the MPC framework is depicted.

There is a difference between the cost in the day-ahead scheduling and in the MPC part as the former cost reflects absolute measures, while in the cost is associated with deviations

from the optimized schedule, and it can be written in a general form as:

$$J_{\text{MPC}} = \sum_{k=0}^{N} l(\boldsymbol{x}_k - \boldsymbol{x}_{\text{sch},k}, \boldsymbol{u}_k - \boldsymbol{u}_{\text{sch},k}), \tag{4.18}$$

where the signals $\boldsymbol{x}_{\text{sch},k}$ and $\boldsymbol{u}_{\text{sch},k}$ are the corresponding scheduled counterparts of variables. In MPC, moreover, the perfect matching constraint should be replaced by the updated version of it taking into account the forecast values. Similarly, the demand should be perfectly met by the available resources on the microgrid and/or the distribution system. It should be noted that in an island mode, the MGCC may shut down some non-critical loads to maintain service for critical ones. In such a case the demand quantities in the MPC problem should be replaced by just the critical loads concerned.

The objective function of an MPC problem, conventionally, is a summation of various quadratic costs. This form of objective function results in a convex problem provided that the associated constraints satisfy the convexity conditions as well. Availability of efficient quadratic solvers makes it straight-forward to formulate the problem in such a way as what Anderson *et al.* used [149]. A general form of this type of cost function is:

$$J_{\text{quad}} = \sum_{k=0}^{N-1} (\boldsymbol{x}_k - \boldsymbol{x}_{\text{sch},k})^T Q (\boldsymbol{x}_k - \boldsymbol{x}_{\text{sch},k}) + (\boldsymbol{u}_k - \boldsymbol{u}_{\text{sch},k})^T R (\boldsymbol{u}_k - \boldsymbol{u}_{\text{sch},k}) \tag{4.19}$$

Although simple and convenient to solve, quadratic programming approach does not reflect the realistic financial costs of a technology, which is the major concern for actual implementation. For example, the cost of using fuel in a gas engine is a linear cost; the cost of using two units of fuel is twice of using one unit. Also, the degradation cost can be better approximated by norm-1 costs. Thus, the costs introduced in the day-ahead optimization part are modified to capture the deviation costs here.

4.5.1 Recursive Feasibility

In an MPC framework, an online procedure repeatedly solves an optimization problem to specify a set of control actions that minimizes an objective function. This framework is

interesting as it can work with uncertainties that a system may face in reality. But unlike the conventional controllers, where the control input is pre-calculated and available, an MPC procedure is not guaranteed to be feasible inherently; solving the optimization problem may fail after some steps, and the problem will become infeasible. Thus, it should be guaranteed that the solution at one step does not violate feasibility of the problem in the successive steps. This condition should be taken care of a-priori. The standard approach in dealing with this problem is to add a final state constraint or a final state cost to the original problem. The former method comes either in the form of an equality constraint or putting a boundary around the final state, while the latter approach alters the cost function with an additional term as a function of the final state

In the present study, the terminal constraint technique is used for maintaining the feasibility of the problem. The developed terminal constraint guarantees recursive feasibility for the problem and is derived from the viable set concept in control theory. The constraint of interest when added to the original problem provides a sufficient condition for fulfilling recursive feasibility requirement, and is derived from the physical characteristics of system elements.

As a descriptive example, consider a storage device the state of which is determined by its stored energy E_k at time step k and its instantaneous output power P_k. The difference equation that describes the device behavior is given by eq. 4.1. As an extreme case, assume that the device is working at its maximum power capacity and has almost run out of its stored energy, meaning that $E_k \approx 0$. It can be seen that with a limited ramping capacity which is the control input of the device, it is not possible to avoid violation of the minimum energy constraint in the successive time step $k + 1$. In other words the amount of stored energy will become less than zero, making the problem infeasible.

In Fig. 4.9, a scheme of possible vector fields $f(x_k, u_k)$ associated with the studied problem is depicted by a spectrum of arrows. Associated with each state, there is a spectrum of fields $f(x_k, u_k)$ that can exist depending on the chosen value of the control input u_k.

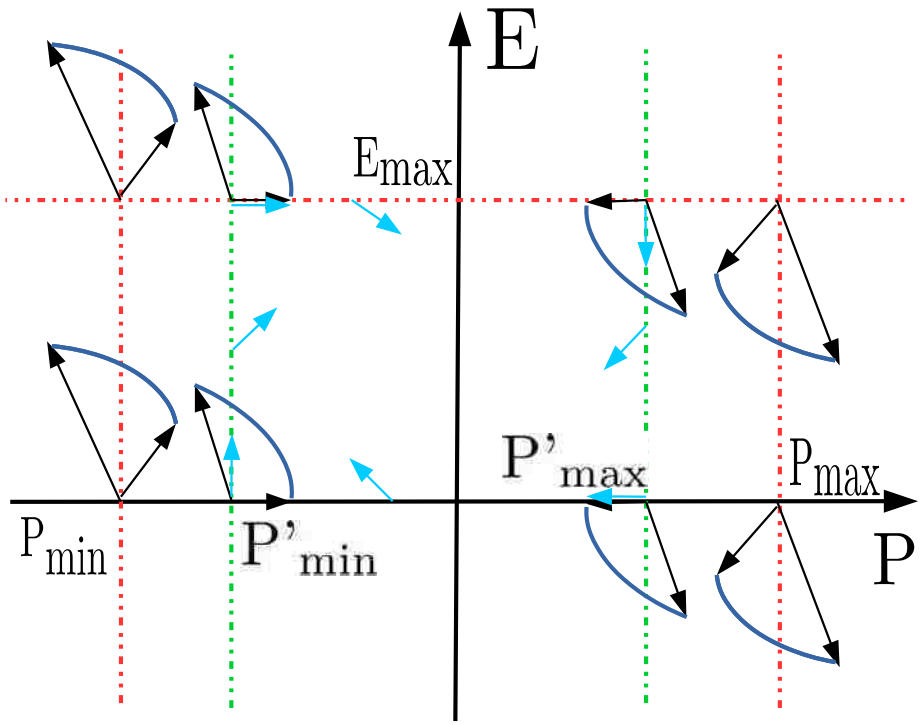

Figure 4.9: An spectrum of vector fields associated with $f(x_k, u_k)$. The green boundary depicted by $P'_{\min} \leq P_k \leq P'_{\max}$ and $E_{\min} \leq E_k \leq E_{\max}$ is a subset of the viable set corresponding to the system of interest.

Another concept is the viable set, discussed in section 4.6. Briefly, a viable set is a subspace of the state space for which there exist control input associated with each state that guarantees the successive states will not leave the subspace of interest. Using the viable set associated with the dynamical model of the system, a recursive feasibility condition will be developed.

Lemma. For the admissible set of ramp rate input signal $u_{\min} = -u_{\max} \leq u_k \leq u_{\max}$, the subset of the state space specified by

$$\begin{aligned} 0 \quad &\leq \quad E_k \quad \leq \quad E_{\max} \\ P'_{\min} = -P'_{\max} \quad &\leq \quad P_k \quad \leq \quad P'_{\max} \end{aligned} \tag{4.20}$$

is a subset of the viable set, where

$$P'_{\max} = \text{min. } \{\frac{t_s}{2} u_{\max}, \frac{E_{\max}}{t_s}\} \tag{4.21}$$

Proof. The claimed boundary set determines a rectangle in the state space. It is shown that on the sides of this rectangle there exists a vector filed, the direction of which is towards inside of the boundary. Here, the proof for two successive sides of the rectangle is provided. The proof for the other two sides is similar and straight-forward.

First, it is assumed that the boundary of the rectangle is determined by $0 \leq E_k \leq E_{\max}$ and $-\frac{t_s}{2}u_{\max} \leq P_k \leq \frac{t_s}{2}u_{\max}$. Consider the side of the rectangle that is determined by $E_k = 0$. For the state with $P_k = \frac{t_s}{2}u_{\max}$ on this side, it suffices to choose $u_k = -u_{\max}$ to make sure that the direction of the vector is not outwards with respect to the rectangle. For all states with $E_k = 0$ on the rectangle for which $P_k \leq \frac{t_s}{2}u_{\max}$, choosing $u_k \geq -u_{\max}$ (which is permitted) guarantees that $E_{k+1} \geq 0$.

For the state $(E_k, P_k) = (0, -\frac{t_s}{2}u_{\max})$ which is the intersection of two sides of the boundary of interest, choosing $u_k = 0$ results in the vector field to be $(\frac{t_s^2}{2}u_{\max}, 0)^T$ meaning that the successive state will be $(\frac{t_s^2}{2}u_{\max}, -\frac{t_s}{2}u_{\max})^T$. Thus, the direction of the vector field will not be outwards with respect to the rectangle again. Also, for all the states on this side of the rectangle with $P_k = -\frac{t_s}{2}u_{\max}$, it suffices to choose $u_k \geq 0$ to make sure that $P_{k+1} \geq -\frac{t_s}{2}u_{\max}$, meaning that the direction of the field will be towards inside the boundary.

The only condition that should be considered here is to make sure that choosing the control action of $u_k = 0$ will not cause the successive state to lie outside of the boundary. If the intersection of the two so far considered sides is specified by $(E_k, P_k) = (0, -P')$, choosing $u_k = 0$ results in the successive state to be $(E_{k+1}, P_{k+1}) = (t_s P', -P')$. It is now just needed to make sure that $t_s P' \leq E_{\max}$, meaning that $P' \leq \frac{E_{\max}}{t_s}$. This condition now can be merged with the primary boundary $P' \leq \frac{t_s}{2}u_{\max}$, resulting in the boundary $P_k \leq P'_{\max} = \text{min. } \{\frac{t_s}{2}u_{\max}, \frac{E_{\max}}{t_s}\}$. Note that for the other intersection state $(E_k, P_k) = (0, P')$, the successive state is guaranteed to stay on the boundary, given that by choosing $u_k \geq -\frac{2P'}{t_s}$.

Following the same analysis, it can be shown that there exists control input u_k for each state x_k on the other two sides of the specified rectangle which guarantees that the successive

states will not leave the boundary. The dynamical system of interest with the guaranteed set of control inputs determined over the specified boundaries now provides a closed-loop system for which the Poincare-Bendixon criterion is met [155]. Consequently, each state staring within the specified boundary will stay in the boundary.

Following the above lemma, it is claimed that appending the original MPC problem with the terminal constraint defined by the specified boundary guarantees the recursive feasibility of the problem.

Theorem. For the MPC problem defined as the recursive programming:

$$\begin{aligned}
\underset{\underline{\boldsymbol{U}}_i=\{\underline{\boldsymbol{u}}_i,\cdots,\underline{\boldsymbol{u}}_{i+n-1}\}}{\text{minimize}} \quad & J(\underline{\boldsymbol{x}}_i,\underline{\boldsymbol{u}}_i,\ldots,\underline{\boldsymbol{u}}_{i+n-1}) = \sum_{k=0}^{n-1} J_k(\underline{\boldsymbol{x}}_{i+k},\underline{\boldsymbol{u}}_{i+k}) \quad i=0,1,\ldots \\
\text{subject to} \quad & \underline{\boldsymbol{x}}_{i+k+1} = A\underline{\boldsymbol{x}}_{i+k} + B\underline{\boldsymbol{u}}_{i+k} \qquad k=0,1,\ldots,N-1 \\
& \underline{\boldsymbol{x}}_{\min} \leq \underline{\boldsymbol{x}}_{i+k} \leq \underline{\boldsymbol{x}}_{\max} \\
& \underline{\boldsymbol{u}}_{\min} \leq \underline{\boldsymbol{u}}_{i+k} \leq \underline{\boldsymbol{u}}_{\max} \\
& \underbrace{(0\ 1\ \ldots\ 0\ 1)}_{2m\times 1} \cdot \underline{\boldsymbol{x}}_{i+k} = P_{\text{ref},i+k}.
\end{aligned} \tag{4.22}$$

where $\underline{\boldsymbol{U}}_i = \{\boldsymbol{u}_i, \boldsymbol{u}_{i+1}, \ldots, \boldsymbol{u}_{i+N-1}\}$ and the quantities are the updated forecasts, adding the terminal constraint presented in eq. 4.20 guarantees the recursive feasibility of the problem.

Proof. Assume that for the time step $i = 0$, the problem is feasible. Thus, there exists a control input set $\underline{\boldsymbol{U}}_0 = \{\underline{\boldsymbol{u}}_0, \underline{\boldsymbol{u}}_1, \ldots, \underline{\boldsymbol{u}}_{N-1}\}$ for which the problem at the time step $i = 0$ is feasible. For the successive time step $i = 1$, the control input set $\tilde{\underline{\boldsymbol{U}}}_1 = \{\underline{\boldsymbol{u}}_1, \underline{\boldsymbol{u}}_2, \ldots, \underline{\boldsymbol{u}}_{N-1}, \underline{\boldsymbol{u}}_N = \bar{\underline{\boldsymbol{u}}}\}$ is considered. In this set, the control inputs $\{\underline{\boldsymbol{u}}_1, \underline{\boldsymbol{u}}_2, \ldots, \underline{\boldsymbol{u}}_{N-1}\}$ are taken from the control input set $\underline{\boldsymbol{U}}_0$. Thus, by applying these control actions, it is guaranteed that the state $\boldsymbol{x}_N$ lies in the subspace of eq. 4.20. In the lemma, it was shown that associated with each state within the boundary, there exists a control input, applying which guarantees that the successive state lies within the same subspace. If the corresponding control input with the specific state $\boldsymbol{x}_N$ that keeps the successive state within the same boundary is denoted by $\bar{\underline{\boldsymbol{u}}}$, then it can be concluded that the control input set $\tilde{\boldsymbol{U}}_1$ is a feasible solution for the MPC problem.

4.5.2 Simulation Results

The computational environment for simulation purposes of this study is MATLAB. Specifically, *CVX* which is an open-source MATLAB toolbox for convex optimization problems available in public domain is used [156], [157]. This toolbox is developed for disciplined convex programming, and thus, a good candidate for our developed convex problem.

As an example, a scenario where a net demand on a distribution feeder microgrid is supposed to be met by various available resources is considered. The day-ahead scheduling has determined the set points of each device based on normal operation conditions in the previous section. Then, the MPC is in charge of filling the gap between the actual and predicted net loads. This difference is fed as a reference signal into the MPC part. Then by solving the optimization problem, a re-dispatch process over the resources available takes place.

To make the case more interesting, it is assumed that one of the resources is not able to completely fulfill its predetermined contribution to the generation profile. For example, there is a stress on the grid which necessitates a reduction in the scheduled share of the grid to meet the demand. Such conditions can be induced by a range of conditions from a slight frequency regulation request to a severe disturbance such as a super-storm. This translates into a sharp change in the input signal of the MPC part of the framework. Two curves are shown in Fig. 4.10. The blue one (which is covered by the red signal for the periods of time that the two signals are the same) represents the uncontrollable net load for a regular case, which is the reference signal fed into the MPC mechanism. The red curve describes the case where the grid is undergoing a stress, and a portion of the scheduled power is lost accordingly.

The control framework in this study responds to a price-driven DR scheme. Thus, different prices are used for the MPC optimization problem than those of the day-ahead optimization part, reflecting unforeseen changes in operating circumstances. Moreover, it is assumed that a continuous service should be provided for the end-users. Thus, it is still possible to use

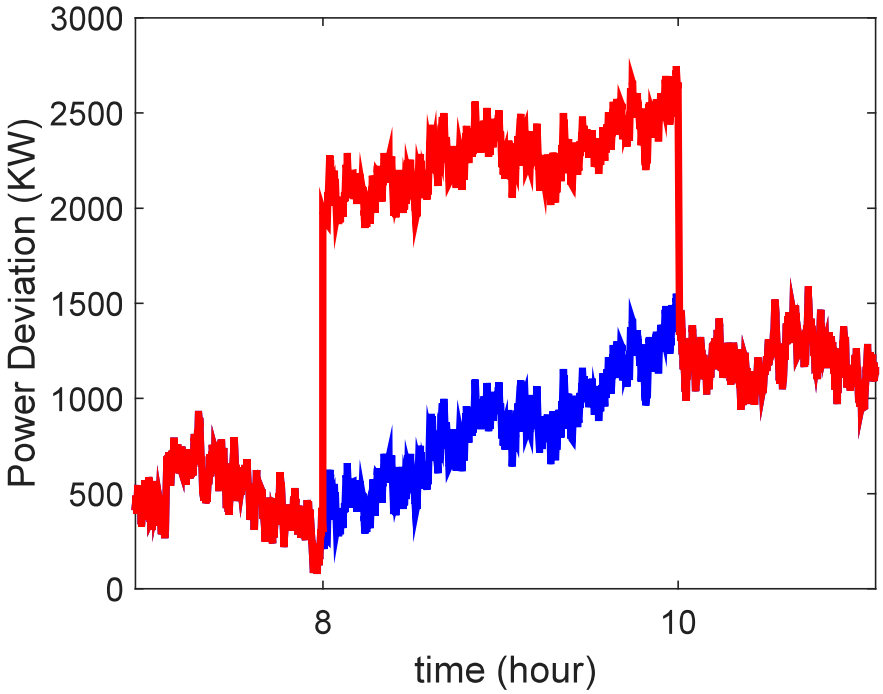

Figure 4.10: Example of a tracking signal fed into the MPC part of the control mechanism, under normal conditions (blue) and under stress (red).

the grid for meeting the demand, but with an excessive cost. For load reduction purposes, a slight increase in the grid tariffs suffices, while extreme costs can represent an emergency situation. Higher prices, no matter how much, can be used as a mechanism to direct the response of the microgrid in a way that it uses the grid less and possibly as the last resource, relying on its own local resources to the extent financially justifiable. It is assumed that this mechanism is used for a certain period of time within a day to induce a distribution feeder microgrid to reduce its demand, assisting the transmission system to handle the stress. In cases that the grid cannot provide service, MGCC can switch to island mode with the help of installed inverters on it. As an example, the system operator enacts step-wise increase in the price of power from 8 AM to 10 AM; the price of importing power from the grid during a stress situation is assumed 200 ¢/KWH. For the purpose of emergency response also the

utility is not able to provide advanced notice of energy prices.

In Fig. 4.11, the share of each resource for covering the deviation is shown during the request period. Because at 8 AM, the fuel cell has already started working with full capacity, it cannot provide any further capacity to help the MGCC for reducing the load on the grid. However, the BESS has been in the full charge state at 8 AM. The BESS had been supposed to deplete its stored energy at early evening, but as the price of importing power from the grid has been increased, the MGCC starts using this stored energy in the BESS at its maximum capacity. Note that the depicted powers show the contribution of each resource to the re-dispatch problem. Thus, the actual values should be calculated by adding-up these values to the scheduled ones.

In Fig. 4.12, the response of the microgrid to the reserve request is depicted for the time window from 8 AM to 10 AM. The scheduled power flow at the point of common coupling is depicted by the blue curve. In the absence of emergency situation, the actual power flow would have been what is depicted by the green curve. Finally, the red curve depicts the actual power flow at the PCC as a result of executing a load reduction scheme via the MGCC.

4.6 Appendix: Viable Sets

For the dynamical system

$$x_{k+1} = f(x_k, u_k); \quad u \in \mathcal{U}, x \in \mathcal{X} \tag{4.23}$$

the **Unsafe** set is defined as a subspace that is prohibited for all possible time within a time-window $\{0, 1, \ldots, \tau\}$. Also, the $\mathbf{Viab}^\tau$ set is defined as follows:

$$\mathbf{Viab}^\tau := \{x_0 \in \mathcal{X} | \exists u_t \in \mathcal{U}, x_t \notin \mathbf{Unsafe}; t = 0, \ldots, \tau\} \tag{4.24}$$

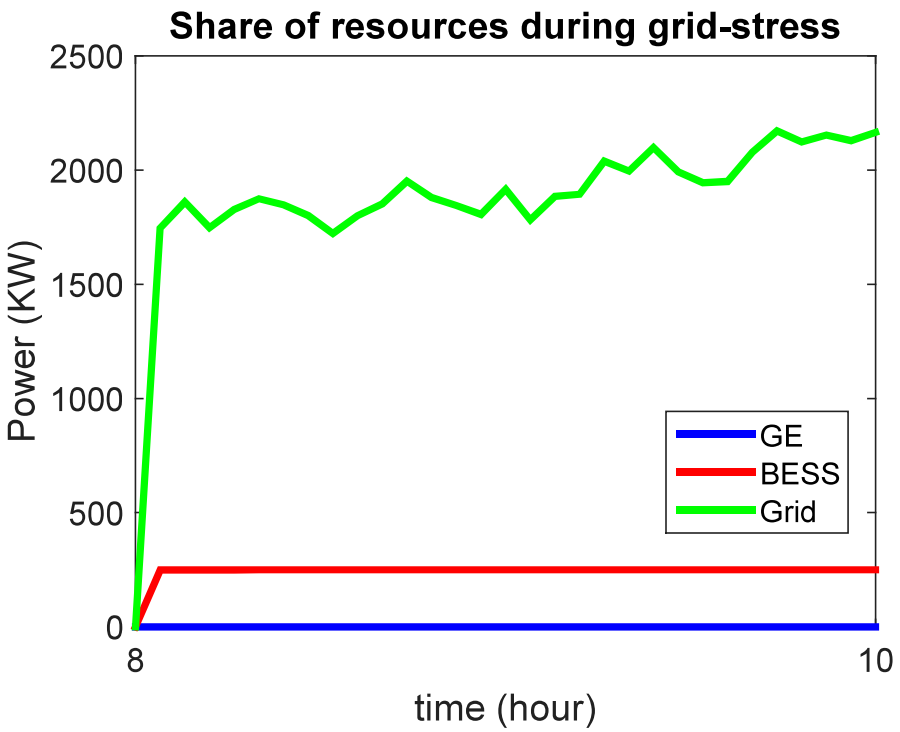

Figure 4.11: Contribution of each resource to the re-dispatch problem, induced by the grid-stress situation. The GE cannot contribute more as it has been already scheduled to work with its full capacity. The MGCC starts depleting the energy stored in the BESS at maximum power capacity.

It can be easily concluded that

$$\mathbf{Viab}^0 \supseteq \mathbf{Viab}^1 \supseteq \mathbf{Viab}^2 \supseteq \ldots \supseteq \mathbf{Viab}^\infty. \tag{4.25}$$

The term **Viab** refers to the $\mathbf{Viab}^\infty$ in this study.

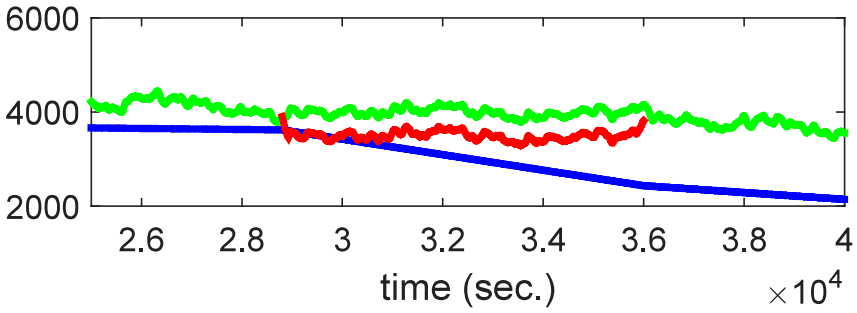

Figure 4.12: The response of the system for a load reduction request from the utility; Blue: scheduled load at the PCC, Green: actual power imported from the grid in the absence of an emergency request, and Red: reduced load at the PCC during the emergency period.

Chapter 5

Cascading Model Predictive Control

The framework introduced in the previous chapter, which was composed of a day-ahead scheduling and an online adjustment optimization in the form of a model predictive control, is extended here with respect to the computational complexity aspect of the dispatching problem.

5.1 Introduction

Deviations from the schedule are mainly the consequence of the fluctuations associated with either the load or renewable power generation. The MPC process optimally dispatches resources to compensate the mismatch between forecasts and actual system state values. Because the number of resources could be large, solution of this problem could become computationally expensive. Specifically it is shown in this chapter that the computational cost grows exponentially with the number variables. To reduce the size of the problem, the characteristics of each resource is matched to an appropriate part of the mismatch frequency spectrum.

Some resources are able to respond effectively to rapid variations, while some others are too

slow. On the other hand, fast devices may not have significant storage capacity, limiting their usefulness in applications where sustained power delivery or absorption is required. On the other hand, slow devices such as energy batteries or thermal storage systems are well-matched to the low-frequency part of the real-time versus schedule mismatch spectrum. Thus, decomposition of the deviations into various frequency bands seems reasonable.

5.2 Time Filter

The reference signal that must be tracked by resources dispatched by the MPC controller results from the net effect of deviation of renewable generation and the load from their schedule counterparts. For reasons of computational efficiency, a real-time digital series filter is used to decompose the mismatch signal into three frequency bands. The linear filter of interest has the general form of

$$y_n = \sum_{k=0}^{L} c_k z_{n-k} + \sum_{j=1}^{L} d_j y_{n-j}, \tag{5.1}$$

takes an input sequence $\{z_n\}$ and produces the output sequence $\{y_n\}$ [158]. In this study, $L = 2$ and $M = 1$. For a band-pass filter with the lower and upper bands a and b, respectively, the appropriate coefficients c_ks and d_js are determined as

$$\begin{aligned} c_0 &= -\tfrac{b}{(1+a)(1+b)}, \\ c_1 &= 0, \\ c_2 &= \tfrac{b}{(1+a)(1+b)}, \\ d_1 &= \tfrac{(1+a)(1-b)+(a-1)(1+b)}{(1+a)(1+b)}, \\ d_2 &= -\tfrac{(1-a)(1-b)}{(1+a)(1+b)}. \end{aligned} \tag{5.2}$$

In this problem, two different set of values are used as the tuple (a, b). The corresponding values are $(0, \frac{\pi}{300})$ and $(\frac{\pi}{300}, \frac{5}{100})$ respectively. These numbers are chosen from heuristic search in the available historical data. However, they can be replaced by other numbers that are derived from an optimal parameter selection routine. In an advanced extension, moreover,

these numbers can be chosen adaptively in cases that the available resources on a microgrid dynamically change, e.g. some resources fail. The outputs of these two filters are then added together and subtracted from the primary signal to generate the high frequency component of the signal. The application of this set of filters is illustrated in Fig. 5.1.

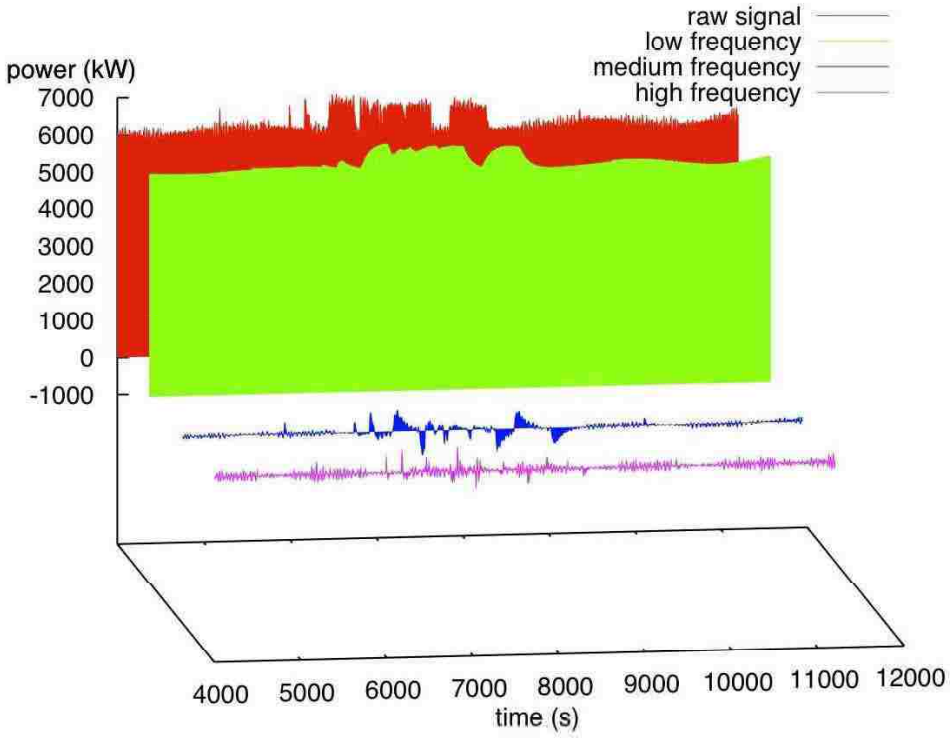

Figure 5.1: Decomposition of a typical signal, for example the net load on a feeder. The low frequency component carries a higher level of energy, while the higher frequency content of the signal encompass small values of energy.

The tracking signal shown in the red is decomposed into a slow signal shown in green, a medium speed signal shown in blue and a fast signal depicted in purple. Also, power spectral density (PSD) plots of the net load and the three associated components are shown in Fig. (5.2). It is illustrated that the applied filter could reasonably decompose the signal into appropriate bands, as each component has a frequency band in which most of its corresponding energy lies.

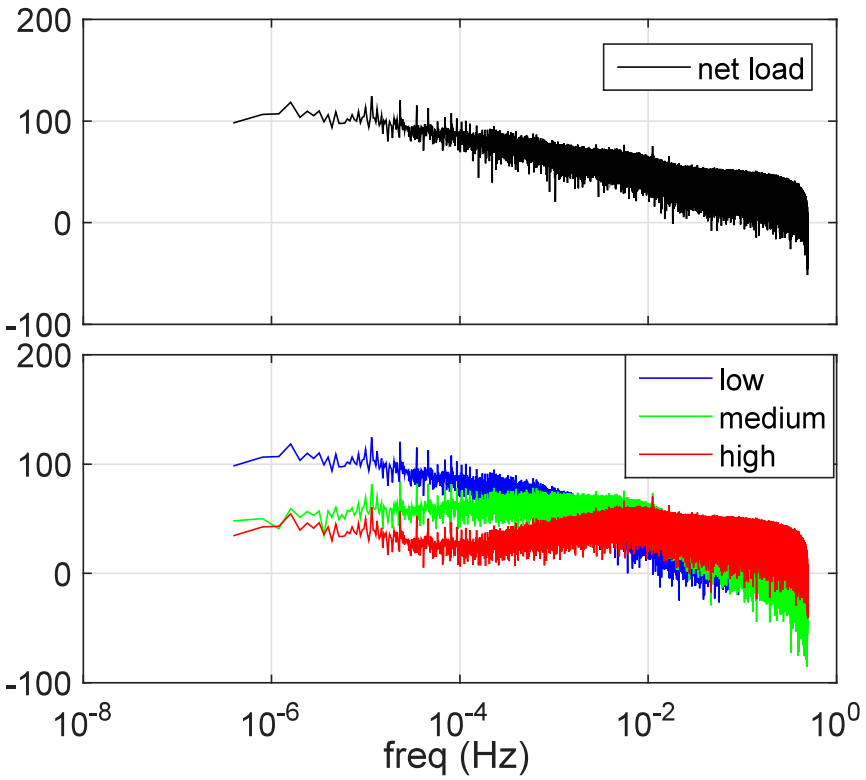

Figure 5.2: Power spectral density of the net load (top) and its filtered components (bottom). It is observed that each component has a frequency band in which most of its corresponding energy lies.

The time-scale characteristics of the slow, medium and fast signals are respectively:

Hour: This time-scale is associated with the share of variations that are slow but have high levels of energy. Examples of phenomena causing deviations in this time-scale are errors in average cloud cover forecast such as those typically provided by the National Weather Service in 1 to 3 hour-long intervals, or unpredicted failures in generation equipment. According to the slow rate of change, the sampling frequency that can capture this component can be in the order of a few minutes. The resources needed for the control purposes do not need to have a high ramp rate capacity, but they may need to have considerable amounts of power and energy capacities.

Minutes: This time-scale is the part of the problem which needs faster resources to respond, but not necessarily needing a significant energy capacity. Medium-speed deviations could be caused by demand-patterns or clouds intermittent occluding the sun. The sampling frequency in this time-scale should be in the order of about 10 seconds as highlighted in Fig.5.1.

Seconds: This category is addressing the portion of the deviations associated with the fastest fluctuations caused by start-up transient of devices or the edge of clouds passing in front of the sun. Thus, the sampling frequency is in the order of one second. The resources in this category need to have the highest ramp rates. However, the energy capacity can be relatively low.

Based on the above description, a cascading control mechanism is considered to follow a tracking signal. The decomposition component of the system subdivides the problem into three subproblems. A schematic of this structure is shown in Fig. (5.3).

In the cascading MPC framework, the low-frequency component of the tracking signal is addressed first. The time horizon for this component of the problem is 40 minutes discretized into 20 steps, each with a 120 seconds duration. Resources are allocated at each time step according to the solution of the optimization problem. The medium frequency tracking signal is obtained by first subtracting the low-frequency response from the master signal and then applying a band pass filter with appropriate range. The MPC algorithm dispatches medium frequency resources with the time horizons of 200 seconds discretized into 20 time intervals, each with 10 seconds duration. Finally, the high-frequency tracking signal is obtained by subtracting the low and medium responses from the master signal. Fast resources are similarly dispatched by the MPC process on the time horizons of 20 seconds discretized by $20 \times$ 1-second time steps.

5.3 Numerical Example

The ability of the proposed structure in reserve request problem to reduce the stress on the grid is evaluated here. For this purpose, a real-time pricing (RTP) mechanism is used to affect the amount of load on the grid placed by the distribution feeder microgrid of interest. The characteristics of the resources are summarized in Table 5.1, where a set of plausible specifications of resources that could be found on a distribution feeder is presented, including conventional ones such as batteries, and unconventional ones such as load-following chillers, ventilation fans and TCLs. In addition, it is assumed that uncontrollable distributed generations, in the form of a large PV array, is present in the system, and acts as a negative load.

Except for the energy battery that has a degradation cost, all other resources come with zero cost. The rationale behind this assumption is that the associated cost with them has

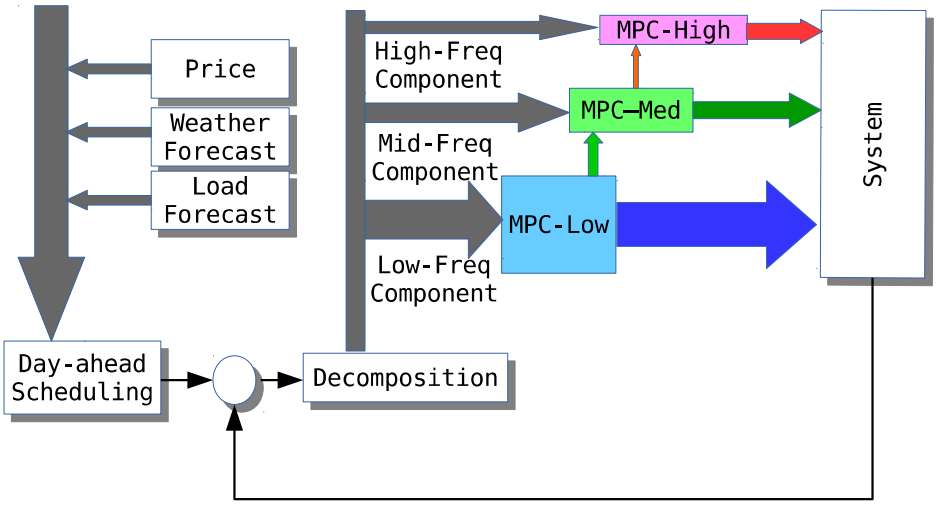

Figure 5.3: Configuration of the control mechanism studied here. The day-ahead scheduling set points optimized in advance are adjusted throughout the day by cascading MPC structure.

been already considered when importing power from the grid to place their state within their associated dead-band. Also, non-conventional resources such as load following chillers offer their storage capacity for operating reserve services as an auxiliary task, and not as a primary task. Furthermore, resources that come with significant ramping capacity offer less energy storage capacity, and vice versa.

The problem considered here is the case where the system is working based on a regular routine for which the day-ahead scheduling has been previously solved. However, as a result of a system level emergency, a rapid load-shed is requested from the microgrid. To achieve the desired result, the system operator enacts step-wise increase in the price of power from 8 AM to 10 AM. As mentioned in the previous chapter, the emergency situation acts translates into a sharp change in the reference input signal of the MPC part. An example of the reference input signal as well as its decomposition into three different frequency bands are shown in Fig. 5.4.

The low frequency content of the reference signal is then fed into the MPC part of the control framework that is associated with local resources that are more appropriate to deal with such a component. The part of the low frequency component of the reference signal that is not met by the corresponding low frequency MPC is combined with the medium range frequency component of the original signal and fed into the part of the MPC framework that is associated to work with resources that respond faster. The procedure follows the structure

Table 5.1: Resource Characteristics for Cascading MPC

Resource	Power capacity	Energy capacity	Ramp rate
Energy Battery	[-250,250] KW	1000 KWH	1.67 %/sec
Chillers	[-150,150] KW	300 KWH	0.56 %/sec
Ventilation system	[-150,150] KW	300 KWH	20 %/sec
Ventilation system	[-50,50] KW	100 KWH	40 %/sec
TCLs	[-300,300] KW	25 KWH	100 %/sec

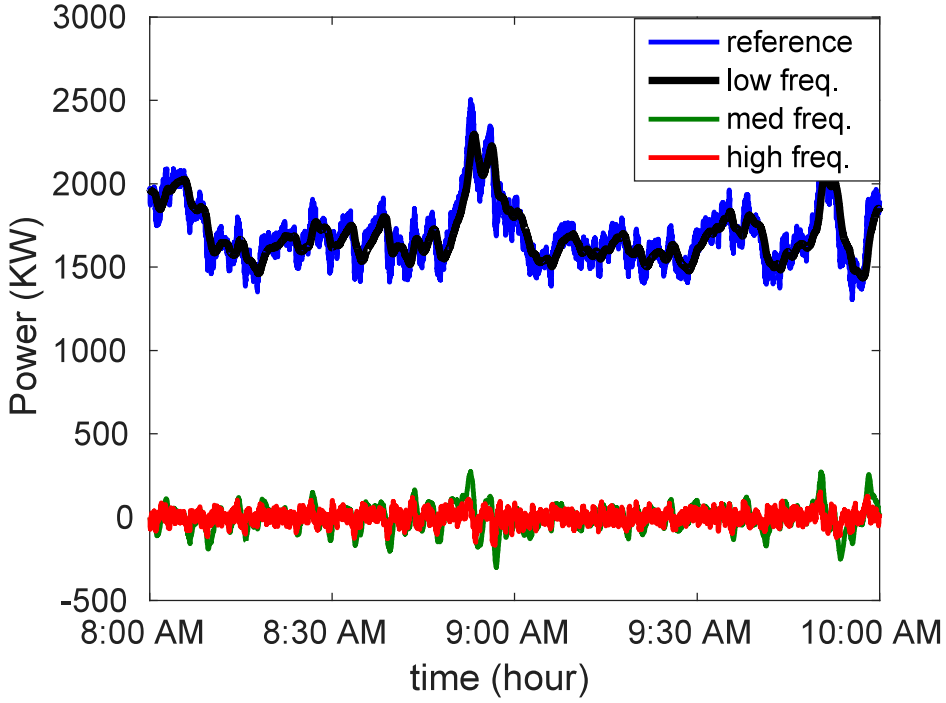

Figure 5.4: An example of the reference input signal and its decomposition into three frequency bands.

shoudn in Fig. 5.3. In Figs. 5.5, 5.6, 5.7 the share of each resource in low, medium and high frequency categories is shown respectively during the request period.

In the collection of the available resources, chillers and ventilation systems are present. As be hysteresis-driven loads, they are treated similar to an energy storage device such as a battery. It is assumed that the specified levels of change over the aggregated capacity of such devices do not affect the behavior of the loads in the system in comparison with their overall power consumption.

The available resources in the low frequency part of the MPC problem start working with their maximum power capacity. However, they are not able to fully cover the requested power reduction. Because chillers are assumed to have the energy capacity of working for 2 hours at their maximum power capacity, moreover, their collective contribution falls after a

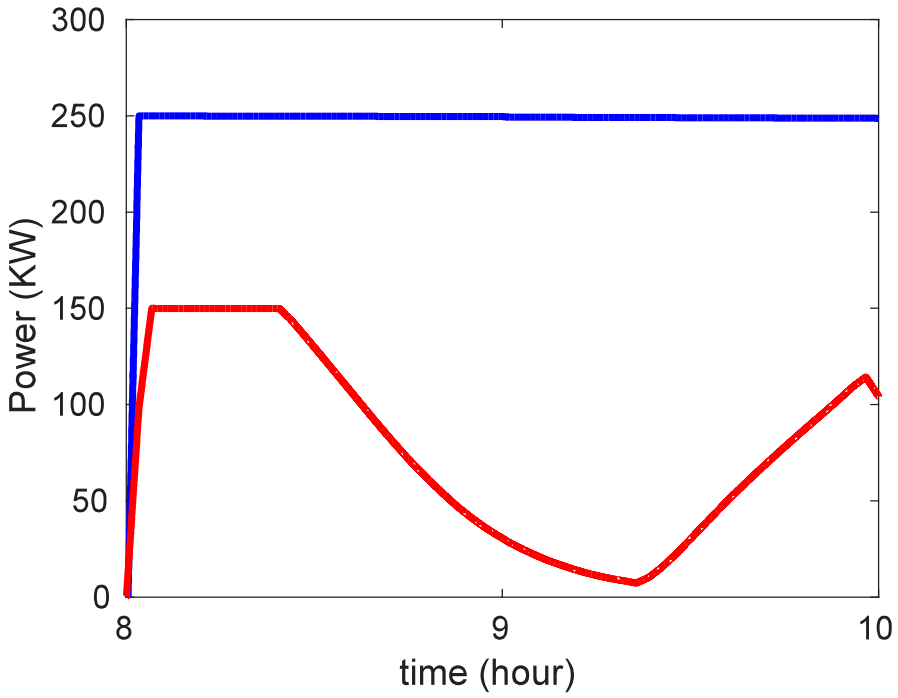

Figure 5.5: Contribution of the energy battery and chillers to the demand reduction request in the low frequency part of the problem.

while due to the recursive feasibility constraint added to the online optimization. Also, the medium and high frequency components of the master signal are completely absorbed in the microgrid by the corresponding resources.

The advantage of using this cascading form is in reducing the computational costs. In Fig. 5.8, the computational cost in terms of the actual time needed to solve the low-frequency part of the problem by MATLAB in an 8GB RAM, Intel Core i5-3470 CPU @ 3.20 GHz machine running under Windows 8.1 operating system is shown.

Based on the derived computational times, the problem grows exponentially by the length of the MPC horizon. Also, increasing the time resolution of the problem, reflected in t_s, significantly increases the computational complexity. Even more, it is not possible to solve

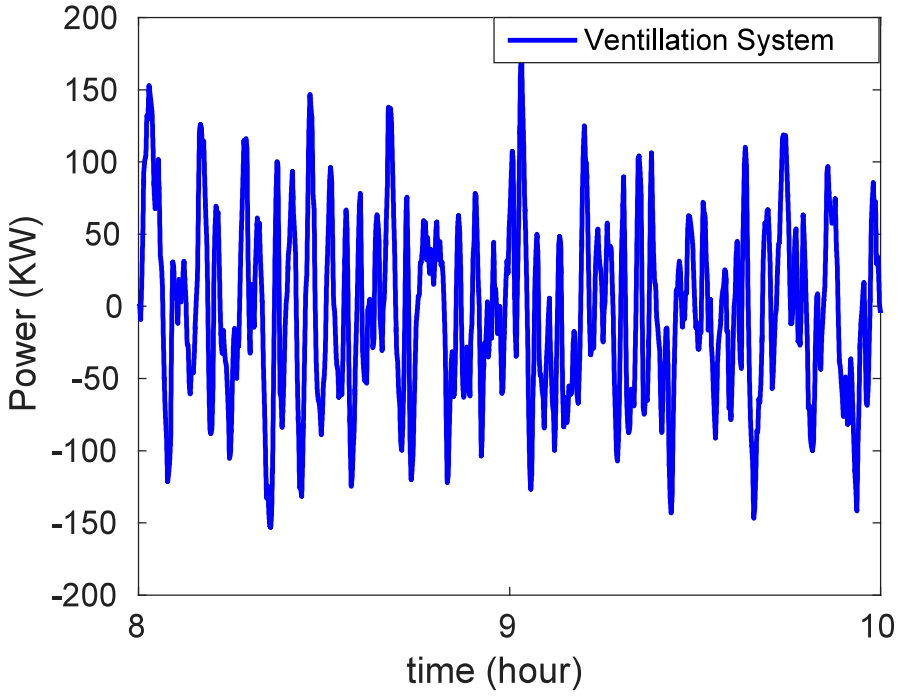

Figure 5.6: Collective contribution of the ventilation systems in the medium frequency range of the MPC framework.

the MPC problem with a certain horizon after passing a time resolution threshold. This is mainly because of the low ramping capacity of available local resources that are not able to meet the terminal constraint that ensures recursive feasibility. More precisely, a local resource needs a minimum amount of time that its state reach the subspace that ensures recursive feasibility. Increasing the time resolution by reducing the sampling time, necessitates to increase the horizon to a minimum amount to avoid infeasibility.

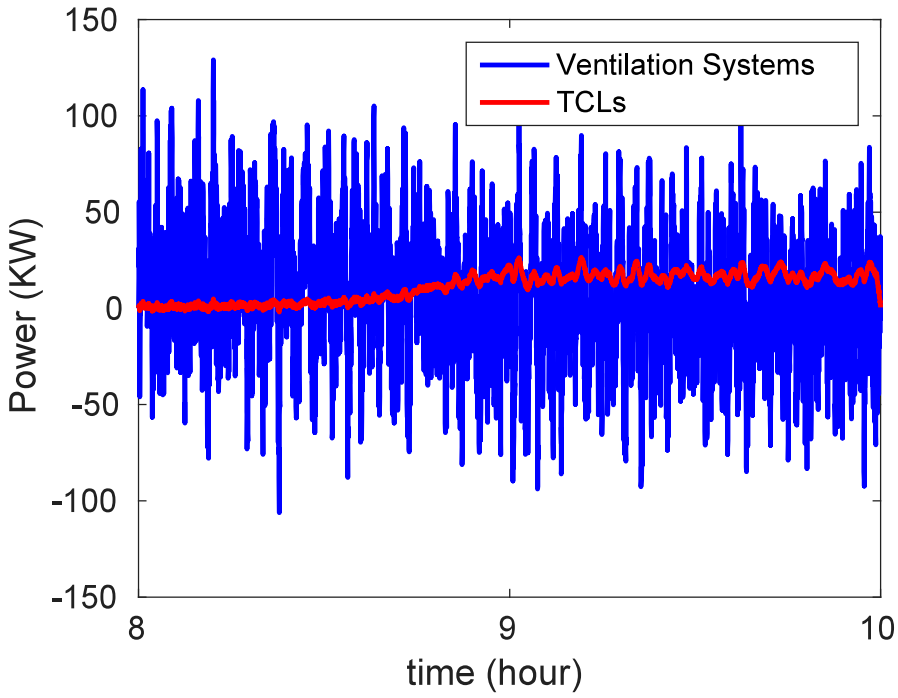

Figure 5.7: Collective contribution of the ventilation systems and TCLs to the demand reduction request. The resources utilized in this part of the problem, completely absorb the high frequency fluctuations.

5.4 Discussion

In the studied example of this chapter, two local resources were used in each mode of the MPC problem. In reality, the number of resources can hypothetically increase to an arbitrary number that consequently increases the computational cost. Due to the real-time nature of the problem, it is thought that faster processors are essential, especially for higher frequencies.

It is also showed that separation of the reference signal into various frequency bands came with the advantage of saving computational efforts that can yield to extending the horizon of the dynamic programming problem to the order of an hour. This was done by increasing

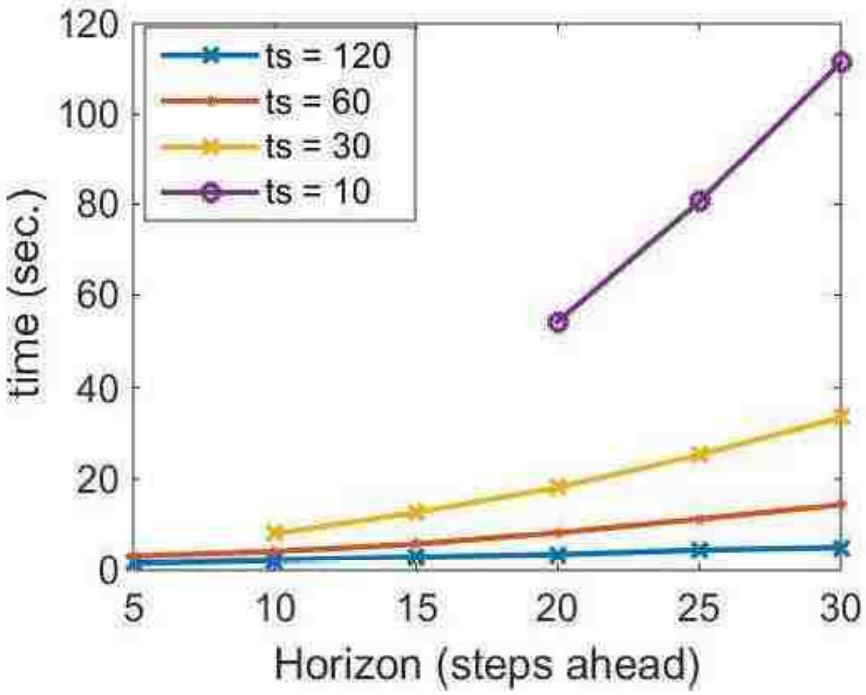

Figure 5.8: Computational complexity diagram for low frequency procedure. As the time resolution of the problem is increased, the computational cost in terms of the time needed to solve the problem is increased.

the sampling period, and achieving the essential performance without compromising system stability. As well as the computational cost, deploying non-conventional distributed resources provide an opportunity to reduce the size of electrical storage. In fact, a kind of storage is needed to meet the demand which is generally met by utilizing batteries. Non-conventional resources can replace batteries in case and reduce the costs.

Chapter 6

Distribution Feeder Microgrids And Grid Reconfiguration

Although the power system in the United States, arguably one of the most complex engineered systems, has evolved to provide an extensively reliable electricity resource, the last decade was marked by numerous large blackouts that raised questions about the system's resiliency against severe disturbances. The control paradigm of the power system is altered, and the potential associated with reconfiguration of the control architecture based on a recently proposed platform for stress mitigation purposes is evaluated quantitatively in this chapter. The results of the proposed reconfiguration are promising in the sense that the studied transformation shows a significant improvement in grid's reaction against severe disturbances. Such an improvement is two-folded; the system reacts faster yet endures longer against disruption. The reconfiguration of interest also shifts the network towards a more decentralized system in comparison to the current highly centralized structure.

6.1 Introduction

Disruptions that the U.S. power system is exposed to have the potential of triggering large blackouts. According to the President's Council of Economic Advisers, the U.S. Department of Energy (DoE)'s Office of Electricity Delivery and Energy Reliability, and the White House's Office of Science and Technology, 670+ widespread power outages in the United States between 2003 and 2012 were induced by severe weather conditions [9]. The (inflation-adjusted) average annual net cost of weather-related power outages has been approximated as between US$18 to US$33 billion.

Severe weather conditions are not the only cause of failures in the system. Malicious attacks in the future can put the electricity infrastructure at risk of large blackouts with the cost of billions of dollars. Whether the electricity infrastructure can better handle unpredicted stresses, including weather-related ones, has become a main concern in the power engineering society. There has been a significant number of studies recently on modeling and analyzing the observed large blackouts in order to design appropriate mechanisms that can mitigate system vulnerabilities. Baldick *et al.* [16] have provided an initial review on the essential concepts, methods and tools needed for analyzing what happens in large outages. Also, Hines *et al.* [8] have studied large blackouts in North America from a statistical point of view; the occurrence frequency of large blackouts conveys information that can be used for planning purposes in the power system.

Moreover, the importance of implementing a new architecture for the power system to better handle disruptive stresses on the grid has been addressed in several studies, e.g. by Che *et al.* [22] that emphasized on utilizing microgrids to mitigate large disruptions on the grid or by Ramakumar *et al.* [118] that have reported the benefits associated with implementing microgrids for the resiliency and efficiency purposes at both the transmission and the distribution layers of the grid. The new proposed platforms are not limited to the concept of microgrid. Virtual power plant concept has also been addressed in this regard [21]. These two platforms

offer finer control over loads in the system via reconfiguring the control architecture of the grid. Along with offering an improvement in the resiliency of the system, these architectures provide opportunities for extending resource heterogeneity in the generation-mix.

In the current study, the potential associated with a recently proposed platform by Yasaei *et al.* [159] for power system structure to improve system robustness against disturbances is investigated. The platform is based on a special type of microgrid, namely the distribution feeder microgrid. Reconfiguration of the power system architecture based on this platform shifts the grid towards having a more decentralized structure than the current highly centralized one. Specifically, the potential of such an architecture to suppress/mitigate stress is evaluated in a probabilistic sense. Also, a connection is made between the present study and a recently published paper by Rahnamay-Naeini *et al.* [35], where the authors have provided a framework to characterize the cascading component failures phenomenon in a power network as an important underlying mechanism of large blackouts.

The remainder of this chapter is structured as follows. In section 6.2, a literature review on the effect of system structure on its resiliency is provided. The concept of microgrid and the potential associated with it for mitigating stress on the system is reviewed. This chapter is, then, continued with a specific type of microgrid in section 6.3, namely distribution feeder microgrid. The influence of load on cascading component failures when the system is under stress is also discussed. Opportunities that a reconfiguration of the system architecture around this type of microgrid can offer for mitigating stress is assessed in a probabilistic sense in section 6.4, and a discussion is provided in section 6.5.

6.2 Large Blackouts and The Structure of the Network - Literature Review

Cascading component failures is a well-known phenomenon that describes what has happened in many large blackouts [15]. In a cascading failures event, a disruptive factor imposes stress on the grid, and causes component failures in a part of the grid. The induced failures consequently impose further stress on the grid, and a chain of outages propagates in the network, resulting in a large blackout [17, 18]. In such a situation, the amount of load on the system as well as the capability of the control mechanism to exert remedy reactions in proper time are two major factors in the progress of component outages [20, 19].

The load in the system affects the frequency stability via the supply-demand balancing issue. A mismatch between the load and the demand causes a deviation in the system frequency. Once the deviation becomes excessive, protection relays trip generation sources. Failure of supply facilities, moreover, increases the stress on available generation sites, which consequently increases the power flow on the corresponding transmission lines to meet the unchanged demand. Lines also fail once the power flow passing through them exceeds their capacity. This phenomenon was among main causes of what happened during the August 2003 large blackout [15]. A possible approach in the current control paradigm to deal with cascading failures event would be directed load curtailment. For a modern paradigm, however, a microgrid-based architecture seems a compelling solution for stress mitigation purposes as it addresses two major concerns at the same time; load and control architecture.

According to the DoE, a microgrid is a group of interconnected loads and distributed energy resources with clearly defined electrical boundaries that acts as a single controllable entity with respect to the grid and can connect and disconnect from the grid to enable it to operate in both grid connected or island mode [23].

As stated by Asmus [21], “perhaps the most compelling feature of a microgid is the ability

to separate and isolate itself from the utility's distribution system during brownouts or blackouts". This feature, when considering the cascading component failures phenomenon, is promising for mitigating stress on the system as it is possible to completely disconnect an entity and its associated load from the grid in the worst case scenario in a contingency. This is different from a regular load curtailment scheme as a microgrid is still able to serve its critical loads autonomously, even in an island mode, whereas in a simple load curtailment all loads lose their service uniformly.

A special type of microgrid, namely, the distribution feeder microgrid has received attention recently [160]. In this type of microgrid, a distribution feeder adopts a microgrid structure, and provides a controllable entity to the utility company at the point of common coupling (PCC). This adoption is facilitated in part by an appropriate control mechanism that can address performance objectives as well as stability requirements. Also, the switching mode of the distribution feeder microgrid structure is implemented via inverter-based technology that connects such a structure to the distribution system. The controllability feature of the distribution feeder microgrid is derived from integration of different types of distributed energy resources (DERs) available on the corresponding feeder. Distributed resources include but are not limited to local fossil fuel generation, battery energy storage systems (BESSs), dispatchable loads as well as renewable resources such as solar photovoltaic (PV) panels. The Borrego Springs microgrid, owned by the San Diego Gas & Electric (SDG&E) utility company, is an example of such a structure.

In another work, Yasaei *et al.* developed an appropriate control platform to be used as the central controller needed to facilitate turning a distribution feeder into a microgrid [159]. In the designed platform, a control mechanism is in charge of optimal integration of distributed resources as well as meeting stability requirements. Specifically, the frequency stability of the system was concerned in [159]. As the microgrid central controller (MGCC) maintains the internal stability of the microgrid, the aggregated capacity of available resources can be used as a whole by system operators in load management schemes [145].

In this study, the previous work [159] has been extended to statistically characterize the potential of a distribution feeder microgrid-based architecture for the power system control mechanism in reducing the chance of outage propagation during a cascading failure-induced blackout. This is performed by a stress reduction application, deploying distributed resources available on distribution feeders.

6.3 Cascading Component Failures, Load and Distribution Feeder Microgrids

Controllability of load plays an important role in mitigating stress on the grid, especially during a cascading event, and preventing large blackouts. In this section the improvement that a microgrid can offer for the controllability of the system is discussed.

6.3.1 Cascading Component Failures and Effect of Load

The probabilistic model for cascading failure in a power network provided by Rahnamay-Naeini *et al.* [35] describes such a phenomenon by a Markov model-based dynamical system. The model is based on a network of interconnected substations (nodes) through lines, and is denoted by the term *stochastic abstract-state evolution* (SASE). The SASE model captures the main attributes of a power system that influence propagation of failures in a cascading event and provides conceptual knobs for reducing the chance of successive failures in a probabilistic way.

A standard practice in dealing with cascading component outages event is load curtailment. This approach can reduce the stress on the system and consequently mitigate the chance of further outages as reported in [35]. Moreover, Rahnamay-Naeini *et al.* studied the effect of the ability to curtail substation loads on the progress of failures in a probabilistic sense.

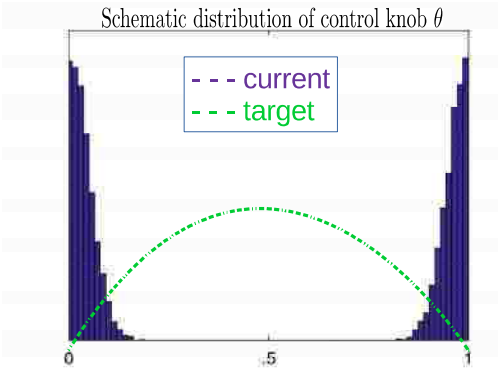

Figure 6.1: Schematic representation of the distribution of the controllability knob θ. Currently, it has a bimodal behavior; no control or complete cut off. The objective is to distribute it over the current extremes.

Such a capability which has roots in the control architecture of the system was represented by the parameter θ in their study. This parameter indicates a uniform partial controllability over a substation load, using a number between 0 and 1. The more controllable substation loads are, the less chance of further outages is.

Moreover, load control is limited to shutting down the demand, or at best to limited demand-response (DR) schemes activated by load aggregators in the current power system control paradigm. Due to the limits of the load control over a substation, there is a bimodal distribution for θ, with two sharp peaks corresponding to full-service (no-load-shedding) and complete cut off respectively, and nothing in between. A schematic distribution of the control knob over substation load is shown in Fig. 6.1 for two cases: current situation versus targeted one in the future. The objective is to distribute the control knob over the current extremes.

The current situation limits the ability of grid operators to use load-shedding as an effective tool to enhance system robustness. Specifically, there is a reluctance to shed load because of the drastic reduction in service at the affected substation, not to mention the cost of compensation that a utility company may have to pay in return for cutting the service to the

consumers. Also loads are likely removed from the system when the window of opportunity for corrective action may have passed. Even worse, a shut down action may not only reduce the load, but also generate a new peak in the system at a later time [161], which is known as the rebound effect. For example, once cooling load of buildings come back to the grid after being cut for a while in a hot summer day, they put a significant demand on the network simultaneously. Consequently, the grid faces a peak that potentially can have a destabilizing effect.

The question is whether it would be possible to provide a load reduction scheme without excessive disruption to end-users' quality of service (QoS). More precisely, if the load of a substation/node becomes at least partially controllable, system operators can use it as an elastic resource for an optimal dispatch process. Such an elasticity of loads empowers system operators when dealing with a disturbance, and thus, improves system resiliency [20].

6.3.2 Distribution Feeder Microgrids and the MPC-Based Control Mechanism

The suggestion of this study is to replace the load curtailment policy in the SASE model by controllable entities that are equipped with the proposed control mechanism suggested by Yasaei *et al.* in [159]. The goal is to smooth the current load curtailment limited schemes between the two aforementioned extremes (zero load shed versus total shut down) by enabling/increasing the controllability of loads. Specifically, there is a potential to capture a significant collective capacity through an aggregation over a considerable number of substations in a power network that have adopted a distribution feeder microgrid architecture. The resultant controllability over substation nodes makes it less threatening for grid operators to access the "control knob" θ. This approach is aligned with the recently published study by the electric power research institute (EPRI) in which the benefits of a grid connected microgrid is discussed in detail [162].

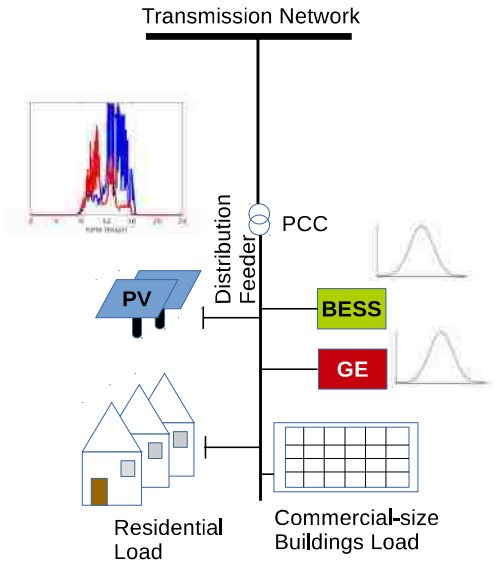

Figure 6.2: Example of a distribution feeder microgrid. Two main local DERs are gas engine and battery energy storage system. The feeder of interest also embodies distributed solar PV generation, which is treated in an aggregated form and as a negative load.

The platform of interest consists of two parts: infrastructure and control. The infrastructure coincides with the physical implementation of a system based on distribution feeder microgrid structure. In this structure a distribution feeder acquires many of the characteristics of a microgrid, presenting itself to the outside world as a single controllable load. Although this structure is defined at the distribution level, the enhanced level of controllability provided boosts the stability of the the power system at higher levels against major disturbances.

The prototype distribution feeder microgrid considered here has an architecture with high photovoltaic (PV) penetration in either centralized (utility-owned) or distributed (customer-owned) forms, supported by large storage batteries, combined heat and power (CHP) and two forms of real-time demand-response, designed for the residential and the commercial sectors respectively. In Fig. 6.2, a scheme of a typical distribution feeder microgrid is shown.

The platform of interest also follows the current trend to shift from a centralized structure to a more decentralized one capturing under-utilized capacity of distributed energy resources [163]. The trend towards increased use of distributed resources for meeting power demand also necessitates new control policies. The control mechanism by Yasaei *et al.* [159], which is also used here, is closely aligned with this trend, and constitutes the second part of the platform. It is composed of a dynamic programming problem formulated as a day-ahead optimized scheduling combined with model predictive control (MPC).

In the day-ahead scheduling part, an optimization problem is solved to determine the set points of various devices on the microgrid to minimize the cost of meeting the demand based on the variable price of electricity provided by the grid and forecasts of load and local renewable generation.

Based on the fact that no forecast is perfectly accurate, an online dispatch controller adjusts the output of the resources in a way that the cost of deviating from the day-ahead schedule to meet the demand is minimized. The cost of deviation must account for battery degradation, costs associated with increased ramp rates, fuel costs, regular maintenance costs, and so on. In this control technique, an optimization problem is solved at each time step to specify a set of control actions over a finite time horizon. The first calculated control action, then, is applied at each time step to the system. The same process takes place at each successive time step taking into account the updated estimates of future quantities based on available information. The control policy is a feedback system as it uses the measured values of the current system states at each time step. The details on modeling as well as stability and performance requirement of the platform is provided in [159].

In summary, the MPC mechanism is in charge of filling the gap between the actual and predicted net load. This gap reflects the unforeseen changes in operating circumstances including normal variations of the demand and/or generation as well as the deviations associated with stresses on the system, e.g. caused by line/generator failures in a part of the grid.

It is assumed here that the utility company uses a price-driven demand response mechanism to obtain its desired behavior from the nodes, as it is more aligned with the characteristics of a future liberalized market. Thus, a variable price for power imported from the grid to an entity is assumed for this purpose. Nationwide, time-of-use rates are prevalent, but these are likely to be replaced by dynamic real-time pricing schemes as controllability of distributed infrastructure improves. Variable prices reflect real costs of generating power. Generally, the cost of importing power from the grid during some periods of the day (e.g., in the afternoon and early evening) is high in order to induce customers to reduce their demand from the grid. If storage devices are present and legally permitted, there is an option for customers to purchase and store energy from the grid when prices are low, and use it later, when prices are high. Based on the variable price of the electricity provided by the grid and forecasts of load and local renewable generation, an optimization problem is solved to determine the set points of controllable DERs on the microgrid so that the overall cost of meeting demand over the course of a day is minimized. In general, the day-ahead scheduling optimization tries to charge storage devices when the cost of grid power is low, and discharges them when the cost is high. In some cases, for example during the peak hours, local fossil-fuel-generation may cost lower than importing power from the grid. Finally, controllable loads can be scheduled to coincide with renewable generation. A comprehensive discussion on the process of choosing cost functions, the hierarchical structure of the MPC framework as well as other computational issues and solver specification is provided in [159].

As mentioned earlier, the standard practice in dealing with stress on the system is to curtail load which comes with decreasing the quality of service for consumers. In this study, the effect of enhanced controllability over loads facilitated by implementing a microgrids-based architecture for the power network in stress reduction applications is investigated. The stress reduction procedure of interest, however, does not come with disruptive actions on costumers' demand, meaning that the quality of service is maintained. In other words, it is the flexibility of the load in the system that facilitates the stress reduction by decreasing the power grid's share for meeting the demand, and increasing the share of local resources

to compensate the lost capacity.

To formulate this problem into an MPC framework, and based on the objective of using price-based mechanisms, different prices are used for the dynamic optimization problem than that of the day-ahead scheduling part. These new prices reflect the unforeseen change in operating circumstances. An unforeseen circumstance can be, for example, induced by a weather-related stress over the grid. Higher prices can be used as a tool to prioritize the available resources in the automated system, and thus, to use the grid as the last resource by relying on local distributed resources to the extent possible. It is assumed that this mechanism is used for a certain period of time within a day to induce a microgrid to reduce its demand from the grid, assisting the transmission system to handle the stress. In the context of the SASE model, this action is equivalent to increasing the value of the parameter θ. If the available local resources are not able to handle the situation, the microgrid will use the grid as the last resource to perfectly meet its local demand. In that case, it cannot fully provide service to the grid. Another scenario, that might happen in the future, could be to disconnect non-critical loads, for example via smart breakers, and providing service for just the critical loads.

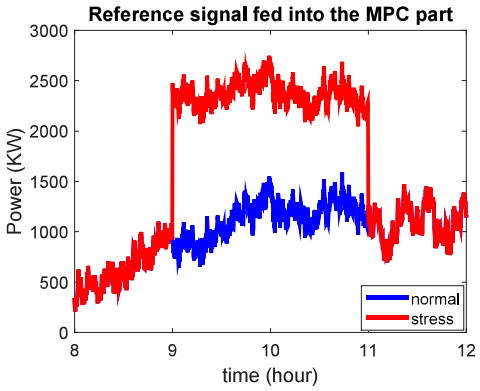

Figure 6.3: Example of a tracking signal fed into the MPC part of the control mechanism, under normal conditions (blue) and under stress (red). The tracking signal reflects the gap between the scheduled demand and the actual one, which should be met by available resources in an optimized fashion.

The gap between the actual net load and the predicted one should be filled by available resources. The MPC part of the control mechanism optimizes the redispaching of resources for this purpose. Two curves are shown in Fig.6.3. The blue one (which is covered by the red signal for the periods of time that the two signals are the same) represents the uncontrollable net load for a regular case, which is the reference signal fed into the MPC mechanism. The red curve describes the case where the grid is undergoing a stress, and a portion of the scheduled power is lost accordingly. This translates into a sharp change on top of the regular deviations in the reference signal for the MPC part as shown in the plot.

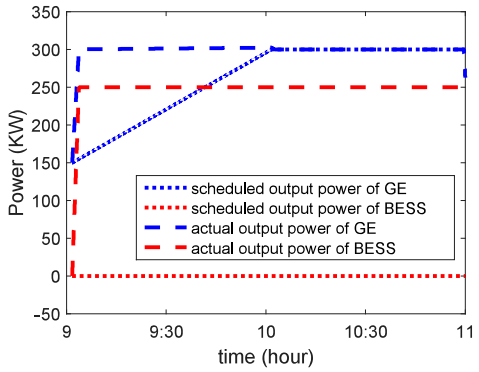

Figure 6.4: Response of the MGCC system to a load-shedding request from the grid. Local resources started working with their full capacity once the grid sent demand reduction request.

Factors that affect the response of the MGCC include time at which the event occurs (which specifies the scheduled state of charge and power level of individual resources) as well as technical specifications of the microgrid. Also, the presence of renewable resources in the microgrid structure affects its response. As shown in Fig. 6.2, PV panels produce different amount of power in various days.

It is assumed that a gas engine (GE) and a battery energy storage system (BESS) were present for this simulation in the configuration of the microgrid. In Fig.6.4, the share of each of the local resources to partially help meeting the demand for the stress case depicted in

Fig. 6.3 is shown. There are two curves associated with each of the resources. The dotted curves depict the scheduled output power, while the dashed lines represent the corresponding actual quantities derived from redispatching resources by the MPC part of the control framework. As shown, the GE had been scheduled to gradually reach its maximum power by 10 AM. However, as the result of the reserve request, reflected in the real-time price, it ramps up more to reach the maximum output power faster. Similarly, the BESS was fully charged at 9 AM and had been scheduled to release the energy stored later in early evening. Followed by the reserve request from the grid, the microgrid sets the BESS to work with its full capacity in response to the reserve request.

6.4 Statistical Characteristics of Distribution Feeder Microgrids for Load Reduction Applications

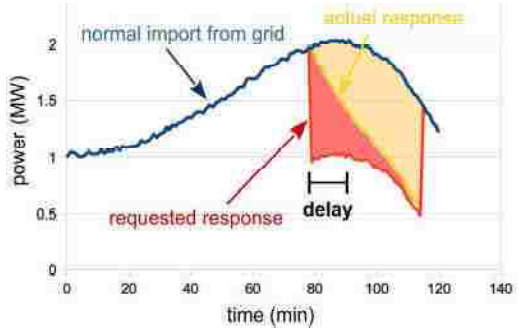

Figure 6.5: Performance metrics of a microgrid as related to load-shedding requests in times of grid-stress.

Two issues matter when facing a stress situation in the power network: 1) How quick the corrective actions can be implemented and 2) How long the system can endure a stress. In this regard, two metrics are introduced in Fig. 6.5 to assess the performance of a distribution

feeder microgrid while providing a non-disruptive service to the end-users: 1) delay and 2) energy ratio.

The delay metric is defined as the time that it takes an MGCC to reduce the imported power from the grid by 50% of what the utility has asked for to curtail. It is consistent with the definition of delay of a dynamical system in control systems theory in responding to a step change. Indeed, the reserve request from the utility in reducing the power demand is a step change in the scheduled quantities.

The other metric is the ratio of the energy that such a structure can contribute to, to the overall requested energy reduction. Ratios closer to unity indicate that the microgrid will be better able to handle long-term contingencies. In Fig. 6.5, the energy ratio is defined as the share provided by the microgrid resources (the yellow area) to the overall requested reduction (yellow + red) during the contingency.

The performance of a given microgrid in the face of a grid-stress event, however, is not deterministic. It depends on the weather (particularly as affecting PV power production) and on the time of day that the grid-stress event takes place. For example, if a grid-stress event takes place at the end of an on-peak tariff, it is likely that storage would be depleted, resulting in lower performance. Thus, a statistical characterization of microgrid performance is necessary.

An individual feeder is characterized by different installed resources. For this study, a distribution feeder microgrid equipped with a gas engine and a BESS along with PV generation is considered. The size of the gas engine and the BESS represent the variability of the physical characteristics of systems deployed regionally. For example, colder and cloudier regions would have a higher penetration of gas engine, while sunny, warm regions would be characterized by more BESS.

As an example, a load reduction request is sent to a microgrid which embodies a 300 KW GE, and a 250 KW BESS. The load reduction request is equivalent to 1500 KW of total power

consumption for a 10 GW feeder. The load reduction request takes place at 9 AM, when the BESS is fully charged and the GE is off. Consequently, the microgrid central controller (MGCC) starts using the available resources with their maximum capacity, meaning 550 KW contribution to the load reduction. It is also assumed that the energy capacity of the battery is 500KWH. Thus, the BESS is able to work with its maximum power capacity at most for 2 hours. The results of the simulation is shown in Fig.6.6.

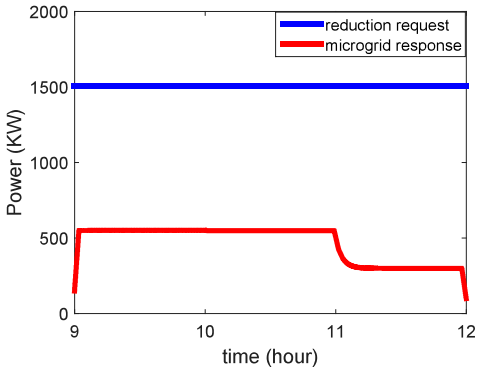

Figure 6.6: Response of the microgrid to a load reduction request from the grid. The microgrid can contribute 550 KW to the demand reduction request for a limited time. Once the battery is exhausted, the contribution reduces consequently.

It is assumed that the load reduction request lasts for three hours. Thus, the battery can no longer contribute to the load reduction service after 11 AM. It is shown that the limited power capacity of the available resources determines whether a microgrid can even reach the threshold of 50% for determining the corresponding delay. In the illustrated scenario, the associated delay with the microgrid of interest is ∞!

As another example, a load reduction of 1700 KW on the same feeder is requested from the microgrid. This time the BESS of the previous example is replaced with another one that has 700 KW power capacity. However, the energy capacity of this new BESS is equivalent to 1 hour of operation at the maximum capacity; 700 KWH. As the battery is fully charged by 8 AM, the MGCC starts using it at the maximum capacity. Thus, the system is able to meet the 50% threshold, and the delay is a limited quantity. The simulation results are

shown in Fig. 6.7.

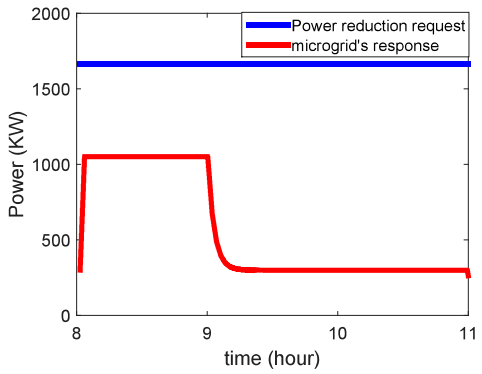

Figure 6.7: Response of the microgrid to a load reduction request from the grid. The microgrid can contribute 1050 KW to the demand reduction request for a limited time.

Two uniform distributions were sampled to form the resources available, with gas engine installations ranging from 0 to 3MW that can run infinitely, and BESS sizes ranging from 0 to 5MW that have the capacity to run at maximum power for an hour. In addition, the grid-stress event can occur at various times of the day, for different weather conditions. 10 battery sizes and 10 fuel cell sizes were sampled, and the response from an event occurring at 5 different times of day were calculated for 5 different days. Finally, 2 case of an 8MW capacity microgrid (50% capacity) and a 16MW capacity microgrid (100% capacity) were examined. It is also assumed that the load reduction request lasts three hours in all cases. The resulting performance statistics for 2×2500 different scenarios are shown in Figs. 6.8 and 6.9, for the delay and energy ratio distributions respectively.

Regarding the delay, it is shown that the distribution of the metric is almost a bimodal one. This is resulted from the fact that the important feature of the microgrids of interest in specifying the delay was the power capacity. Given that they have an acceptable ramping capacity, the only issue that matters is whether they have sufficient power capacity to reach a certain level of output power. Otherwise, they are not able to meet the requested reduction at all during the assumed 3 hours stress period.

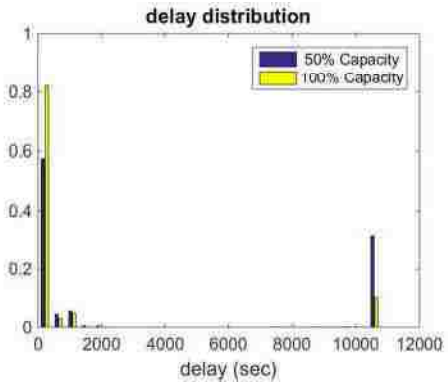

Figure 6.8: Histogram of delay distribution resulting from 2500 microgrid simulations for two cases. Note the strongly bimodal distribution of delays.

Concerning the energy metric, the distribution is skewed right for microgrids with smaller energy capacities, while the corresponding one for those with larger energy capacities is skewed left. The former case indicates that the microgrids endure less, while the latter case represents microgirds that are less dependent to the grid.

6.5 Discussion

By solving the dynamic programming problem and implementing an MPC controller in combination with optimized day-ahead scheduling, it was shown how a microgrid can put into effect an acceptable stress reduction procedure to help the transmission system during a grid-stress. More specifically, some meaningful distributions for useful metrics were derived in a distribution feeder microgrid-based power network, namely delay and energy ratio. The knowledge of such distributions can then be fed into the analytical and numerical models of the cascading-failure phenomena to facilitate developing a cascading-failure-aware power flow optimization with controllable distribution nodes.

In this study, two important characteristics were derived regarding time and energy. Re-

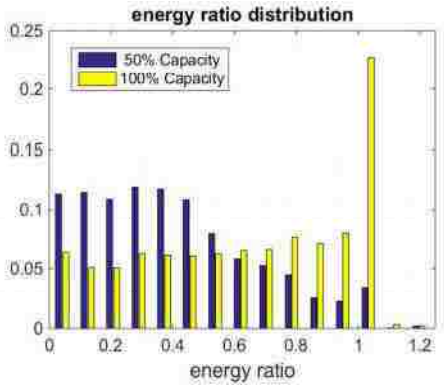

Figure 6.9: Energy ratio distribution for 2500 simulations for two cases. For microgrids with smaller resources (blue), the energy ratio is skewed towards right, while the distribution for larger resource microgrids (yellow) is skewed left. The former case indicates that the microgrids endure less, while the latter case represents microgirds that are less dependent to the grid.

garding the connection of this study with the SASE model, it is suggested that the static parameter θ in the SASE model is replaced with a dynamic attribute. Such an attribute is two-folded, including time and spatial distribution of the control knob θ. In this way, the two introduced metrics can be injected to the model and a significant amount of information is taken into account in the SASE model.

Moreover, there is a trade-off between the economic efficiency of the structure and its robustness. In order to enhance the robustness of the system, the cost function can be altered to make sure that there will be a level of stored energy in the storage devices to be used in severe cases. In other words, by adding some soft constraints to the dynamic programming problem, the robustness of the system will be improved to handle grid-stress situations more effectively.

Chapter 7

Conclusions

In this manuscript, the effect of the control architecture in the power system on enhancing system's resiliency against major disturbances was investigated. This enhancement was facilitated through integration of distributed energy resources into the grid. The main objective was to provide an implementable framework by which, aggregation of small scale distributed resources would have become possible. The platform introduced was based on distribution feeder microgrids as the physical structure combined with an appropriate control mechanism that addresses stability and performance requirements. The developed platform offered an aggregated capacity as an alternative for the capital-intensive resources in a grid, a chance to increase renewable resources share in the generation-mix and an enhancement regarding the resiliency of the system against severe disturbances.

For the objectives of this research it was first needed to derive a model that could be used in control process of interest. Specifically, a novel framework was proposed to capture the dynamical behavior of distributed resources such as TCLs in a power system. The framework was based on capturing the behavior of aggregated TCLs in the frequency domain. This framework, then, can be used to design a desired control signal to be followed by the system. Also, the presence of dead-time effect in thermostatic loads was presented. Based on my

knowledge, this feature is not addressed at least directly in the current literature.

The design of an appropriate mechanism that could facilitate participation of distributed resources was also presented. Model predictive control provided a framework to address both optimal performance and stability concerns. The objective function of interest was formulated in a way that it better reflects the realistic costs associated with implementing distribution feeder microgrids in the system. For such a purpose, a combination of linear and absolute value costs was considered. Specifically, linear costs were used for representing fuel costs in the system, while absolute value costs were used to show the degradation costs. This formulation is novel and has not been addressed to the best of obtained knowledge.

Another contribution of the present study was addressing the maintenance cost of using a local fossil-fuel-based generator. This cost is usually omitted in the literature due to the difficulty associated with solving the problem. A branch and bound methodology was used in the present study to solve the optimization problem of interest, while capturing the mixed-boolean convex parts corresponding to the maintenance cost.

An important contribution that was made in this study was addressing the recursive feasibility conditions in the MPC part. The common practice in this regard is appending the MPC problem with soft constraints that reduces the chance of infeasibility. However, using soft constraints does not guarantee the feasibility of the problem.

Moreover, the new methodology implemented on the distribution feeder microgrid, was used for the power system to integrate a wider range of distributed resources into the generation-mix. The cooperation between loads, generation and storage devices via an MPC mechanism could make it possible to reduce the size of electrical energy storage devices, and consequently the integration cost in a consistent way independent of the nature of the resources utilized.

The MPC based platform was extended in a cascading mechanism that could significantly reduce the computational costs associated with using an online adjustment method. For such a purpose, two static filters were used to decompose the deviation signal into three

different frequency bands and address each subproblem with appropriate available resources. The method can be substituted with dynamic filters in case and can be extended to finer frequency bands if needed.

Finally, The ability of the proposed platform to provide reserve services was addressed in a deterministic sense for standalone case, and in a statistical sense for system-wide implementation. The connected nature of future devices through ever-developing communication infrastructures makes it possible to extend control levels over demand. Also, the proposed framework would enable utility companies to go beyond the current limits of deploying renewable resources on the grid. This increased level of control could also increase the resiliency of the whole grid against large failures. An important factor in a grid-stress situation is the amount of load on the grid, and the common approach is to curtail the load in an emergency situation. This policy is also based on the inelastic presence of load in the grid. Utilizing distribution feeder microgrids provides an opportunity to make the load elastic to some extent. This elasticity enables a system operator not to cut the service during a stress situation necessarily, but to use load flexibility instead.

A load reduction scheme can potentially have a destabilizing effect as well. For example, if all the controllable entities start to reduce their associated loads to a large extent, generation may exceed demand. The direct consequence of such a phenomenon is thus a positive frequency deviation in the system, which is as harmful as the negative frequency deviation for which the load reduction scheme is implemented. Thus, a microgrid is informed by a real-time pricing alert as well as the needed load reduction level in the studied platform. Specifically, the grid does not ask for more than a certain level of load reduction by the real-time pricing mechanism.

A microgrid-based structure offers several opportunities ranging from reducing greenhouse gas emissions and resiliency against correlated failures to mitigating vulnerability of the system. Specifically, a distribution feeder microgrid, while equipped with an appropriate control mechanism, provides such benefits for the current existing feeders. Also, the microgrid cen-

tral controller is in charge of its own stability. Thus, correlated failures that happen in for example an extreme case of WMD-attacks have less impact on the system as a microgrid can run independently from the rest of the grid at least for a while.

Reconfiguration of the current power system based on distribution feeder microgrids was shown to have an improving effect on the resiliency of the network. The studied architecture is aligned with the current trend for a shift from centralized power system structure towards a more decentralized network as well.

References

[1] California ISO. Demand response and energy efficiency roadmap: Maximizing preferred resources, 2013.

[2] wikipedia. Electrical grid, 2016.

[3] CAISO. 2013 annual report on market issues and performance, 2013.

[4] Energy Information Administration. Electric power annual 2013, 2015.

[5] P Kundur, C Taylor, and P Pourbeik. Blackout experiences and lessons, best practices for system dynamic performance, and the role of new technologies. *IEEE Task Force Report*, 2007.

[6] Vaithianathan Venkatasubramanian and Yuan Li. Analysis of 1996 western american electric blackouts. *Bulk Power System Dynamics and Control-VI, Cortina dAmpezzo, Italy*, pages 22–27, 2004.

[7] S Abraham and R Efford. Final report on the august 14th blackout in the united states and canada. *US-Canada Power System Outage Task Force*, 2004.

[8] Paul Hines, Jay Apt, and Sarosh Talukdar. Large blackouts in north america: Historical trends and policy implications. *Energy Policy*, 37(12):5249–5259, 2009.

[9] Executive Office of the President. Economic benefits of increasing electric grid resilience to weather outages-august 2013.

[10] Alexis Kwasinski. Lessons from field damage assessments about communication networks power supply and infrastructure performance during natural disasters with a focus on hurricane sandy. In *FCC Workshop on Network Resiliency 2013*, 2013.

[11] WN Bryan. Emergency situation reports: Hurricane sandy. *Office of Electricity Delivery and Energy Reliability of US Department of Energy, Hurricane Sandy Situation Report*, 20, 2012.

[12] Aneesh Chopra and Vivek Kundra. A policy framework for the 21st century grid: Enabling our secure energy future. 2011.

[13] Andrea Sarzynski, Jeremy Larrieu, and Gireesh Shrimali. The impact of state financial incentives on market deployment of solar technology. *Energy Policy*, 46:550–557, 2012.

[14] Frauke Oldewurtel, Theodor Borsche, Matthias Bucher, Philipp Fortenbacher, Marina Gonzalez Vaya, Tobias Haring, Johanna L Mathieu, Olivier Megel, Evangelos Vrettos, and Goran Andersson. A framework for and assessment of demand response and energy storage in power systems. In *Bulk Power System Dynamics and Control-IX Optimization, Security and Control of the Emerging Power Grid (IREP), 2013 IREP Symposium*, pages 1–24. IEEE, 2013.

[15] Task Force. Final report on the august 14, 2003 blackout in the united states and canada. *US Department of Energy*, 2004.

[16] Ross Baldick, Badrul Chowdhury, Ian Dobson, Zhaoyang Dong, Bei Gou, David Hawkins, Henry Huang, Manho Joung, Daniel Kirschen, Fangxing Li, et al. Initial review of methods for cascading failure analysis in electric power transmission systems ieee pes cams task force on understanding, prediction, mitigation and restoration of cascading failures. In *Power and Energy Society General Meeting-Conversion and Delivery of Electrical Energy in the 21st Century, 2008 IEEE*, pages 1–8. IEEE, 2008.

[17] Ian Dobson, Benjamin A Carreras, Vickie E Lynch, and David E Newman. Complex systems analysis of series of blackouts: Cascading failure, critical points, and self-organization. *Chaos: An Interdisciplinary Journal of Nonlinear Science*, 17(2):026103, 2007.

[18] Ian Dobson, Benjamin A Carreras, and David E Newman. A loading-dependent model of probabilistic cascading failure. *Probability in the Engineering and Informational Sciences*, 19(01):15–32, 2005.

[19] Charles D Brummitt, Raissa M DSouza, and EA Leicht. Suppressing cascades of load in interdependent networks. *Proceedings of the National Academy of Sciences*, 109(12):E680–E689, 2012.

[20] Mahshid Rahnamay-Naeini, Zhuoyao Wang, Andrea Mammoli, and Majeed M Hayat. A probabilistic model for the dynamics of cascading failures and blackouts in power grids. In *Power and Energy Society General Meeting, 2012 IEEE*, pages 1–8. IEEE, 2012.

[21] Peter Asmus. Microgrids, virtual power plants and our distributed energy future. *The Electricity Journal*, 23(10):72–82, 2010.

[22] Liang Che, Mohammad Khodayar, and Mohammad Shahidehpour. Only connect: Microgrids for distribution system restoration. *Power and Energy Magazine, IEEE*, 12(1):70–81, 2014.

[23] Dan T Ton and Merrill A Smith. The us department of energy's microgrid initiative. *The Electricity Journal*, 25(8):84–94, 2012.

[24] Yuri V Makarov, Clyde Loutan, Jian Ma, and Phillip De Mello. Operational impacts of wind generation on california power systems. *Power Systems, IEEE Transactions on*, 24(2):1039–1050, 2009.

[25] Shmuel S Oren. Ensuring generation adequacy in competitive electricity markets. *Electricity Deregulation: Choices and Challenges*, pages 388–414, 2005.

[26] P Trichakis, Philip Charles Taylor, Padraig F Lyons, and Richard Hair. Predicting the technical impacts of high levels of small-scale embedded generators on low-voltage networks. *IET Renewable Power Generation*, 2(4):249–262, 2008.

[27] S Conti and S Raiti. Probabilistic load flow using monte carlo techniques for distribution networks with photovoltaic generators. *Solar Energy*, 81(12):1473–1481, 2007.

[28] Paul Denholm and Robert M Margolis. Evaluating the limits of solar photovoltaics (pv) in traditional electric power systems. *Energy policy*, 35(5):2852–2861, 2007.

[29] JJ Alba Rios, P Birkner, F Hakan, A Kroll, P Lawson, P Lebreton, et al. Decentralised storage: impact on future distribution grids. *Brussels, Belgium: Union of the Electricity Industry*, 2012.

[30] Douglas Halamay, Ted KA Brekken, Asher Simmons, Shaun McArthur, et al. Reserve requirement impacts of large-scale integration of wind, solar, and ocean wave power generation. *Sustainable Energy, IEEE Transactions on*, 2(3):321–328, 2011.

[31] Mohamed H Albadi and EF El-Saadany. Demand response in electricity markets: An overview. In *IEEE power engineering society general meeting*, volume 2007, pages 1–5, 2007.

[32] Peter Asmus. Microgrids, virtual power plants and our distributed energy future. *The Electricity Journal*, 23(10):72–82, 2010.

[33] P Denholm and R Margolis. Very large-scale deployment of grid-connected solar photovoltaics in the united states: challenges and opportunities. *National Renewable Energy Laboratory*, 2006.

[34] Amir-Hamed Mohsenian-Rad and Alberto Leon-Garcia. Coordination of cloud computing and smart power grids. In *Smart Grid Communications (SmartGridComm), 2010 First IEEE International Conference on*, pages 368–372. IEEE, 2010.

[35] Mahshid Rahnamay-Naeini, Zhuoyao Wang, Nasir Ghani, Andrea Mammoli, and Majeed M Hayat. Stochastic analysis of cascading-failure dynamics in power grids. *Power Systems, IEEE Transactions on*, 29(4):1767–1779, 2014.

[36] Jed Kolko. How suburban are big american cities?, 2015.

[37] Claus Ballegaard Nielsen, Peter Gorm Larsen, John Fitzgerald, Jim Woodcock, and Jan Peleska. Model-based engineering of systems of systems. *Submitted to ACM Computing Surveys*, 2013.

[38] DoD. Systems engineering guide for systems of systems essentials, 2010.

[39] Mark W Maier. Architecting principles for systems-of-systems. In *INCOSE International Symposium*, volume 6, pages 565–573. Wiley Online Library, 1996.

[40] Nancy S Andreas. Space-based infrared system (sbirs) system of systems. In *Aerospace Conference, 1997. Proceedings., IEEE*, volume 4, pages 429–438. IEEE, 1997.

[41] RS Fang and AK David. Optimal dispatch under transmission contracts. *Power Systems, IEEE Transactions on*, 14(2):732–737, 1999.

[42] NERC. United states mandatory standards subject to enforcement, 2016.

[43] US Federal Energy Regulatory Commission et al. Promoting wholesale competition through open access non-discriminatory transmission services by public utilities; recovery of stranded costs by public utilities and transmitting utilities. *Order*, 888:24, 1996.

[44] EIA. Annual energy review 2011. *Energy Information Administration*, 2012.

[45] Galen Barbose. Tracking the sun vi: An historical summary of the installed price of photovoltaics in the united states from 1998 to 2012. 2014.

[46] Jeremiah X Johnson and Joshua Novacheck. Emissions reductions from expanding state-level renewable portfolio standards. *Environmental science & technology*, 49(9):5318–5325, 2015.

[47] PJM. Pjm renewable integration study report, 2014.

[48] David Manz, Reigh Walling, Nate Miller, Beth LaRose, Rob D'Aquila, and Bahman Daryanian. The grid of the future: Ten trends that will shape the grid over the next decade. *Power and Energy Magazine, IEEE*, 12(3):26–36, 2014.

[49] CAISO. Smart grid, roadmap and architecture, 2010.

[50] V Cagri Gungor, Dilan Sahin, Taskin Kocak, Salih Ergut, Concettina Buccella, Carlo Cecati, and Gerhard P Hancke. A survey on smart grid potential applications and communication requirements. *Industrial Informatics, IEEE Transactions on*, 9(1):28–42, 2013.

[51] Ye Yan, Yi Qian, Hamid Sharif, and David Tipper. A survey on smart grid communication infrastructures: Motivations, requirements and challenges. *Communications Surveys & Tutorials, IEEE*, 15(1):5–20, 2013.

[52] Olli Kilkki, Antti Alahaivala, and Ilkka Seilonen. Optimized control of price-based demand response with electric storage space heating. *Industrial Informatics, IEEE Transactions on*, 11(1):281–288, 2015.

[53] Yann G Rebours, Daniel S Kirschen, Marc Trotignon, and Sébastien Rossignol. A survey of frequency and voltage control ancillary servicespart i: Technical features. *Power Systems, IEEE Transactions on*, 22(1):350–357, 2007.

[54] Yann G Rebours, Daniel S Kirschen, Marc Trotignon, and Sébastien Rossignol. A survey of frequency and voltage control ancillary servicespart ii: economic features. *Power Systems, IEEE Transactions on*, 22(1):358–366, 2007.

[55] Erik Ela, Michael Milligan, and Brendan Kirby. Operating reserves and variable generation. *Contract*, 303:275–3000, 2011.

[56] Kaveh Dehghanpour and Saeed Afsharnia. Electrical demand side contribution to frequency control in power systems: a review on technical aspects. *Renewable and Sustainable Energy Reviews*, 41:1267–1276, 2015.

[57] Shashi Kant Pandey, Soumya R Mohanty, and Nand Kishor. A literature survey on load–frequency control for conventional and distribution generation power systems. *Renewable and Sustainable Energy Reviews*, 25:318–334, 2013.

[58] Pascal Mercier, Rachid Cherkaoui, and Alexandre Oudalov. Optimizing a battery energy storage system for frequency control application in an isolated power system. *Power Systems, IEEE Transactions on*, 24(3):1469–1477, 2009.

[59] Pengwei Du and Ning Lu. Appliance commitment for household load scheduling. *Smart Grid, IEEE Transactions on*, 2(2):411–419, 2011.

[60] Hao Jiang, Jin Lin, Yonghua Song, Wenzhong Gao, Yu Xu, Bin Shu, Xiaomin Li, and Jianxun Dong. Demand side frequency control scheme in an isolated wind power system for industrial aluminum smelting production. *Power Systems, IEEE Transactions on*, 29(2):844–853, 2014.

[61] Prasenjit Basak, S Chowdhury, S Halder nee Dey, and SP Chowdhury. A literature review on integration of distributed energy resources in the perspective of control, protection and stability of microgrid. *Renewable and Sustainable Energy Reviews*, 16(8):5545–5556, 2012.

[62] David S Watson. Fast automated demand response to enable the integration of renewable resources. 2013.

[63] David Dallinger, Schubert Gerda, and Martin Wietschel. Integration of intermittent renewable power supply using grid-connected vehicles–a 2030 case study for california and germany. *Applied Energy*, 104:666–682, 2013.

[64] Rashid A Waraich, Matthias D Galus, Christoph Dobler, Michael Balmer, Göran Andersson, and Kay W Axhausen. Plug-in hybrid electric vehicles and smart grids: Investigations based on a microsimulation. *Transportation Research Part C: Emerging Technologies*, 28:74–86, 2013.

[65] Alexandre Oudalov, Daniel Chartouni, and Christian Ohler. Optimizing a battery energy storage system for primary frequency control. *Power Systems, IEEE Transactions on*, 22(3):1259–1266, 2007.

[66] Jim Eyer and Garth Corey. Energy storage for the electricity grid: Benefits and market potential assessment guide. *Sandia National Laboratories*, 20(10):5, 2010.

[67] M Braun and T Stetz. Multifunctional photovoltaic inverters–economic potential of grid-connected multifunctional pv-battery-systems in industrial environments. In *23rd European Photovoltaic Solar Energy Conference, Valencia, Spain*, volume 1, 2008.

[68] KC Divya and Jacob Ostergaard. Battery energy storage technology for power systemsan overview. *Electric Power Systems Research*, 79(4):511–520, 2009.

[69] Peter J Hall and Euan J Bain. Energy-storage technologies and electricity generation. *Energy policy*, 36(12):4352–4355, 2008.

[70] Noriko Kawakami, Yukihisa Iijima, Yoshinori Sakanaka, Motohiro Fukuhara, Koji Ogawa, Matsuo Bando, and Takeshi Matsuda. Development and field experiences of stabilization system using 34mw nas batteries for a 51mw wind farm. In *Industrial*

Electronics (ISIE), 2010 IEEE International Symposium on, pages 2371–2376. IEEE, 2010.

[71] DM Rastler. *Electricity energy storage technology options: a white paper primer on applications, costs and benefits*. Electric Power Research Institute, 2010.

[72] Marc Beaudin, Hamidreza Zareipour, Anthony Schellenberglabe, and William Rosehart. Energy storage for mitigating the variability of renewable electricity sources: An updated review. *Energy for Sustainable Development*, 14(4):302–314, 2010.

[73] Hussein Ibrahim, Adrian Ilinca, and Jean Perron. Energy storage systemscharacteristics and comparisons. *Renewable and sustainable energy reviews*, 12(5):1221–1250, 2008.

[74] Scott B Peterson, Jay Apt, and JF Whitacre. Lithium-ion battery cell degradation resulting from realistic vehicle and vehicle-to-grid utilization. *Journal of Power Sources*, 195(8):2385–2392, 2010.

[75] J Vetter, P Novak, MR Wagner, C Veit, K-C Moller, JO Besenhard, M Winter, M Wohlfahrt-Mehrens, C Vogler, and A Hammouche. Ageing mechanisms in lithium-ion batteries. *Journal of power sources*, 147(1):269–281, 2005.

[76] McKinsey & Company. A portfolio of power-trains for europe: a fact-based analysis, 2010.

[77] Theodor Borsche, Andreas Ulbig, Michael Koller, and Goran Andersson. Power and energy capacity requirements of storages providing frequency control reserves. In *IEEE PES General Meeting, Vancouver*, 2013.

[78] Alexandre Oudalov, Daniel Chartouni, and Christian Ohler. Optimizing a battery energy storage system for primary frequency control. *Power Systems, IEEE Transactions on*, 22(3):1259–1266, 2007.

[79] Olivier Megel, Johanna L Mathieu, and Goran Andersson. Maximizing the potential of energy storage to provide fast frequency control. In *Innovative Smart Grid Technologies Europe (ISGT EUROPE), 2013 4th IEEE/PES*, pages 1–5. IEEE, 2013.

[80] Erhan Demirok, Dezso Sera, Remus Teodorescu, Pedro Rodriguez, and Uffe Borup. Evaluation of the voltage support strategies for the low voltage grid connected pv generators. In *Energy Conversion Congress and Exposition (ECCE), 2010 IEEE*, pages 710–717. IEEE, 2010.

[81] Ali Nourai. Installation of the first distributed energy storage system (dess) at american electric power (aep). *Sandia Report SAND2007-3580*, 2007.

[82] Shahin Abdollahy, Olga Lavrova, A Mammoli, Steve Willard, and B Arellano. Pnm smart grid demonstration project from modeling to demonstration. In *Innovative Smart Grid Technologies (ISGT), 2012 IEEE PES*, pages 1–6. IEEE, 2012.

[83] Mary Ann Piette, David Watson, Naoya Motegi, Sila Kiliccote, and Peng Xu. Automated critical peak pricing field tests: Program description and results. *Lawrence Berkeley National Laboratory*, 2006.

[84] Froylan E Sifuentes and Taylor Keep. Estimating demand response potential of buildings using a predictive hvac model. In *ASME 2014 Power Conference*, pages V002T14A005–V002T14A005. American Society of Mechanical Engineers, 2014.

[85] Johanna L Mathieu, Ashok J Gadgil, Duncan S Callaway, Phillip N Price, and Sila Kiliccote. Characterizing the response of commercial and industrial facilities to dynamic pricing signals from the utility. In *ASME 2010 4th International Conference on Energy Sustainability*, pages 1019–1028. American Society of Mechanical Engineers, 2010.

[86] He Hao, Timothy Middelkoop, Prabir Barooah, and Sean Meyn. How demand response from commercial buildings will provide the regulation needs of the grid. In *Commu-*

nication, Control, and Computing (Allerton), 2012 50th Annual Allerton Conference on, pages 1908–1913. IEEE, 2012.

[87] Sila Kiliccote. Field testing of automated demand response for integration of renewable resources in california's ancillary services market for regulation products. 2013.

[88] Mary Ann Piette. Open automated demand response communications specification (version 1.0). *Lawrence Berkeley National Laboratory*, 2009.

[89] Sila Kiliccote, Mary Ann Piette, Edward Koch, and Dan Hennage. Utilizing automated demand response in commercial buildings as non-spinning reserve product for ancillary services markets. In *Decision and Control and European Control Conference (CDC-ECC), 2011 50th IEEE Conference on*, pages 4354–4360. IEEE, 2011.

[90] Johanna L Mathieu, Phillip N Price, Sila Kiliccote, and Mary Ann Piette. Quantifying changes in building electricity use, with application to demand response. *Smart Grid, IEEE Transactions on*, 2(3):507–518, 2011.

[91] Frauke Oldewurtel, Andreas Ulbig, Alessandra Parisio, Goran Andersson, and Manfred Morari. Reducing peak electricity demand in building climate control using real-time pricing and model predictive control. In *Decision and Control (CDC), 2010 49th IEEE Conference on*, pages 1927–1932. IEEE, 2010.

[92] Yudong Ma, Francesco Borrelli, Brandon Hencey, Brian Coffey, Sorin Bengea, and Philip Haves. Model predictive control for the operation of building cooling systems. *Control Systems Technology, IEEE Transactions on*, 20(3):796–803, 2012.

[93] Evangelos Vrettos, K Lai, Frauke Oldewurtel, and Goran Andersson. Predictive control of buildings for demand response with dynamic day-ahead and real-time prices. In *European Control Conference (ECC), Zurich, Switzerland*, 2013.

[94] Duncan S Callaway and Ian A Hiskens. Achieving controllability of electric loads. *Proceedings of the IEEE*, 99(1):184–199, 2011.

[95] Duncan S Callaway. Tapping the energy storage potential in electric loads to deliver load following and regulation, with application to wind energy. *Energy Conversion and Management*, 50(5):1389–1400, 2009.

[96] Stephan Koch, Marek Zima, and Goran Andersson. Active coordination of thermal household appliances for load management purposes. In *IFAC Symposium on Power Plants and Power Systems Control, Tampere, Finland*. Citeseer, 2009.

[97] Taylor M Keep, Froylan E Sifuentes, David M Auslander, and Duncan S Callaway. Using load switches to control aggregated electricity demand for load following and regulation. In *Power and Energy Society General Meeting, 2011 IEEE*, pages 1–7. IEEE, 2011.

[98] Badri Ramanathan and Vijay Vittal. A framework for evaluation of advanced direct load control with minimum disruption. *Power Systems, IEEE Transactions on*, 23(4):1681–1688, 2008.

[99] Duncan S Callaway. Can smaller loads be profitably engaged in power system services? In *Power and Energy Society General Meeting, 2011 IEEE*, pages 1–3. IEEE, 2011.

[100] A Aruzuaga, Inigo Berganza, Alberto Sendin, Manu Sharma, and Badri Varadarajan. Prime interoperability tests and results from field. In *Smart Grid Communications (SmartGridComm), 2010 First IEEE International Conference on*, pages 126–130. IEEE, 2010.

[101] Theodor Borsche, Frauke Oldewurtel, and Goran Andersson. Minimizing communication cost for demand response using state estimation. In *PowerTech (POWERTECH), 2013 IEEE Grenoble*, pages 1–6. IEEE, 2013.

[102] Yasser Yasaei and Andrea Mammoli. A novel framework for characterizing the aggregated response of thermostatically controlled loads in distribution networks, 2016. Accepted for 2016 IEEE PES Genral Meeting.

[103] Mardavij Roozbehani, Munther A Dahleh, and Sanjoy K Mitter. Volatility of power grids under real-time pricing. *Power Systems, IEEE Transactions on*, 27(4):1926–1940, 2012.

[104] J Mathieu, Mark Dyson, Duncan Callaway, and A Rosenfeld. Using residential electric loads for fast demand response: The potential resource and revenues, the costs, and policy recommendations. *Proceedings of the ACEEE Summer Study on Buildings, Pacific Grove, CA*, 1000(2000):3000, 2012.

[105] Saeid Bashash and Hosam K Fathy. Modeling and control insights into demand-side energy management through setpoint control of thermostatic loads. In *American Control Conference (ACC), 2011*, pages 4546–4553. IEEE, 2011.

[106] Soumya Kundu, Nikolai Sinitsyn, Scott Backhaus, and Ian Hiskens. Modeling and control of thermostatically controlled loads. *arXiv preprint arXiv:1101.2157*, 2011.

[107] Stephan Koch, Johanna L Mathieu, and Duncan S Callaway. Modeling and control of aggregated heterogeneous thermostatically controlled loads for ancillary services. In *Proc. PSCC*, pages 1–7, 2011.

[108] Johanna L Mathieu and Duncan S Callaway. State estimation and control of heterogeneous thermostatically controlled loads for load following. In *System Science (HICSS), 2012 45th Hawaii International Conference on*, pages 2002–2011. IEEE, 2012.

[109] Johanna L Mathieu, Stephan Koch, and Duncan S Callaway. State estimation and control of electric loads to manage real-time energy imbalance. *Power Systems, IEEE Transactions on*, 28(1):430–440, 2013.

[110] PG& E. Smart ac programs, 2016.

[111] Evangelos Vrettos, Andreas Witzig, Roland Kurmann, Stephan Koch, and Goran Andersson. Maximizing local pv utilization using small-scale batteries and flexible thermal loads. *EU PVSEC*, 2013.

[112] Chris Marnay, Raquel Blanco, Kristina S Hamachi, Cornelia P Kawaan, Julie G Osborn, and F Javier Rubio. Integrated assessment of dispersed energy resources deployment. *Lawrence Berkeley National Laboratory*, 2000.

[113] Estefania Planas, Asier Gil-de Muro, Jon Andreu, Inigo Kortabarria, and Inigo Martinez de Alegria. General aspects, hierarchical controls and droop methods in microgrids: A review. *Renewable and Sustainable Energy Reviews*, 17:147–159, 2013.

[114] Chun-Hao Lo and Nayeem Ansari. Decentralized controls and communications for autonomous distribution networks in smart grid. *Smart Grid, IEEE Transactions on*, 4(1):66–77, 2013.

[115] Robert Lasseter, Kevin Tomsovic, and Paolo Piagi. Scenarios for distributed technology applications with steady state and dynamic models of loads and micro-sources. *Consortium for Electric Reliability Technology Solutions, PSERC*, 2000.

[116] Danny Pudjianto, Charlotte Ramsay, and Goran Strbac. Virtual power plant and system integration of distributed energy resources. *Renewable power generation, IET*, 1(1):10–16, 2007.

[117] Michael Angelo Pedrasa and Ted Spooner. A survey of techniques used to control microgrid generation and storage during island operation. In *Proceedings of the 2006 Australasian Universities Power Engineering Conference (AUPEC'06)*, pages 1–6, 2006.

[118] R Ramakumar. Role of distributed generation in reinforcing the critical electric power infrastructure. In *Power Engineering Society Winter Meeting, 2001. IEEE*, volume 1, pages 139–139. IEEE, 2001.

[119] Xingguo Tan, Qingmin Li, and Hui Wang. Advances and trends of energy storage technology in microgrid. *International Journal of Electrical Power & Energy Systems*, 44(1):179–191, 2013.

[120] NWA Lidula and AD Rajapakse. Microgrids research: A review of experimental microgrids and test systems. *Renewable and Sustainable Energy Reviews*, 15(1):186–202, 2011.

[121] Gianfranco Chicco and Pierluigi Mancarella. Distributed multi-generation: a comprehensive view. *Renewable and Sustainable Energy Reviews*, 13(3):535–551, 2009.

[122] Joseba Jimeno, Jon Anduaga, Jose Oyarzabal, and Asier Gil de Muro. Architecture of a microgrid energy management system. *European Transactions on Electrical Power*, 21(2):1142–1158, 2011.

[123] Robert H Lasseter and Paolo Paigi. Microgrid: a conceptual solution. In *Power Electronics Specialists Conference, 2004. PESC 04. 2004 IEEE 35th Annual*, volume 6, pages 4285–4290. IEEE, 2004.

[124] Farid Katiraei, Reza Iravani, Nikos Hatziargyriou, and Aris Dimeas. Microgrids management. *Power and Energy Magazine, IEEE*, 6(3):54–65, 2008.

[125] Kumudhini Ravindra, Balaraman Kannan, and Nagaraja Ramappa. Microgrids: A value-based paradigm: The need for the redefinition of microgrids. *Electrification Magazine, IEEE*, 2(1):20–29, 2014.

[126] Fang Z Peng, Yun Wei Li, and Leon M Tolbert. Control and protection of power electronics interfaced distributed generation systems in a customer-driven microgrid. In *Power & Energy Society General Meeting, 2009. PES'09. IEEE*, pages 1–8. IEEE, 2009.

[127] Adeel Abbas Zaidi and Friederich Kupzog. Microgrid automation-a self-configuring approach. In *Multitopic Conference, 2008. INMIC 2008. IEEE International*, pages 565–570. IEEE, 2008.

[128] David P Chassin, Pengwei Du, and Jason C Fuller. The potential and limits of residential demand response control strategies. In *Power and Energy Society General Meeting, 2011 IEEE*, pages 1–6. IEEE, 2011.

[129] Erik Ela, Michael R Milligan, Aaron Bloom, A Botterud, A Townsend, and T Levin. *Evolution of wholesale electricity market design with increasing levels of renewable generation*. National Renewable Energy Laboratory, 2014.

[130] Michael J Krok and S Gene. A coordinated optimization approach to volt/var control for large power distribution networks. In *American Control Conference (ACC), 2011*, pages 1145–1150. IEEE, 2011.

[131] Zhi Chen, Lei Wu, and Yong Fu. Real-time price-based demand response management for residential appliances via stochastic optimization and robust optimization. *Smart grid, IEEE transactions on*, 3(4):1822–1831, 2012.

[132] Wencong Su, Jianhui Wang, Kuilin Zhang, and Alex Q Huang. Model predictive control-based power dispatch for distribution system considering plug-in electric vehicle uncertainty. *Electric Power Systems Research*, 106:29–35, 2014.

[133] Xinan Zhang, D Mahinda Vilathgamuwa, King-Jet Tseng, Bikramjit S Bhangu, and Chandana J Gajanayake. Power buffer with model predictive control for stability of vehicular power systems with constant power loads. *Power Electronics, IEEE Transactions on*, 28(12):5804–5812, 2013.

[134] Mubbashir Ali, Juha Jokisalo, Kai Siren, and Matti Lehtonen. Combining the demand response of direct electric space heating and partial thermal storage using lp optimization. *Electric Power Systems Research*, 106:160–167, 2014.

[135] Matthias D Galus, Stephan Koch, and Goran Andersson. Provision of load frequency control by phevs, controllable loads, and a cogeneration unit. *Industrial Electronics, IEEE Transactions on*, 58(10):4568–4582, 2011.

[136] Evangelos Vrettos and Goran Andersson. Combined load frequency control and active distribution network management with thermostatically controlled loads. In *Smart Grid Communications (SmartGridComm), 2013 IEEE International Conference on*, pages 247–252. IEEE, 2013.

[137] Evangelos Vrettos, K Lai, Frauke Oldewurtel, and Goran Andersson. Predictive control of buildings for demand response with dynamic day-ahead and real-time prices. In *European Control Conference (ECC), Zurich, Switzerland*, 2013.

[138] J Michaels and T Leckey. Commercial buildings energy consumption survey. *URL http://www. eia. doe. gov/emeu/cbecs*, 2003.

[139] PNM. Public service new mexico electric energy efficiency potential study, 2006.

[140] Wei Zhang, Karanjit Kalsi, Jason Fuller, Marcelo Elizondo, and David Chassin. Aggregate model for heterogeneous thermostatically controlled loads with demand response. In *Power and Energy Society General Meeting, 2012 IEEE*, pages 1–8. IEEE, 2012.

[141] Maryam Kamgarpour, Christian Ellen, Sadegh Esmaeil Zadeh Soudjani, Sebastian Gerwinn, Johanna L Mathieu, Nils Mullner, Alessandro Abate, Duncan S Callaway, Martin Franzle, and John Lygeros. Modeling options for demand side participation of thermostatically controlled loads. In *Bulk Power System Dynamics and Control-IX Optimization, Security and Control of the Emerging Power Grid (IREP), 2013 IREP Symposium*, pages 1–15. IEEE, 2013.

[142] Johanna L Mathieu, Maryam Kamgarpour, John Lygeros, and Duncan S Callaway. Energy arbitrage with thermostatically controlled loads. In *Control Conference (ECC), 2013 European*, pages 2519–2526. IEEE, 2013.

[143] Andrea Mammoli, C Birk Jones, Hans Barsun, David Dreisigmeyer, Gary Goddard, and Olga Lavrova. Distributed control strategies for high-penetration commercial-

building-scale thermal storage. In *Transmission and Distribution Conference and Exposition (T&D), 2012 IEEE PES*, pages 1–7. IEEE, 2012.

[144] Evangelos Vrettos, Frauke Oldewurtel, Matteo Vasirani, and Goran Andersson. Centralized and decentralized balance group optimization in electricity markets with demand response. In *PowerTech (POWERTECH), 2013 IEEE Grenoble*, pages 1–6. IEEE, 2013.

[145] Arindam Maitra, Ben York, Haresh Kamath, Tom Key, and Vikas Singhvi. Microgrids: A primer. 2013.

[146] SDG&E. Sdg&e borrego springs microgrid demonstration project, 2012.

[147] Massoud Amin. Toward self-healing energy infrastructure systems. *Computer Applications in Power, IEEE*, 14(1):20–28, 2001.

[148] Kai Heussen, Stephan Koch, Andreas Ulbig, and Göran Andersson. Unified system-level modeling of intermittent renewable energy sources and energy storage for power system operation. *Systems Journal, IEEE*, 6(1):140–151, 2012.

[149] Michele Arnold and Göran Andersson. Model predictive control of energy storage including uncertain forecasts. In *Power Systems Computation Conference (PSCC), Stockholm, Sweden*, 2011.

[150] Michael Grant, Stephen Boyd, and Yinyu Ye. *Disciplined convex programming*. Springer, 2006.

[151] Ramon E Moore. Global optimization to prescribed accuracy. *Computers & mathematics with applications*, 21(6):25–39, 1991.

[152] Fred Glover. Tabu search-part i. *ORSA Journal on computing*, 1(3):190–206, 1989.

[153] Fred Glover. Tabu searchpart ii. *ORSA Journal on computing*, 2(1):4–32, 1990.

[154] Jacob Mattingley, Yang Wang, and Stephen Boyd. Receding horizon control. *Control Systems, IEEE*, 31(3):52–65, 2011.

[155] Hassan K Khalil and JW Grizzle. *Nonlinear systems*, volume 3. Prentice hall New Jersey, 1996.

[156] Michael Grant and Stephen Boyd. CVX: Matlab software for disciplined convex programming, version 2.1, March 2014.

[157] Michael Grant and Stephen Boyd. Graph implementations for nonsmooth convex programs. In V. Blondel, S. Boyd, and H. Kimura, editors, *Recent Advances in Learning and Control*, Lecture Notes in Control and Information Sciences, pages 95–110. Springer-Verlag Limited, 2008.

[158] William H Press, Saul A Teukolsky, William T Vetterling, and Brian P Flannery. Numerical recipes in fortran, 1992.

[159] Yasser Yasaei, Majeed Hayat, and Andrea Mammoli. Response of distribution feeder microgrids to system-level reserve requests, 2016. Accepted for 2016 IEEE PES Genral Meeting.

[160] Peter Asmus. Private, public power, and remote utility networks for renewable energy integration, grid reliability, and load reduction: Global market analysis and forecasts. Research report, Pike Research, 2012.

[161] Peter Palensky and Dietmar Dietrich. Demand side management: Demand response, intelligent energy systems, and smart loads. *Industrial Informatics, IEEE Transactions on*, 7(3):381–388, 2011.

[162] The integrated grid: Realizing the full value of central and distributed energy resources. Technical Results 3002002733, Electrical Power Research Institute, February 2014.

[163] Mohamed H Albadi and EF El-Saadany. A summary of demand response in electricity markets. *Electric power systems research*, 78(11):1989–1996, 2008.